Tome 12 *Février* *1974* Numéro 1

うみ

La mer

昭和 49 年 2 月

日 仏 海 洋 学 会

La Société franco-japonaise
d'océanographie
Tokyo, Japon

日 仏 海 洋 学 会

編 集 委 員 会

投 稿 規 定

1. 報文の投稿者は本会会員に限る。
2. 原稿は簡潔にわかりやすく書き，図表を含めて印刷ページで12ページ以内を原則とする。原稿（正1通，副1通）は，(〒101)東京都千代田区神田駿河台2-3　日仏会館内　日仏海洋学会編集委員会宛に送ること。
3. 編集委員会は，事情により原稿の字句の加除訂正を行うことがある。
4. 論文（欧文，和文とも）には必ず約200語の英文（または仏文）の Abstract (Résumé) をつけること。欧文論文には英文（又は仏文）の Abstract (Résumé) のほかに必ず約500字の和文の要旨をつけること。
5. 図及び表は必要なもののみに限る。図はそのまま版下になるように縮尺を考慮して鮮明に黒インクで書き，論文の図及び表には必ず英文（又は仏文）の説明をつけること。
6. 初校は原則として著者が行う。
7. 報文には1編につき50部の別刷を無料で著者に進呈する。これ以上の部数に対しては，実費（送料を含む）を著者が負担する。

RECOMMANDATIONS A L'USAGE DES AUTEURS

1. Les auteurs doivent être des Membres de la Société franco-japonaise d'océanographie.
2. Les notes ne peuvent dépasser douze pages. Les manuscrits à deux exemplaires, dactylographiés sur papier fort, doivent être envoyés au Comité de rédaction de la Société franco-japonaise d'océanographie, c/o Maison franco-japonaise, 2-3 Kanda, Surugadai, Chiyoda-ku, Tokyo, 101 Japon.
3. Le Comité de rédaction se réserve le droit d'apporter, le cas échéant, des modifications mineuses aux manuscrits ainsi que de demander aux auteurs de les corriger.
4. Des résumés en langue japonaise ou langue française sont obligatoires.
5. Les figures au trait seront tracées à l'encre de Chine noire sur papier blanc ou sur calque. Les légendes des figures et des tableaux sont indispensables.
6. Les premières épreuves seront corrigées, en principe, par les auteurs.
7 Un tirage à part des articles en cinquante exemplaires est offert gratuitement aux auteurs. Ceux qui en désirent un plus grand nombre peuvent les faire établir à leurs frais.

La mer (Bulletin de la Société franco-japonaise d'océanographie)
Tome 12, N° 1, pp. 1 à 8. Février 1974

大陸棚上における長周期波の振舞 (I)*

——女川湾沖における観測結果——

益永典昭** 寺本俊彦** 前田明夫**

Behavior of Long Period Waves on the Continental Shelf (I)

——Measurements off Onagawa Bay——

Noriaki MASUNAGA, Toshihiko TERAMOTO and Akio MAEDA

Abstract: Measurements of water temperatures at the surface, 10 m depth and 20 m depth together with velocity measurement at 20 m depth were carried out from R/V *Tansei-maru* anchored 0.9 km north to Miyagi-Enoshima on the continental shelf off Onagawa Bay. Cross-spectral analyses of these measurements and sea-level measurement at Miyagi-Enoshima in addition reveal existence of barotropic long waves with periods of 12 min, 5.5 min and 3 min and baroclinic long waves with periods of 10 to 7 min. Barotropic waves of period of 12 min are the edge waves of leaky mode and Barotropic waves of periods of 5.5 min and 3 min are both seiches produced in association with local geographical configuration of the region under consideration.

1. 序　論

沿岸の浅海には，風波うねりのような短周期の波から，潮汐波あるいは，更に長周期の波まで各種の波があつまってくる。これらのうち，数分から数時間までの周期範囲の波についての沖合における実測に基づく研究は少ない。このような波の伝播には，海底地形が重要な役割を果たすものと考えられる。

この研究は，大局的にみると，一様な幅の大陸棚が海岸に沿って長くつづいている三陸沖 (Fig. 1) を選び，数分から数十分の周期範囲の波の振舞を実測を通して調べたものである。このような波の研究は，その現象を理解する上で重要なだけではなく，津波のバックグラウンド・ノイズにあたることから実際面でも重要である。なお，この研究は，三陸沖と異なり海底が沖へ向って一様な勾配で深くなっている相模湾沿岸での観測に基づく研究を含む研究計画の一環をなすものである。

歴史的には，STOKES (1847年) は，真直ぐな海岸の海底が沖に向って一様に傾斜している場合，海

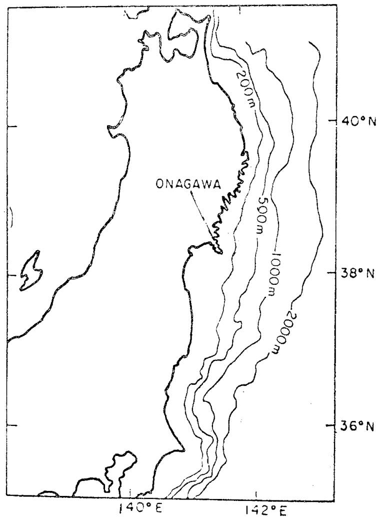

Fig. 1. Bottom topography off Northeastern Districts of Japan.

* 1973年12月13日受理
** 東京大学海洋研究所　東京都中野区南台 1-15-1
Ocean Research Institute, University of Tokyo, Minamidai, Nakano-ku, Tokyo, 164 Japan

岸に沿って伝わり海岸からの距離が遠ざかるにつれて減衰するような一種の長波が存在することを理論的に見いだした (LAMB[1] 参照)。更に，MUNK, SNODGRASS ら[2)3)4)] は，大陸棚に沿ってハリケーンが通過するとき観測した分散性の波についてその可能性を指摘し，ついで理論的に大陸棚上の長周期波に二つのモードすなわち，捕捉モード (trapped mode)と漏洩モード (leaky mode)とがあることを見いだし，その理論的研究結果に照らしてカリフォルニア沖の大陸棚上で観測された水位変動のエネルギーの大部分が，捕捉モードの長周期波に基づくものであることを示した。また，LARSEN[5] は，陸棚上の長周期波の理論を地球の自転を考慮に入れた場合へと発展させた。1966年 AIDA[6] は，MUNK らによる理論的研究結果を用い，宮城江の島付近の海底地形を考慮に入れて，捕捉モードと漏洩モードの長周期波の周波数特性，更に漏洩モードの長周期波については振幅特性を計算した。その結果，東大地震研究所江の島津波観測所の長波記録から求めたスペクトルと，計算に基づいて推定した海面振動スペクトルとが極めて良く一致することを見いだした。

著者らは，宮城江の島付近の大陸棚上で，流速・水温の同時測定を行い，同時にとられた東大地震研究所江の島津波観測所の水位記録と合わせて解析した。今までの観測と異なり，この観測では，水位観測等に比べて困難な流速測定を行ったので波による水粒子の運動の方向，ひいては伝播の方向を知ることができ，水位記録には現われない内部モードの波についても合せて調べることができた。流速や水位と共に水温測定を同時に行ったのは，内部モードと表面モードの波の区分けに利用するためである。

2. 観 測

1967年7月17日から19日にかけて，三陸女川湾沖江の島より約 0.9 km の水深 50 m 地点 (38° 24.3′N, 141°35.8′E, Fig. 2) に碇置された淡青丸より 20 m 層における水平二方向の流速，表面・10 m・20 m 層の水温の測定を行った。この期間風はほとんどなく，海はないでいたため船の動揺（ローリング，ピッチング周期約6秒）はほとんどなかったので，船からつるされた流速計（固有振動の周期約10秒）もほとんど揺れ動かなかった。流速測定には超音波式流速計が，水温測定には表面水温計及び2台の電気式 BT が用いられた。流速のデータについては，ある直交する二方向成分とその方向の方位がディジタル形式で得られ，10秒間の平均値が 12.5秒ごとに紙テープに記録された。又，水温のデータは各層共アナログ形式で得られ，チャート上に連続記録された。

3. 解 析

1. 流速変化と水位変化

この研究に用いられた流速データは，記録1（7月17日，16時～18日2時）と記録2（18日，17

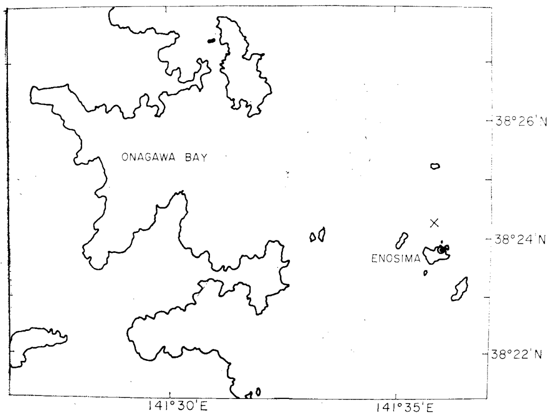

Fig. 2. Location of measurements.

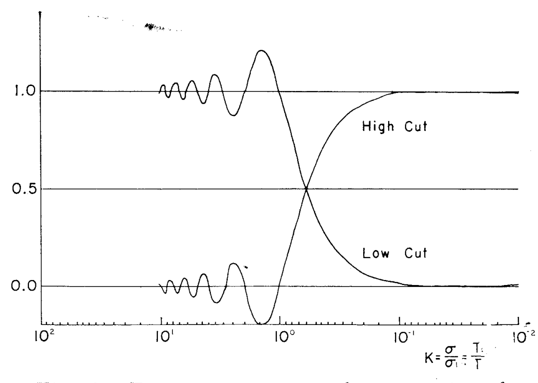

Fig. 3. Frequency-response characteristics of running averaging used in preliminary data processing.

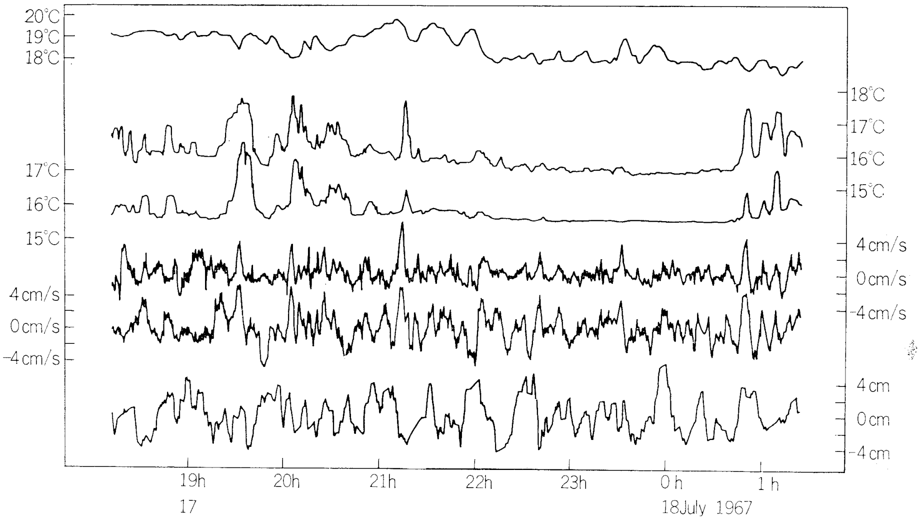

Fig. 4. Records used (1). From the top, water temperatures at the surface, 10 m depth, 20 m depth, velocity components in the east-west and north-south directions and sea level, respectively.

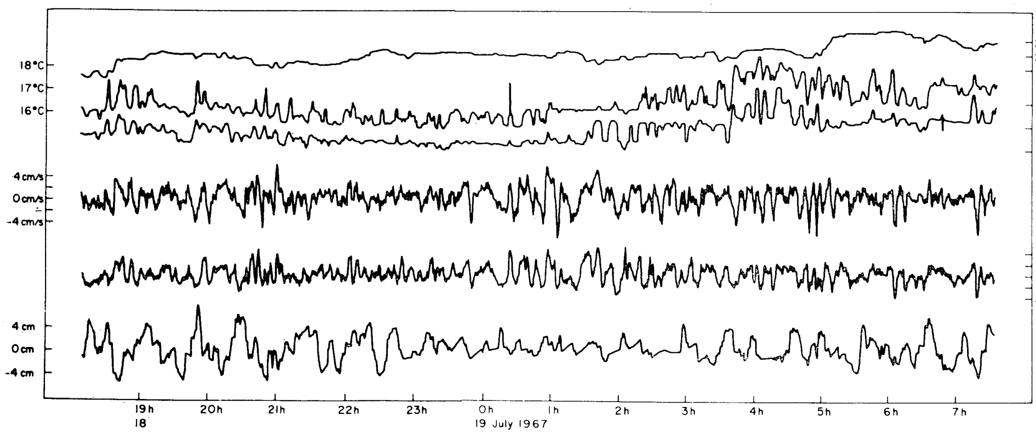

Fig. 5. Records used (2). From the top, water temperatures at the surface, 10 m depth, 20 m depth, velocity components in the east-west and north-south directions and sea level, respectively.

時37分～19日8時1分）である。見かけ上の変動成分を除くために，これらのデータは 12.5秒×3＝37.5秒にわたる移動平均[7)8)]を掛け，更に研究の目的に沿わない定常流及び30分以上の周期の変動を除くために60分にわたる移動平均を掛け，60分の移動平均を掛ける前のデータから差引いた。これらの移動平均の周波数特性を示すため Fig. 3 に，移動平均時間 T_1 でノーマライズした高周波周波域ろ波及び低周波域ろ波フィルターの特性を目盛ってある。水温データは，表層については 37.5秒ごと，10 m・20 m 層についてはそれぞれ 25秒ごとに読取られ再び目盛られた。

江の島津波観測所の水位データは25秒ごとに読取られ，流速データの処理と同様に30分以上の周期成分を除くため，30分にわたる移動平均に掛けられた。以上の処理を行った結果は Fig. 4（記録1）及び Fig. 5（記録2）に示されている。流速記録は比較的規則正しい変化を含んでおり，それら

の周期は10分前後である。流速の東西・南北成分にはかなりよい対応がみられ，それらの振幅は両成分共約 2 cm/s であって 4 cm/s を超えることは少ない。水位記録は30分程度の周期の大きな振幅をもつ変化を含んでおり，それに10分前後の周期をもつ振幅の小さい変化が重畳されている。水温記録は，表面では変化が少なく，記録1では 17°C～20°C, 記録2では 18°C～20°C の間で，なだらかにゆっくりと変化しているのみである。これは表層では混合により海水が均質に近い状態にあるためと考えられる。10 m層・20 m 層では，互に極めてよい相関をもつ周期8分程度，振幅 1.5°C から 2°C の変化がみられる。

これらの変化の性質やそれらの間の関係を調べるため，stationary random に近い変化をしている流速及び水位についてスペクトル解析を行った。Fig. 6, Fig. 7 はそれぞれ記録1，記録2の流速変化のスペクトルを Tukey の方法で求めたものである[9)10)]。この場合，自由度はそれぞれ 16.1, 28.6 であった。Fig. 6 にみられるとおり，記録1では南北成分には，11.6分・7分・5.4分・3.8分・3.2分周期にスペクトルピークがあり，東西成分には，10.4分・5.4分・3.1分周期にスペクトルピークがある。すなわち，両成分にほぼ共通した周期にスペクトルピークが見られる。記録2では，東西及び南北成分で互にスペクトルピークの現われる周期が僅かずつ異なる。すなわち，東西成分では，7.5 分周期にスペクトルピークがあり，南北成分では，12.5分・7分・5.4 分周期に顕著なスペクトルピークがある。

Fig. 8, Fig. 9 に江の島における水位のスペクトルを示してある。記録1に対応する Fig. 8 では，スペクトルピークは 11.9分・5.6分・3分周期に，記録2に対応する Fig. 9 では，12.2分・5.5 分周期にスペクトルピークがみられる。これらの周期は，流速変化の場合の周期とかなりよく一致する。このことから，記録1における約 12 分・5.5分・3分周期の変化及び記録2における約12分・5.5 分の変化は表面モードの長波によるものと考えられる。

2.　流速変化と水温変化

水温変化は一般に，流速変化や水位の変化程定常的でなく過渡的性格を持つように思われる。そこで，水温変化と流速変化との対比は次の方法で行われた。Fig. 10, Fig. 11 に見られるように，記録1，記録2を，主として同層の水温変化の周期と振幅の対応を考慮して Fig. 10, Fig. 11 におけるようにいくつかの期間に区分けした。

記録1では，18日0時45分より1時30分までの期間水温変化と流速変化は極めてよい相関を示し，変化のピーク数より概算した周期はそれぞれ10分である。17日18時10分より21時30分の期間は，水温変化の大きいところ（↓印で示されている）は短時間の間流速との相関はよいが全体的にはよくない。

記録2では，水温変化と流速変化との相関が極めてよいのは，領域 1・2・3・4・6・8・9 であり，周期はそれぞれ 10.6分・9.7分・約11分・10.1分・7.7分・10.1分・7.1分である。領域2・5は水位変化と流速変化の相関は悪く，概算した流速変化の周期は約13分で，振幅は 4 cm/s と大きい。更に，記録1，記録2に共通してみられることは，約12分より13分の周期の変化は水温・流速間の相関は悪く，約7分から10分の周期の変化は水温・流速間の相関はよく，その期間の流速変化の振幅は一般に大きく 4 cm/s である。これは，表面モードに内部モードの波が重畳して流速変化に現われたものと考えられる。

3.　流速の方向特性及び long-crestedness

各瞬間ごとの方向の頻度分布を以下の方法で求めた。流速の東西・南北成分を，それぞれ u, v とし，その各瞬間における値を u_i, v_i とする。更に反時計回りを正の角度とすると，その方向 θ_i は

$$\theta_i=\tan^{-1}\frac{v_i}{u_i}$$

である。

流速の大きさ V_i は

$$V_i^2=u_i^2+v_i^2$$

で求まる。

ΣV_i^2: $\alpha\Sigma\leqq\theta_i<\alpha+15°$ をみたす θ_i に対応する V_i の和

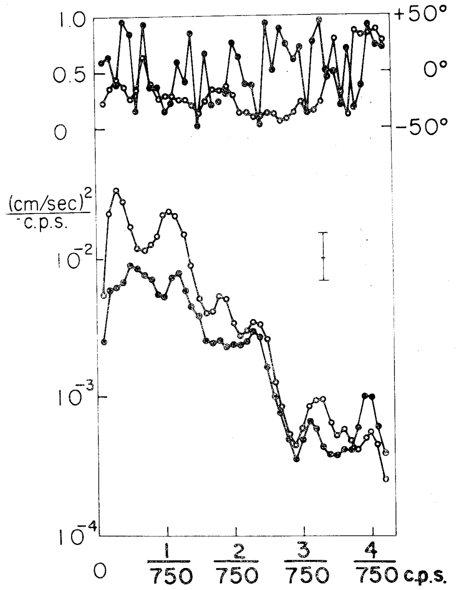

Fig. 6. Results of spectral analysis of velocity components in Records 1. Lower panel; spectral densities of east-west component (illustrated with black circles) and north-south one (illustrated with open circles). Upper panel; long-crestedness (illustrated with black circles) and phase shift (illustrated with open circles) between the two components. A positive phase shift means a lead of east-west component to north-south one.

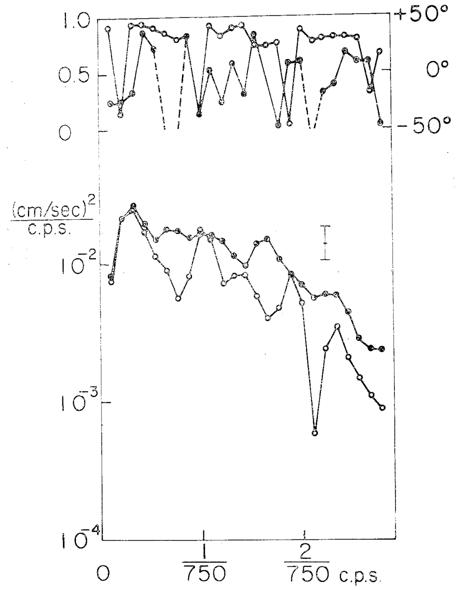

Fig. 7. Results of spectral analysis of velocity components in Records 2. Lower panel; spectral densities of east-west component (illustrated with black circles) and north-south one (illustrated with open circles). Upper panel; long-crestedness (illustrated with black circles) and phase shift (illustrated with open circles) between the two components. A positive phase shift means a lead of east-west component to north-south one.

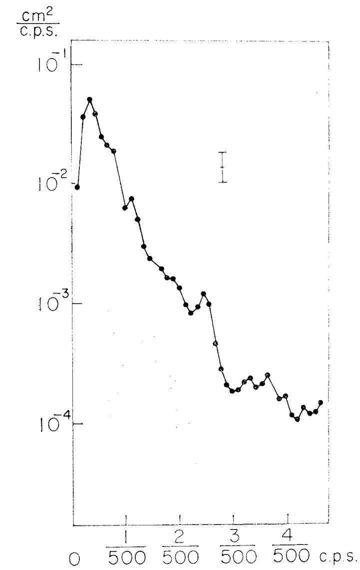

Fig. 8. Spectral density of sea level in Records 1.

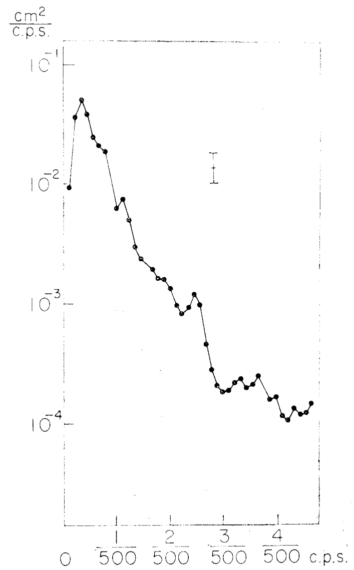

Fig. 9. Spectral density of sea level in Records 2.

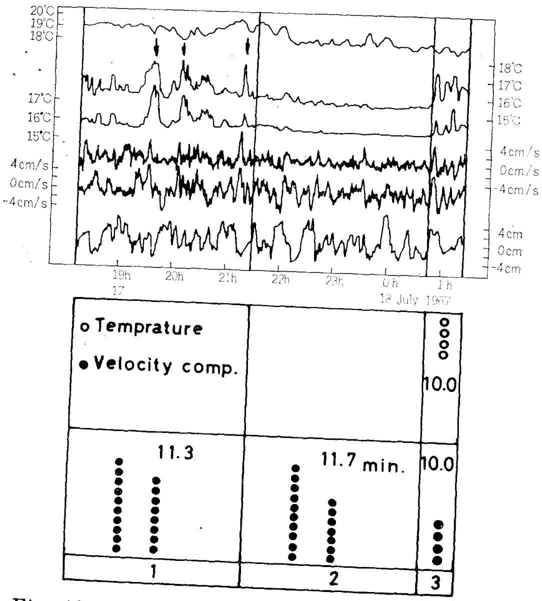

Fig. 10. Comparison-by-eye of velocity records to temperature records (Records 1.). Records were divided into three parts (1, 2 and 3 as illustrated) by considering characteristics of variation of records. Coherent wave peaks of those records are counted and the numbers are illustrated by open circles (temperature) and black circles (velocity). On taking into consideration the corresponding length of records, periods of variations are roughly estimated as indicated in the figure.

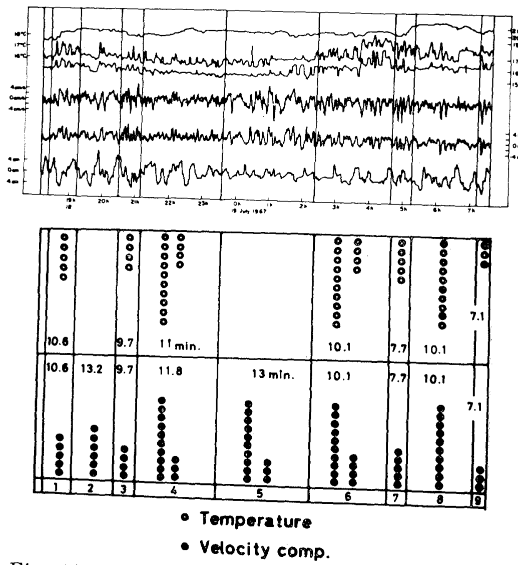

Fig. 11. Comparison-by-eye of velocity records to temperature records (Records 1.). Records were divided into nine parts (1, 2, . . . and 9 as illustrated) by considering characteristics of variation of records. Coherent wave peaks of those records are counted and the numbers are illustrated by open circles (temperature) and black circles (velocity). On taking into consideration the corresponding length of records, periods of variations are roughly estimated as indicated in the figure.

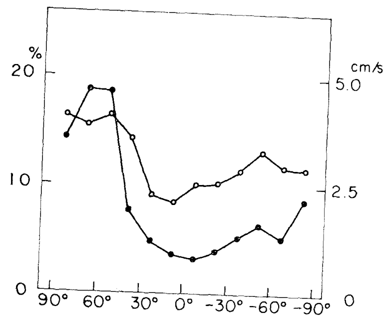

Fig. 12. Frequency distribution of wave direction (black circles) and magnitude of water-particle velocity (open circles) estimated from instantaneous records of east-west and north-south components.

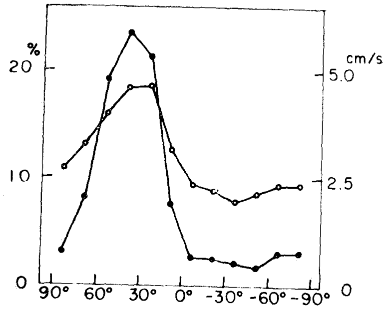

Fig. 13. Frequency distribution of wave direction (black circles) and magnitude of water-particle velocity (open circles) estimated from instantaneous records of east-west and north-south components.

$\sum^{N} V_i : 0° \leqq \theta_i < 360°$ をみたす θ_i に対応する V_i の和

とすると重みをつけた頻度（15° 範囲ごとに区分けした）は

$$\frac{\sum V_i}{\sum^{N} U_i} \times 100\ (\%)$$

で表わされる。

また，$\alpha \leqq \theta_i < \alpha + 15°$ をみたす θ_i に対応する V_i の和の平均 $\bar{V}$ は θ_i の個数を n とすると

$$\bar{V} = \frac{\sum V_i}{n}$$

である。この方法で求めた流速の方向の頻度分布を Fig. 12（記録 1）及び Fig. 13（記録 2）に示した。記録 1 では 45°～75° の方向に振動が集中し，その振幅も僅かに他の方向の振幅より大きいことがわかる。また，Fig. 13 をみると 15°～45° の方向の頻度が大きく，その方向の振動の振幅も記録 1 と異なりかなり大きいのが見られる。このことは，時間により島の間を抜けるような流れがあることから，流速変化が定常流に影響されていること，すなわち，地形が大きく作用していると推定される。

次に各周波数ごとの統計的方向特性及び long-crestedness[11] を求める。各周波数ごとの流速成分の主方向を $\theta(f)$, long-crestedness を $r^{-1}(f)$ とすると，

$$\theta(f) = \frac{1}{2} \tan^{-1} \frac{2M_{11}}{M_{20} - M_{02}}$$

$$\lambda^2(f) = \frac{M_{20} + M_{02} - \sqrt{(M_{20} - M_{02})^2 + 4M_{11}}}{M_{20} + M_{02} + \sqrt{(M_{20} - M_{02})^2 + 4M_{11}}}$$

で定義される。

ここで，

$$M_{20}(f) = 2\int_{-\infty}^{\infty} R_u(\tau) \cos 2\pi f \tau d\tau$$

$$M_{11}(f) = 2\int_{-\infty}^{\infty} R_{uv}(\tau) \cos 2\pi f \tau d\tau$$

$$M_{02}(f) = 2\int_{-\infty}^{\infty} R_v(\tau) \cos 2\pi f \tau d\tau$$

で，M_{20}, M_{02}, M_{11} はそれぞれ流速の東西・南北成分 u, v から求めたスペクトル密度及びクロススペクトル密度である。実際には，データが有限であることから Tukey の方法を用いて M_{20}, M_{11}, M_{02} を求めてある。上記の方法で求めた主方向及び long-crestedness を Fig. 6（記録 1）及び Fig. 7（記録 2）に流速変動のスペクトルと一緒に示した。Fig. 6 をみると，流速変化にみられる 11.6 分・7 分・5.4 分・4 分・3.1分の卓越周期に対する方向は，−22°・−18°・−40°・33° であり，long-crestedness は，γ が 0.16, 0.24, 0.38, 0.14 であることから，それらの周期の波は峰線の長いことがわかる。

Fig. 7 においては，流速変化の卓越周期 12.5 分，7.5分，7 分，5.4 分に対して方向及び γ はそれぞれ，−35°, 24°, −46°, 30°, 0.18, 0.43, 0.58 である。

周波数ごとにみた統計的方向特性及び long-crestedness は，記録 1，記録 2 における周期 12 分前後でかなりよく一致している。この 12分前後の周期の波の方向は，Fig. 1, Fig. 2 からほぼ岸及び陸棚に直角であることがわかる。

4. まとめ

宮城江の島より約 0.9 km の地点（水深 50 m）での 20 m 層における水平二方向の流速測定，表面・10 m・20 m 層での同時水温測定が行われ，流速記録はスペクトル解析された。また，流速記録から波の方向特性及び long-crestedness が求められた。流速記録と水温記録とは目視により比較検討された。一方，東京大学地震研究所江の島津波観測所でとられた水位記録がスペクトル解析された。

以上の結果

1) 約 12 分・5.5 分・3 分周期の波は表面モードの長波である。
2) 約 12分周期の波の方向は，ほぼ岸及び陸棚に直角で峰線も長いことから漏洩の長波であり，5.5 分・3 分周期の波は局地的な地形に結びついたセイシュである。
3) 約 7 分から約 10分周期の波は，内部モードの

波であることが推測される。更に，この観測・研究から，十数分周期以下の波の測定には，水圧測定より超音波による流速測定がより効果的であることが期待される。

観測の行われた女川湾沖は，数分から数十分周期の長波の研究に江の島水位記録が有効に利用できる地点であった。しかしながらこの研究においては，流速に及ぼす内部モードの波と表面モードの波の区別にはっきりとした確証を得られなかった。また，海岸地形の複雑さ，特に観測地点付近は，平島・江の島・足島・笠貝島に近く，対象とされた周期の波に大きな影響を及ぼしていると思われる。この二つの理由から今後，流速・水温及び水位の同時記録の得やすい女川湾沖の観測・研究，更には大陸棚上と大陸斜面上及びその沖の深海での同時測定が必要である。更にまた，海岸・海底地形の単純な仙台沖での観測・研究が望まれる。

謝　辞

数多くの助言を頂いた東京大学地球物理教室の吉田教授，永田助教授，東京大学地震研究所の相田講師に心からの謝意を表します。なお，この観測は，淡青丸の KT-67-13 次研究航海において行われたものであります。同船の乗組員及び同観測に参加されたわれわれ以外の研究者に感謝します。

文　献

1) LAMB, H. (1930): Hydrodynamics. Cambridge Univ. Press, 738 pp.
2) MUNK, W. H., F. E. SNODGRASS and G. F. CAKRIER (1956): Edge waves on the continental shelf. Science, January 23, **123**, 127-131.
3) MUNK, W. H., F. E. SNODGRASS and G. R. MILLEK (1962): Long-period waves over California's Continental Borderland, Part III. Background Spectra. J. Mar. Res., **20**, 119-120.
4) MUNK, W. H., F. E. SNODGRASS and F. GIBERT (1964): Long waves on the continental shelf: an experiment to separate trapped and leaky modes. J. Fluid Mech., **20**, 529-554.
5) LARSEN, J. C. (1969): Long waves along a single-step topography in a semi-infinite uniformly rotating ocean. J. Mar. Res., **27**(1), 1-6.
6) AIDA, I. (1967): Water level oscillations on the continental shelf in the vicinity of Miyagi-Enoshima. Bull. Earthquake Res. Inst., **45**, 61-78.
7) 堀川　明 (196): ランダム変動の解析．共立出版，218 pp,
8) GROVES, G. (1955): Numerical filters for discrimination against tidal periodicities. A.G.T.U,, **36**, 1073-1084.
9) BENDAT, J. S. and A. G. PIERSOL (1966): Measurement and Analysis of Random Data. John Wiley & Sons, Inc., New York. 390 pp.
10) MUNK, W. H., F. E. SNODGRASS and M. J TUCKER (1959): Spectra of low-frequency ocean waves. Bull. Scrips Inst. Oceanography, **7**(4), 283-362.
11) NAGATA, Y. (1964): The statistical properties of orbital waves motion and thier application for the measurement of directional wave spectra. J. Oceanog. Soc. Japan, **19**(4), 169-181.

La mer (Bulletin de la Société franco-japonaise d'océanographie)
Tome 12, N° 1, pp. 9 à 15. Février 1974

Decomposition of Particulate Organic Materials in Tokyo Bay at Summer Stagnation Period in 1972*

Humitake SEKI,** Hideo SHINOYAMA,*** Makoto MUTO***
and Haruo NUMANOI***

Abstract: Studies on some organic composition of particles with microorganisms in the water column of Tokyo Bay show that sedimentation of the particles is much faster than complete decomposition of easily decomposable organic particles before their arrival at the bottom of the sea during summer stagnation period.

1. Introduction

The natural environment of Tokyo Bay is now seriously destroyed partly due to the eutrophication as to form microaerobic zone in the region of the coastal water in the inner part of the bay during summer (TSUJI *et al.*, 1974). Contribution of herbivorous zooplankton to the formation of the microaerobic zone in the bottom layer was shown to be very important through the process of their production of phytodetritus and fecal pellets by repeated production, or multiple crops, of phytoplankton in a red tide at the summer stagnation period in the surface layer of the sea (SEKI *et al.*, 1974).

The present work forms a part of this series of investigations on the mechanism of formation and destruction of microaerobic watermass at the bottom layer of Tokyo Bay, with special reference to the dynamics of some particulate organic materials and the distribution of microorganisms utilizing these substrates.

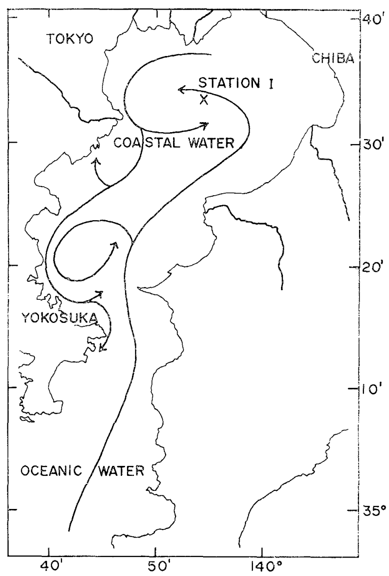

Fig. 1. Station location and general hydrography in Tokyo Bay. Station 1 (35°31.6′N, 139°53.9′E), depth; approximately 20 m.

2. Materials and methods

Hydrographic observations and water sampling were made from August 9 to October 17 in 1972 at Station 1 (Fig. 1). Seawater samples were collected with Van Dorn samplers which had been washed carefully with hydrochloric acid.

Water temperature was determined with a Toho Dentan ET-5 thermometer, salinity by an Auto Lab 601 MK III salinometer, dissolved oxygen by Winkler method, pH by a Toa pH meter DM-1A, redox potential by a Toa redox meter RM-1, light intensity by a Toshiba No. 9 submarine photometer, and microbial respiration in seawater by the method described in TSUJI *et al.* (1974).

---

* Received December 15, 1973
** Ocean Research Institute, University of Tokyo, Minami-dai, Nakano-ku, Tokyo, 164 Japan
*** School of Education, Waseda University, Totsukamachi, Shinjuku-ku, Tokyo, 160 Japan

Particulate matter was collected onto Whatman type C glass fiber filter. The organic carbon and nitrogen were determined by a Yanagimoto CHN analyzer. Carbohydrates, crude fiber (analyzed chiefly as cellulose by the method employed here) and chitin were measured by the methods of STRICKLAND and PARSONS (1968).

Total number of bacteria was directly counted in a bacterial counting chamber (Erma, Japan) under a phase contrast microscope. The number of aerobic heterotrophic bacteria, anaerobic heterotrophic bacteria, cellulose decomposing bacteria and chitin decomposing bacteria were estimated by the plate count method with the following media:

Medium 2216 (ZOBELL, 1941) for aerobic heterotrophic bacteria
- Peptone: 5 g
- Agar: 15 g
- Aged seawater: 1,000 ml
- pH adjusted to 7.8.

Medium for anaerobic heterotrophic bacteria
- Peptone: 5 g
- Sodium thioglycolate: 2 g
- Agar: 15 g
- Aged seawater: 1,000 ml
- pH adjusted to 7.8.

Medium for cellulose decomposing bacteria
- Cellulose powder (Wako): 10 g
- Peptone: 0.1 g
- Agar: 15 g
- Aged seawater: 1,000 ml
- pH adjusted to 7.8.

Medium for chitinoclastic bacteria (SEKI, 1965)
- Chitin particles: 60 ml (wet)
- Peptone: 0.1 g
- Agar: 15 g
- Aged seawater: 1,000 ml
- pH adjusted to 7.8.

3. Results

1. Stratification of watermasses

Watermasses were completely stratified during

Table 1. Distribution of dissolved oxygen in the sea of Tokyo Bay (Station 1). g/m^3 (%)

Sampling depth (m)	August 9	August 31	September 13	September 25	October 17
0	10.7356(154)	12.4489(182)	11.4539(165)	6.7976(92)	7.3562(98)
2	10.5287(148)	12.0300(176)	11.5920(166)	6.7548(91)	7.3358(98)
4	5.1157(73)	9.5899(140)	8.3666(120)	6.3106(85)	6.7212(89)
6	4.4512(64)	7.7008(111)	6.5891(94)	5.3200(72)	6.2698(84)
8	4.1936(59)	6.1932(89)	3.8850(55)	4.2127(58)	6.2569(84)
10	4.2764(61)	3.1752(45)	4.7201(66)	2.6438(36)	5.8535(78)
12	4.0210(57)	3.3021(46)	3.2442(45)	2.4547(34)	5.6269(75)
14	3.8069(54)	2.7291(37)	3.6165(50)	2.5157(34)	5.5040(73)
16	3.3277(47)	1.3716(19)	3.1557(43)	2.0868(29)	5.1736(69)
18	2.3877(33)	2.3860(32)			
20	1.9668(27)				

Table 2. Distribution of pH in the sea of Tokyo Bay (Station 1).

Sampling depth (m)	August 9	August 31	September 13	September 25	October 17
0	8.2	8.4	8.75	8.2	8.2
2	8.3	8.5	8.6	8.25	8.2
4	8.2	8.4	8.4	8.2	8.1
6	8.05	8.4	8.4	8.1	8.1
8	8.0	8.2	8.25	7.85	8.1
10	7.8	7.95	8.05	7.9	8.05
12	7.8	7.8	8.05	7.85	8.05
14	7.8	7.65	7.9	7.8	8.05
16	7.8	7.6	7.55	7.8	8.0
18	7.8	7.8	—	—	—
20	7.8	—	—	—	—

Table 3. Distribution of Eh (mV) in the sea of Tokyo Bay (Station 1).

Sampling depth (m)	August 9	August 31	September 13	September 25	October 17
0	380	350	360	365	418
2	390	353	360	365	423
4	380	338	340	365	418
6	385	343	336	388	413
8	380	328	328	375	413
10	360	350	328	365	413
12	360	352	328	375	408
14	360	333	348	368	408
16	360	343	348	368	388
18	360	372	—	—	—
20	360	—	—	—	—

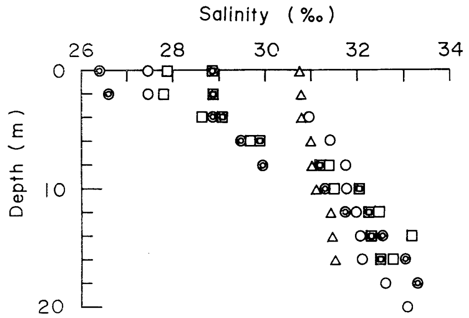

Fig. 2. Salinity of seawater column. ○: August 9, ◎: August 31, □: September 13, ⊡: September 25, △: October 17.

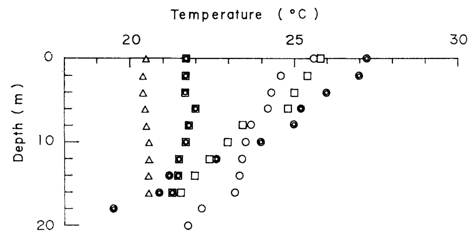

Fig. 3. Distribution of seawater temperature. Symbols are as in Fig. 2.

summer at Station 1 in a gyre of the coastal water in the inner part of the bay (Tables 1, 2 and 3) (Figs. 2 and 3), whereas transition from summer stagnation to fall overturn was observed from August 31 to October 17.

The surface watermass was strongly influenced by freshwater inflow from rivers into the bay during summer stagnation, which was shown by low salinity of the watermass (Fig. 2). The concentration of dissolved oxygen in the watermass was oversaturated (Table 1) because of active photosynthesis of phytoplankton in the red tide as observed simultaneously by SEKI *et al.* (1974).

The compensation depth of photosynthesis measured was approximately 4 m depth. As its depth corresponded to the boundary of the surface and intermediate watermasses, the compensation depth was exactly coincided with the critical depth for photosynthesis. As the photosynthesis of phytoplankton could be carried out only within the surface layer, considerable concentration of chlorophyll detected in the intermediate or bottom layer must have been belonging to phytoplankton in death phase of their growth or dead, because primary production cannot be expected there.

2. Microbial biomass

Distributions of total bacteria, aerobic heterotrophic bacteria, anaerobic heterotrophic bacteria, cellulose decomposing bacteria and chitinoclastic bacteria at the summer stagnation are

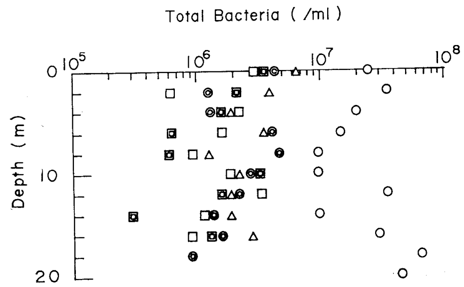

Fig. 4. Total bacteria in seawater. Symbols are as in Fig. 2.

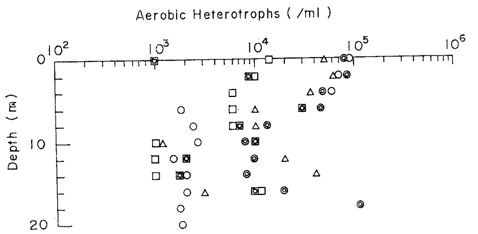

Fig. 5. Aerobic heterotrophic bacteria in seawater. Symbols are as in Fig. 2.

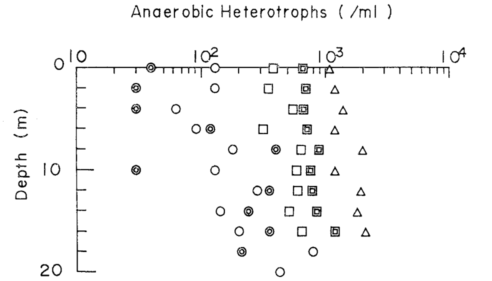

Fig. 6. Anaerobic heterotrophic bacteria in seawater. Symbols are as in Fig. 2.

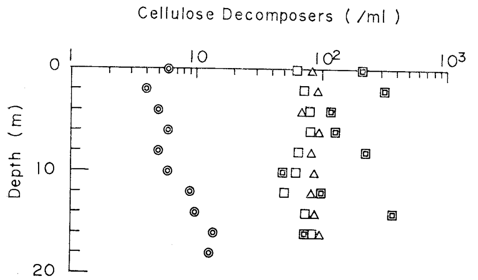

Fig. 7. Cellulose decomposing bacteria in seawater. Symbols are as in Fig. 2.

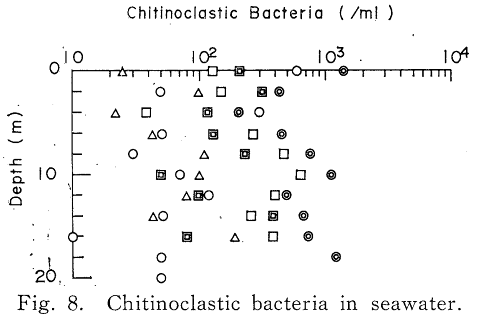

Fig. 8. Chitinoclastic bacteria in seawater. Symbols are as in Fig. 2.

shown in Figs. 4, 5, 6, 7 and 8. Population densities of these microbial groups were from 10 to 100 times higher than those at the pelagic region of oceans (*e.g.*, KRISS, 1963), which are good indications of the progress of eutrophication of Tokyo Bay.

The distribution of total bacteria showed the maxima densities at the surface and the bottom layers and the minimum density at the intermediate layer. Aerobic heterotrophs had the maximum density at the surface, whereas anaerobic heterotrophs distributed without having any particular maximum zone of their densities. Cellulose or chitin showed concentration in the water column without any specific relationship with the vertical distribution of a group of bacteria decomposing each substrate (Figs. 9 and 10).

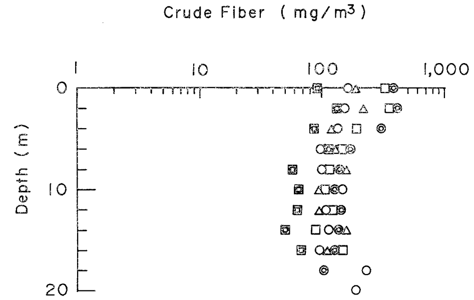

Fig. 9. Concentration of crude fiber in seawater Symbols are as in Fig. 2.

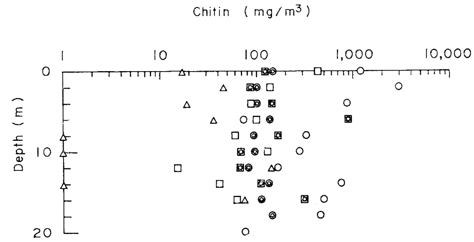

Fig. 10. Concentration of chitin in seawater. Symbols are as in Fig. 2.

3. Dynamics of some particulate carbohydrates

Vertical distributions of crude fiber, chitin, particulate carbohydrates and particulate organic carbon in the sea are shown in Figs. 9, 10, 11 and 12. At the stagnation period, concentra-

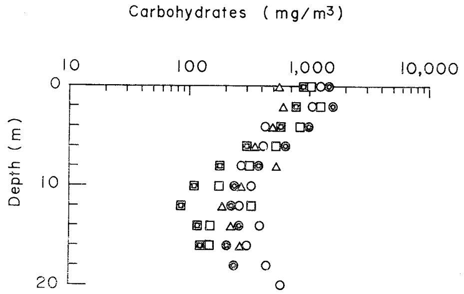

Fig. 11. Concentration of particulate carbohydrates in seawater. Symbols are as in Fig. 2.

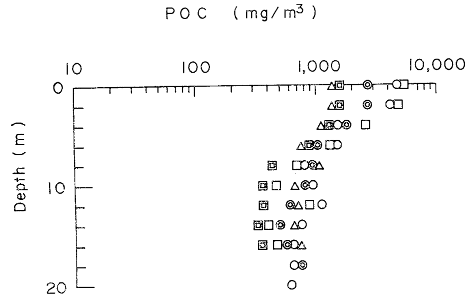

Fig. 12. Concentration of particulate organic carbon in seawater. Symbols are as in Fig. 2.

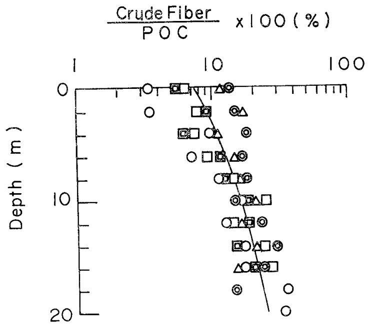

Fig. 13. Fraction of crude fiber in particulate organic carbon in seawater. Symbols are as in Fig. 2.

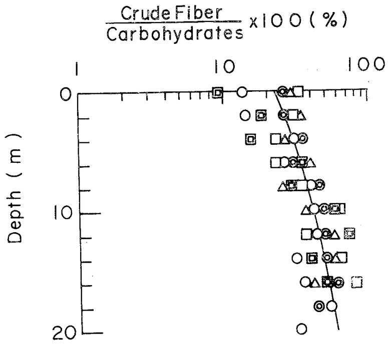

Fig. 14. Fraction of crude fiber in particulate carbohydrates in seawater. Symbols are as in Fig. 2.

tion of crude fiber showed the maximum at the surface layer and decreased with increasing depth. Chitin showed heterogeneous concentration probably as influenced by vertical migration of copepods. Copepods, such as *Oithona* sp. and *Acartia* sp., were predominantly observed with forming patchiness in the planktonic fauna, and about 5 % dry weight of these copepods have been analyzed to be chitin. The concentration of both carbohydrates and organic carbon were high at the surface layer, but low at the intermediate or bottom layer. On the other hand, vertical distribution became more homogeneously on October 17 when fall overturn was obviously observed.

The fraction of crude fiber in particulate organic carbon or in particulate carbohydrates was higher at increasing depth, and there was a significant linear relationship between them (Figs. 13 and 14), *i.e.*,

$$y=1.82x+22.38 \quad \text{or} \quad y=0.86x'+7.48$$

where y=depth (m), x=fraction of crude fiber in particulate carbohydrates, x'=fraction of crude fiber in particulate organic carbon. This result must indicate that crude fiber was decomposed by microorganisms slower than other organic materials in particles during its sedimentation throughout the water column where the sedimentation could not be influenced seriously by vertical mixing, because input of crude fiber at Tokyo Bay was expected chiefly from the surface layer through freshwater inflow and through production by phytoplankton (LEWIN, 1962). Moreover, easily decomposable organic materials must have remained still even in the bottom layer, because the rate of increase for the fraction of crude fiber in particulate carbohydrates or particulate organic carbon was constant during the sedimentation from the surface to the bottom of the sea.

There was no linear relationship between the depth of the sea and the fraction of chitin in particulate organic carbon or in particulate

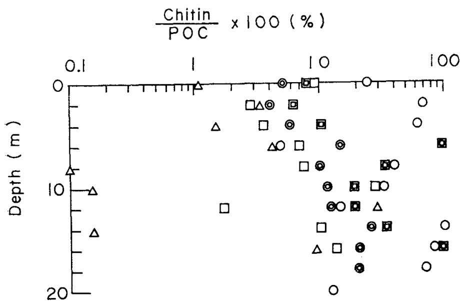

Fig. 15. Fraction of chitin in particulate organic carbon in seawater. Symbols are as in Fig. 2.

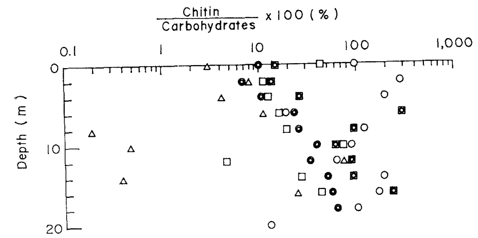

Fig. 16. Fraction of chitin in particulate carbohydrates in seawater. Symbols are as in Fig. 2.

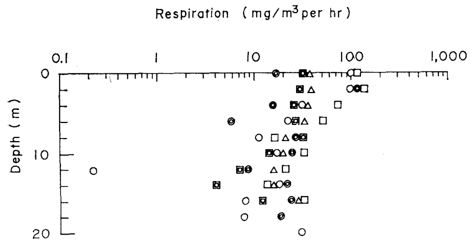

Fig. 17. Microbial respiration in seawater. Symbols are as in Fig. 2.

carbohydrates (Figs. 15 and 16). This might be greatly attributed to chitin being chiefly produced by living copepods which migrate vertically throughout the water column.

The rate of microbial respiration in seawater of the surface layer was not significantly higher than that of the intermediate or bottom layer (Fig. 17) although the biomasses of phytoplankton and zooplankton were significantly different at each watermass (SEKI *et al.*, 1974). This result supports the hypothesis of ZOBELL (1946) that marine microorganisms are chiefly responsible for the consumption of dissolved oxygen in the sea.

4. Discussion

This microbiological study has a good agreement with the former studies in biochemical investigation (TSUJI *et al.*, 1974) and in planktological investigation (SEKI *et al.*, 1974) that efficient transportation of organic matter produced in the surface layer to the bottom layer must be responsible for the formation of microaerobic or anaeobic watermass in the bottom layer of the inner part of Tokyo Bay, *i.e.*, particulate organic materials supplied from land or primary production at the surface layer of the sea are actively decomposed by microorganisms during sedimentation, but the rate of sedimentation is too fast for the complete decomposition of easily decomposable matter before the particles arrive at bottom of the sea. Accumulation of these easily decomposable organic materials in the bottom layer is very favorable for the rapid consumption of dissolved oxygen which induces low oxygen tension in the watermass with slow diffusion rate of dissolved oxygen from the surface layer.

Acknowledgments

This work was partly supported as a special project "Environment and Human Survival" by the Ministry of Education of Japan. This investigation was impossible but for the kind help of Fisheries Experimental Station of Chiba Prefecture.

References

KRISS, A. E. (1963): Marine Microbiology. Oliver & Boyd, London, 536 pp.

LEWIN, R. A. (ed) (1962): Physiology and Biochemistry of Algae. Academic Press, London, 938 pp.

SEKI, H. (1965): Microbiological studies on the decomposition of chitin in marine environment IX. J. Oceanog. Soc. Japan, **21**, 253-260.

SEKI, H., T. TSUJI and A. HATTORI (1974): Effect of zooplankton grazing on the formation of the anoxic layer in Tokyo Bay. Estuarine and Coastal Marine Science, **2**. (in press)

STRICKLAND, J. D. H. and T. R. PARSONS (1968): A practical handbook of seawater analysis. Bulletin

No. 169, Fisheries Research Board of Canada, 311 pp.
TSUJI, T., H. SEKI and A. HATTORI (1974): Results of red tide formation in Tokyo Bay. J. Water Pollution Control Federation, **46**, 165-172.
ZOBELL, C. E. (1941): Studies on marine bacteria I. J. Marine Res., **4**, 42-75.
ZOBELL, C. E. (1946): Marine Microbiology. Chronica Botanica, Waltham, Mass., 240 pp.

夏季停滞期の東京湾における懸濁態有機物の分解

関　文威　篠山秀夫
武藤　誠　沼野井春雄

要旨: 現在，東京湾は都市廃水並びに工場廃水の影響を受けて，富栄養化が著しく進行している。殊に夏季の湾奥部で水塊の成層が認められ，停滞した底層水塊においては低酸素状態あるいは嫌気状態さえも観測されている。われわれは，東京湾におけるこのような嫌気底層水塊の生成機構を，海中に懸濁する有機物の動態と，それを分解する微生物の分布様式とから，主に数種の炭水化物を指標として調査・研究した。

観測点の中層や下層では，動植物プランクトンの現存量が表層に比べ少ないのと対照的に，微生物量並びに水中呼吸速度は表層とそれ程の相違がないことが判明した。

懸濁態有機物と炭水化物の濃度は，ともに表層水塊中で極めて高いが，中層から底層では低いことが判明した。また，キチンは深度に関係ない不均一な分布様式を示していた。この不均一性には，コペポーダの分布が大きく関与しているものと考えられる。比較的分解速度の遅い粗繊維が，懸濁態有機炭素と懸濁態炭水化物中を占める割合は，表層より底層に向って直線的な増加の傾向にあった。すなわち，海底までの沈降中，懸濁懸有機物を占める粗繊維部分の増加率が一定であることは，海底直上層においても分解速度の比較的速い有機物が相当量残留していることを示していることにほかならない。従って，表層からの低い酸素供給速度よりも速い酸素消費を伴う有機物分解が底層水塊中において起こり，溶在酸素濃度が低下するものと解析された。

La mer (Bulletin de la Société franco-japonaise d'océanographie)
Tome 12, N° 1, pp. 16 à 19. Février 1974

Petroleumlytic Bacteria in Different Watermasses of the Pacific Ocean in January, 1973*

Humitake SEKI**, Toshisuke NAKAI** and Hirotaka OTOBE**

Abstract: The population densities of petroleumlytic bacteria were studied in seawater of watermasses with different levels of pollution in the Pacific Ocean in January, 1973. The population densities per liter of seawater were from 10^2 to 10^3 in the very polluted bay of Tokyo, from 10 to 10^2 in the coastal water of Japan and less than 50 in the western North Pacific central water. The density was a little higher in the southern region than in the northern region of the western North Pacific central water.

1. Introduction

It has been suggested that the population density of petroleumlytic microorganisms in seawater is dependent on the degree of petroleum pollution of the seawater and that the petroleumlytic microorganisms are only rarely found in the pelagic region of the ocean (*e.g.*, ZOBELL, 1969). SEKI (1973), however, found the petroleumlytic microorganisms to be a few per 100 ml of seawater from surface to 1,000 m depths even in the pelagic region of the Pacific Ocean, by concentrating microorganisms on a glass fiber and by incubating them on a silica gel medium for the enumeration of petroleumlytic microorganisms.

In this study, the relationship between the population density and the watermass of the Pacific Ocean was investigated and analyzed aboard the research vessel *Hakuho-maru* of the University of Tokyo during Leg KH-73-1 expedition in winter of 1973 (HATTORI (ed.), 1974).

2. Materials and methods

The petroleumlytic microorganisms were enumerated by the method of SEKI (1973), as a viable count using a silica gel medium.

Particulate matter was filtered onto a Gelman glass fiber type A (pore size: 0.3 μ), and organic carbon of the dried samples were determined by Yanagimoto MT-1 CHN analyzer.

The sampling stations at the centers of gyres in the inner part (35° 31.6′ N, 139° 53.9′ E) and in the central part (35° 18.1′ N, 139° 44.2′ E) of Tokyo Bay as well as the coastal water of Japan (35° 08.5′ N, 139° 44.2′ E) were selected based on the report by HATTORI *et al.* (1973).

The determination of watermasses in the western North Pacific central water was made chiefly by the analysis of T-S diagrams and dynamic computation for geostrophic currents, based on the data of the routine oceanographic observations (HATTORI (ed.), 1974).

3. Results

The results of dynamic computation for geostrophic currents along the line of 140° E in the western North Pacific central water (Fig. 1) show the existence of the subtropical counter current (YOSHIDA and KIDOKORO, 1967) between Station 2 and Station 3 at the observation (Fig. 2). The eastward current had the speed of approximately 20 cm per second. On the other hand, the westward currents were observed at Stations 4, 5, 7 and 9. The T-S diagram (Fig. 3) shows that each water of the mixing layer at Stations 1, 2 and 3 or at Stations 4, 5, 7 and 9 has the same characteristics respectively but is a little different each other, *i.e.*, lower seawater temperature with lower salinity at the northern water and higher seawater temperature with higher salinity at the

* Received December 15, 1973
** Ocean Research Institue, University of Tokyo, Minamidai, Nakano-ku, Tokyo, 164 Japan

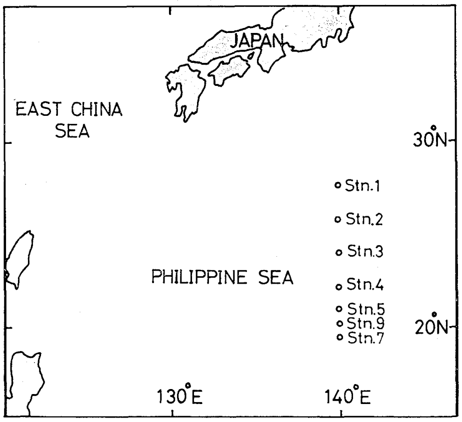

Fig. 1. Station locations in the western North Pacific central water.

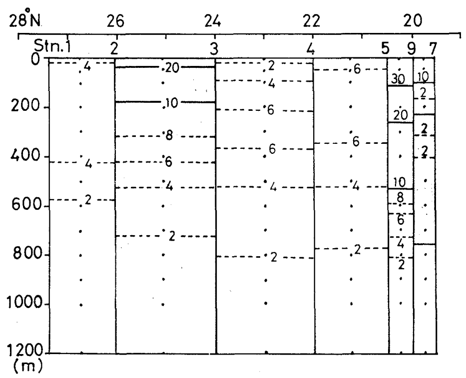

Fig. 2. Zonal geostrophic speed (cm/sec) along 140°E. Dark area: eastward current. Light area: westward current.

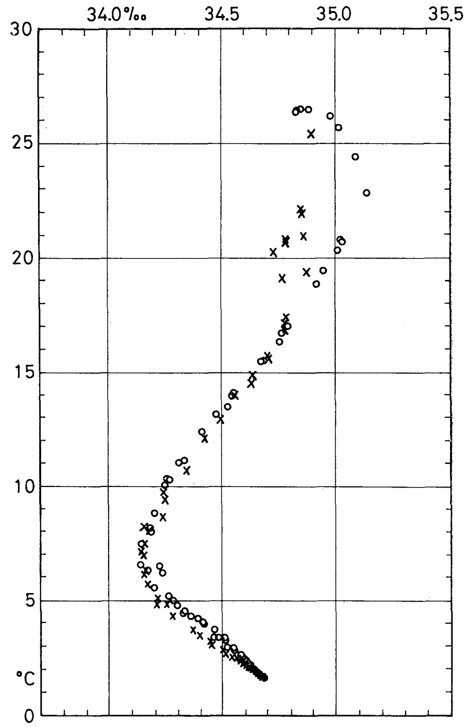

Fig. 3. T-S diagram at the northern region (Stations 1, 2 and 3) (×) and at the southern region (Stations 4, 5, 7 and 9) (○).

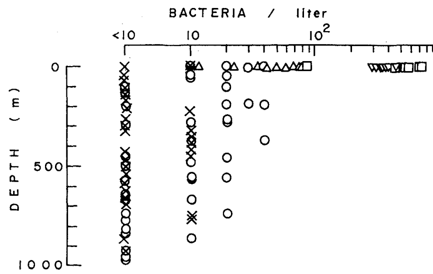

Fig. 4. Population density of petroleumlytic bacteria in each watermass.

□: gyre in the inner part of Tokyo Bay
▽: gyre in the central part of Tokyo Bay
△: the coastal region off Kurihama
○: the southern region of the western North Pacific central water
×: the northern region of the western North Pacific central water

southern water. On the other hand, the watermasses in each deeper layer at every station are little different each other.

The distribution of petroleumlytic bacteria in each water of the very polluted gyre in the inner part of Tokyo Bay, of the polluted gyre in the central part of Tokyo Bay, of the coastal region off Tokyo Bay (TSUJI *et al.*, 1974), and two different water types in the western North Pacific central water was shown in Fig. 4 by using different symbols. The population densities of petroleumlytic bacteria per liter of seawater were from 10^2 to 10^3 in the polluted bay of Tokyo, from 10 to 10^2 in the coastal water of Japan and less than 50 in the western North Pacific central water. The bacterial density in the inner part of Tokyo Bay was the greatest, and the density was lowest in the northern region of the western North Pacific central water. These population densities at different watermasses were approximately in the order of the polluted degrees of watermasses, *i. e.*, particulate organic carbon in seawater was 720 to 1,500 mg/m³ (sample number: 5) in the gyre of the inner part of Tokyo Bay, 550 to 860 mg/m³ (sample number: 5) in the central gyre of Tokyo Bay, 83 to 145 mg/m³ (sample number: 5) in the coastal water and 38 to 62 mg/m³ (sample number: 8) in the western North Pacific central water.

Although there were no difference on the eutrophication indices, such as population densities of total bacteria and heterotrophic bacteria, particulate organic carbon concentration, microbial assimilation of organic matter, etc. for each watermass of the northern and southern regions in the western North Pacific central water (SEKI *et al.*, 1974), petroleumlytic bacteria were a little numerous in the southern region (usually 10–50/*l*) than in the northern region (usually less than 10/*l*). Assuming that the population density of petroleumlytic microorganisms is dependent on the degree of petroleum pollution (ZOBELL, 1969), the southern region must have been more polluted by petroleum, and the petroleumlytic bacteria can be used as a very sensitive indicator for the detection of petroleum pollution. In this case, the baseline density of petroleumlytic microorganisms may be less than one per 100 m*l* of seawater in the watermasses of non-pollution by petroleum.

4. Discussion

The population density of petroleumlytic bacteria was measured in each watermass of the Pacific Ocean in winter of 1973 with special reference to the pollution degree. The densities were approximately in the order of the eutrophication degrees of watermasses as indicated by the concentration of particulate organic matter. To support strictly the hypothesis of ZOBELL that the population density of petroleumlytic microorganisms in seawater is dependent on the degree of petroleum pollution (ZOBELL, 1969), the density should be compared directly with the concentration of petroleum in seawater of each watermass. The degree of eutrophication of watermasses examined at the neritic region here, however, has been shown chiefly caused by the pollution of sewage and industrial wastes as indicated chiefly by the decomposition experiments of organic matter (TSUJI *et al.*, 1974). The organic matter in Tokyo Bay with higher concentrations had generally the higher refractory fractions against the microbial attack, many parts of which are believed to be composed of petroleum and its products discharged into the bay (HANDA, N., personal communication). On the other hand, at the pelagic region of the Pacific Ocean, petroleum discharge from ship, especially the dumping by tankers at the Kuroshio current and the western regions of the western North Pacific central water, must have been chiefly responsible for the petroleum pollution. The main oil movements by sea (*e. g.*, ZOBELL, 1964) indicates the heavier pollution of petroleum at the southern region than in the northern region of the central water. This might have been shown by the different population densities of petroleumlytic bacteria as the indicator species of the petroleum pollution at the two regions in the pelagic watermass.

Acknowledgments

This work was partly supported as special projects "Studies on the Petroleum Pollution of Marine Environments", "Environment and Human Survival" and "Studies on the Dynamic Status of Biosphere" by the Ministry of Education.

References

HATTORI, A. (ed.) (1974): Preliminary report of the *Hakuho-maru* cruise "KH-73-1". Ocean Research Institute, University of Tokyo. (in press)

HATTORI, A., H. SEKI and T. TSUJI (1973): Biochemical and microbiological studies on the eutrophication of Tokyo Bay. Environment and Human Survival. University of Tokyo Press, 67–76. (in Japanese)

SEKI, H. (1973): Silica gel medium for enumeration of petroleumlytic microorganisms in the marine environment. Appl. Microbiol., **26**, 318–320.

SEKI, H., T. NAKAI and H. OTOBE (1974): Turnover rate of dissolved materials in the Philippine Sea at winter of 1973. Arch. Hydrobiol., **73**, 238–244.

TSUJI, T., H. SEKI and A. HATTORI (1974): Results of red tide formation in Tokyo Bay. J. Water

Poll. Cont. Fed., **46**, 165-172.
YOSHIDA, K. and T. KIDOKORO (1967): A subtropical countercurrent in the north Pacific. J. Oceanog. Soc. Japan, **23**, 81-91.
ZOBELL, C. E. (1964): The occurrence, effect and fate of oil polluting the sea. Int. Conf. Water Pollut. Res., **3**, 85-118.
ZOBELL, C. E. (1969): Microbial modification of crude oil in the sea. Proc. API/FWPCA Conference on Prevention and Control of Oil Spills. American Petroleum Institute Publ. No. 4040, 371-326.

1973年1月の太平洋における石油分解菌分布と水塊

関　文威　中井俊介　乙部弘隆

要旨: 1973年1月における北太平洋の各水塊中に分布する石油分解菌密度は次の通りであった。水質汚濁の著しく進行している東京湾水では 10^2～$10^3/l$, 久里浜沖の沿岸水では 10～$10^2/l$, 西部北太平洋中央水の南環流中では 10～50/l 程度が普通に観測されたが, 北環流中ではほとんどの場合 10/l 以下しか検出されなかった。

La mer (Bulletin de la Société franco-japonaise d'océanographie)
Tome 12, N° 1, pp. 20 à 25. Février 1974

船尾方向からの水中超音波信号の伝達角限界について*

加　藤　増　夫**

On the Critical Transmissible Angle of Ultrasonic Wave Signals in Underwater

Masuo KATO

Abstract: It is considered that the ship on sailing in the future will have more chance to receive ultrasonic wave signals from astern remote point in underwater: such as to determine the position of the ship by the transponders which submerged at the sea bottom; to pursue efficient fishery using telemetering instruments, and so on.

We experimented on board to measure the distance of the ultrasonic wave signals to be received in vertical angle on the basis of sea surface.

The results are as follows: a critical angle, which is possible to transmit the ultrasonic wave signals to the vessel, was 3 to 5 degrees on 200 G/T survey and work vessel (engine: 350 PS×750 r.p.m., KAPLAN type nozzle-propeller with four blades operated by oil pressure: 2 sets), and the sea state was 1 to 2 class and the speed of vessel was 4 to 7 knots. The critical angle is comparatively small.

This can be utilized some other measurements on board.

1. 目　的

船の航走中において，その船で船尾方向からの遠隔水中超音波信号を受信することは，時として，はなはだむずかしくなることがある。これは，船の航走によって生起した水中気泡層が船尾方向に流れ広がってゆくからである。船の曳航体からの超音波信号を受けて水中情報の観測を行うことが今後ますますその機会を増すと考えられるので，この問題は一応 check しておく必要がある。

そこで，このたび，200 ton 型調査作業船（本州四国連絡橋公団所属“いつくしま”）に Sonar-Transponder を装備したので，これによって，船尾方向からの超音波信号が，海面を基準にした垂直角で，どのくらいの距離まで受信できるかについて海上観測を試みた。

2. 測定方法

この Sonar-Transponder 装置は，船の縦軸の前方から約 1/3 の位置に装備した送受波器から，船の後方はもとより，全方向にむけて発射された超音波信号を，海底に沈めた Transponder で受信し，その Transponder から折り返し異なった周波数の超音波信号を応答送信し，この信号を船の送受波器で受信するものである。

調査作業船の船体外形，及びこれに装備した送受波器は Fig. 1 に示すとおりである。

船の吃水は 2.5 m で，送受波器は船底から 0.3 m 突出させてある。Engine の最大伝達馬力（入力軸）は 350 PS×750 r.p.m. であり，かつ，推進器は油圧式の 4 翼 KAPLAN 型 Nozzle Propeller 2 基を使用している。

Sonar-Transponder の配置を Fig. 2 に，船に装備された機器の構成を Fig. 3 にそれぞれ示す。

* 1973 年 12 月 20 日受理
1973 年度日本水産学会春季大会において発表
** 古野電気株式会社東京支社　東京都中央区八重州 4-5, Furuno Electric Co., Ltd. Tokyo Branch, 5, 4-chōme, Yaesu, Chūō-ku, Tokyo, 104 Japan

船から送信する超音波周波数は 30 kHz で，Transponder からの応答信号周波数は，A: 37 kHz, B: 40 kHz, C: 43 kHz である。いずれも ring 状のチタン酸バリウム（$BaTiO_3$）振動子を用い，半球状の無指向性のものである。船の送波器振動子への電気入力は尖頭値 200 W であり，Transponder 応答超音波振動子への電気入力は尖頭値 50 W である。応答距離は，船尾方向以外ならば，2,000～3,000 m までは測定可能である。

測定に際しては，船は送・受信時とも，ある一定の速力で Transponder から正確かつ直線的に離れてゆく。この状態は航跡記録器によって確かめられた。このとき，船では Transponder からの応答信号を記録器の記録紙上に表示する。この記録紙上で，受信信号が認識しにくくなるまでの距離を読み取り，この値から伝達角限界を算定した。

3. 結　果

この測定方法によって，昭和47年10月25日，館山湾において，また同年11月30日，淡路島岩屋沖において，それぞれ海上実験を行った。そのとき

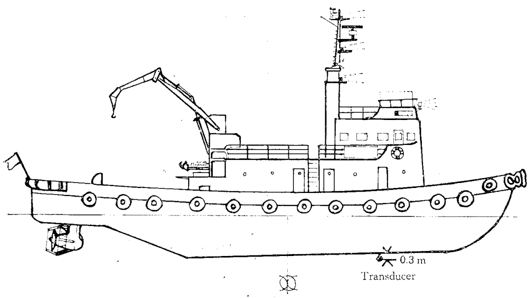

Fig. 1. General sketch of the vessel with installed transducer.

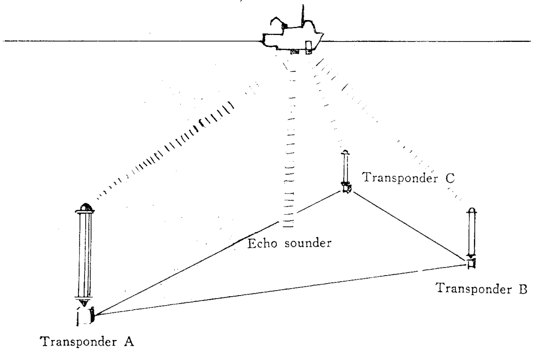

Fig. 2. Transducers arranged in Sonar-Transponder system.

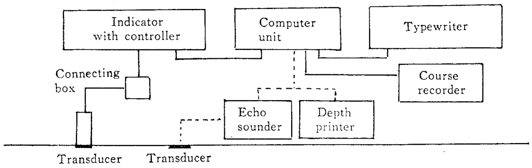

Fig. 3. Block diagram of Sonar-Transponder system on board.

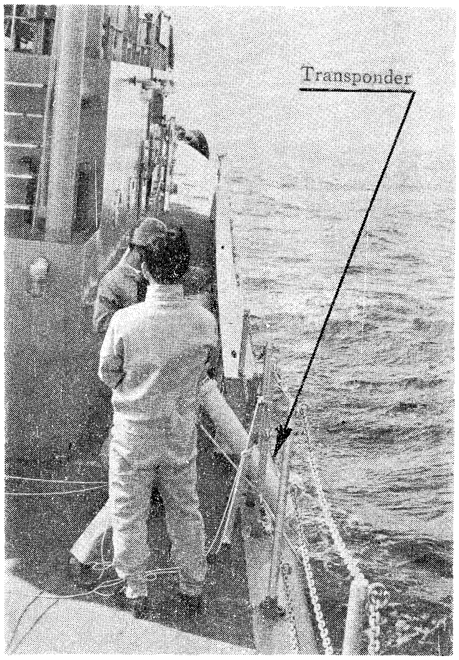

Fig. 4. Transponder just before it is lowered.

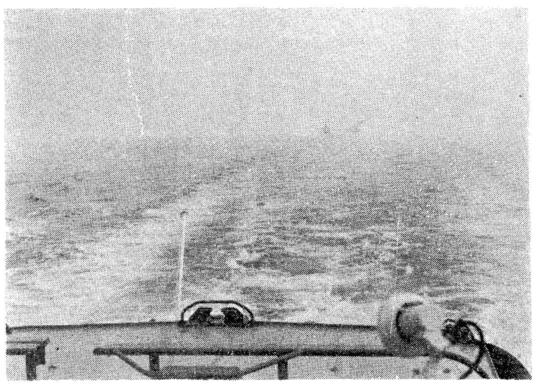

Fig. 5. The wake current of sea surface viewed from stern. Ship speed: 7 kt

Table 1. Results of experiments for limit of answerable distance.

Exper. No.	Date	Station	Speed of ship (kt)	Mark of Transponder (Answer frequency) (kHz)	Depth (h) (Position of submerged Transponder) (m)	Distance (D) (No receiving signal by wake) (m)	Min. transmissible angle (θ) $\sin\theta=\frac{h}{D}$
1	10/25	Tateyama Bay	7	C(43)	90.0	900	5°50′*
2	10/25	Tateyama Bay	4	C(43)	10.0	120	4°50′
3	11/30	off Iwaya	6	A(37)	63.5	1,150	3°10′
4	11/30	off Iwaya	6	B(40)	64.0	1,100	3°40′
5	11/30	off Iwaya	5.5	C(43)	63.5	700	5°10′

Remark: The asterisk * needs correction.

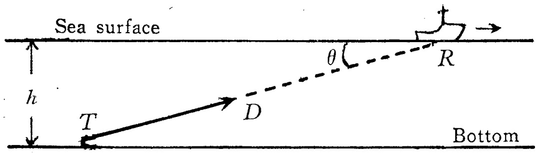

Fig. 6. Transmissible distance (D) between signal source and receiver.
θ: transmissible angle, T: signal source (Transponder), R: receiver (ship), h: depth.

の Transponder 沈設作業の状況を Fig. 4 に示す。

Fig. 5 は船が 7 kt で航走しているときの，船尾方向における海面上の気泡発生状況を示したものである。

このようにして得られた信号伝達距離 (D) の表示記録と，Transponder の沈設された水深 (h) とから，この船の航走中における信号伝達可能角 (θ) の検討を試みた (Fig. 6)。その結果をまとめると，Table 1 のようになる。

それぞれの実験番号に対応する記録を示すと，Fig. 7～11 に見られるとおりである。

深い水深の位置にある送波器から浅い水深に位置する受波器に信号を送る場合，直接波と水面反射波，あるいは海底反射波が存在する[1)]。しかし，この場合には，得られた記録の連続性からみて，明らかに直接波のエネルギーが大きいので，水面あるいは海底からの反射波と見違えることはない。

いずれの実験場所においても，海況は階級 1～2 であった。これに関してデータを補正する必要はないが，ただ，実験海域における鉛直水温分布は Fig. 12, 13 に示すようなものであったので，検討

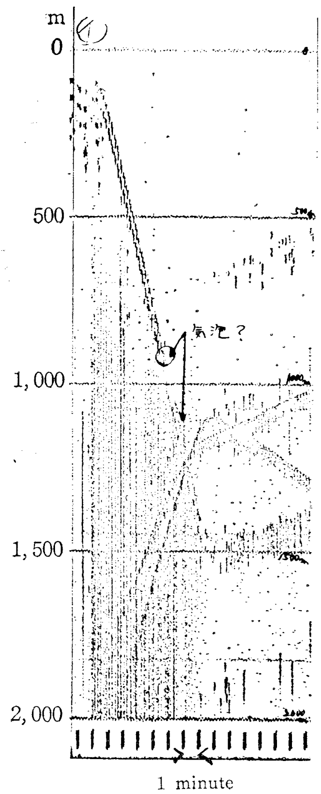

Fig. 7. The record of Experiment No. 1.
The record which the vessel is leaving at a speed of 7 kt after submerging Transponder C at 90 m depth, in Tateyama Bay, Oct. 25, 1972.
Weather: fine
The limit of distance to receive a signal is 900 m.

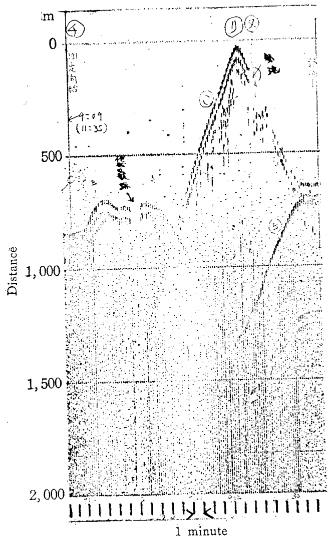

Fig. 8. The record of Experiment No. 2.
The record which the vessel is leaving at a speed of 4 kt from Transponder C submerged at 10 m depth after approaching it, in Tateyama Bay, Oct. 25, 1972. Weather: fine
The limit of distance to receive a signal is 120 m.

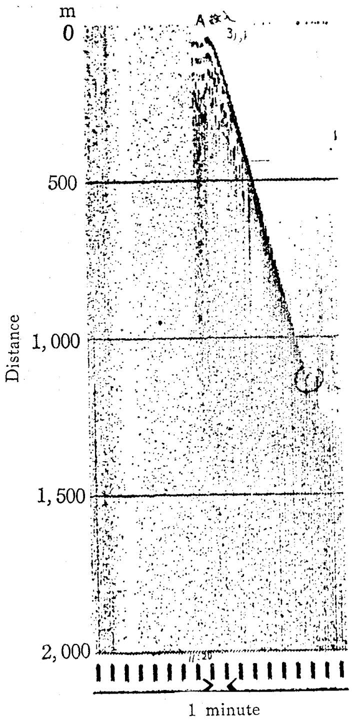

Fig. 9. The record of Experiment No. 3.
The record which the vessel is leaving at a speed of 6 kt after submerging Transponder A at 63.5 m depth, in off Iwaya, Awaji Is., Nov. 30, 1972. Weather: fine
The limit of distance to receive a signal is 1,150 m.

の結果，実験データのうち実験番号1についてのみ補正を行う必要があった。H. Lichte の式[2)]*によって音波の屈折を計算し，これにより補正を行うと，実験番号1の最小伝達角 θ は，$5°50'$ ではなく，$4°$ となった。

以上のことから，今回の実験によって，次のような結論が得られる。

今回行った調査作業船における実験においては，海況1～2で，船速4～7 kt において，水面を基準にした垂直角で，船尾方向からの超音波信号の伝達可能角の限界値はほぼ $3°\sim5°$ であった。このときの超音波周波数は 40 kHz 程度である。この船の場合，信号の伝達可能角の限界値は，かなり小角であるので，いろいろの測定のためには好都合であると考えられる。

* H. Lichte の式

$$y=\frac{1}{\cos^2\delta}10^{-3}\frac{\partial T}{\partial y}x^2+\tan\delta\cdot x$$
$$\fallingdotseq -10^{-3}\frac{\partial T}{\partial y}x^2$$

y: 音波垂直偏移 (m)，δ: 入射角，
T: 水温 (°C)，x: 水平距離 (m).

4. 考　察

船の航走中，船尾方向からの超音波信号を受信しなければならない場合が，海洋調査とか，海底定点を基準にした測位とか，漁業の高能率化を図る計器漁法などにおいて，今後いよいよその機会を増大してゆくものと考えられる。このような場合，船尾方向からどのような範囲であれば受信が可能であるかについて，その基礎資料を得るための糸口を見いだす意味において，一つの測定方法を示すために，今回の実験を行った。

この問題をなお考究するためには，次にあげるようなことを併せて追及しておくべきである。すなわち，水温の鉛直分布が音波伝達経路に影響することはさきに述べたが，それとともに，そのほか，音波の周波数（指向性とともに），音波の強さ，

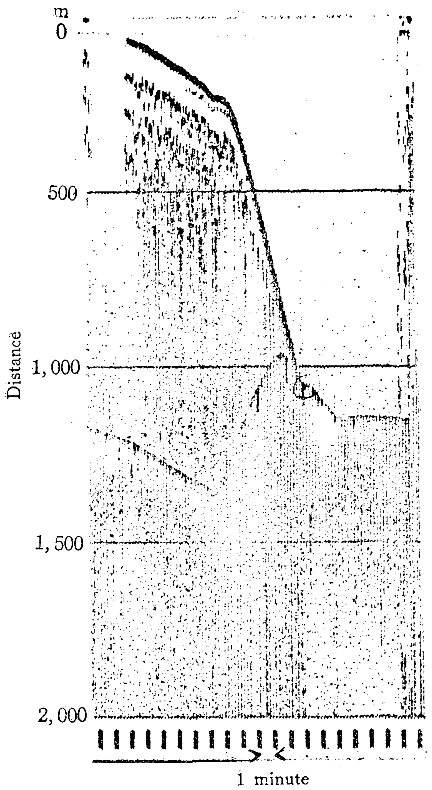

Fig. 10. The record of Experiment No. 4.
The record which the vessel is leaving at a speed of 6 kt after submerging Transponder B at 64 m depth, in off Iwaya, Awaji Is., Nov. 30, 1972. Weather: fine
The limit of distance to receive a signal is 1,100 m.

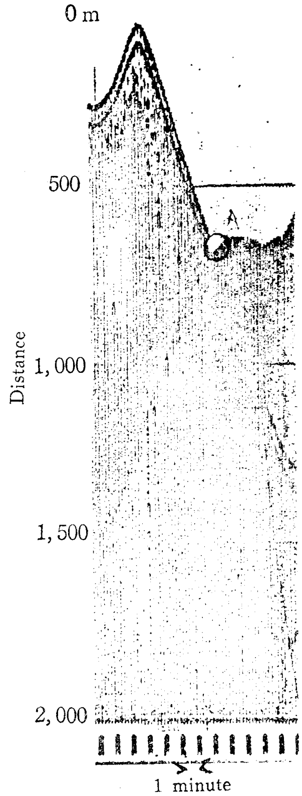

Fig. 11. The record of Experiment No. 5.
The record which the vessel is leaving at a speed of 5.5 kt from Transponder C submerged at 63.5 m depth after approaching it, in Iwaya, Awaji Is., Nov. 30, 1972. Weather: fine
The limit of distance to receive a signal is 700 m.

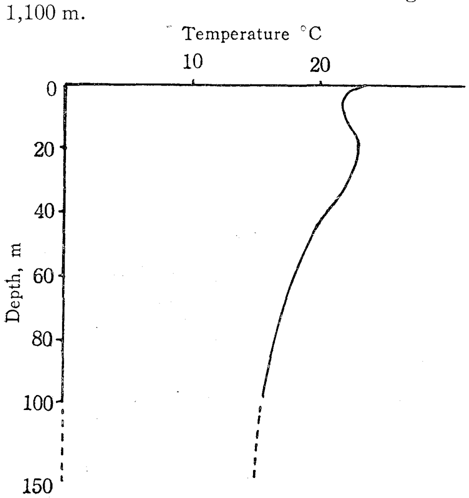

Fig. 12. Vertical temperature distribution in Tateyama Bay, Oct. 25, 1972.
The solid line: observed, the dotted line: assumed.

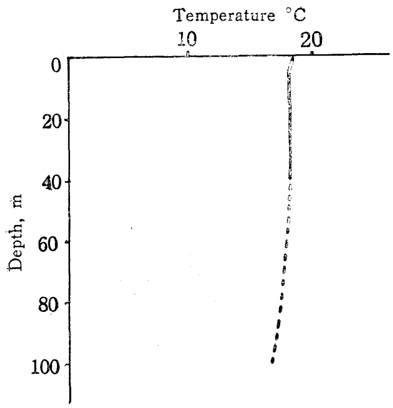

Fig. 13. Vertical temperature distribution in off Awaji Is., Nov. 30, 1972.
The solid line: observed, the dotted line: assumed.

音波信号の質，船型，screw の構造と気泡の生じかた等について，引き続き多くのデータを集めることが必要である。

ただ，超音波で情報を伝送するときに考えられる周波数は，40～60 kHz が最も多く使われるのではないかと思われるので，今回のように，そのうちでも低い方の周波数について実験できたことは幸いであった。一般に，低い方の周波数は，通達条件は良いが，伝送条件の上で，気泡層の影響を悪く受けやすいからである。

謝　辞

この実験を行うにあたり，御援助下さった本州四国連絡橋公団の諸氏，並びに古野電気株式会社の箕原喜代美，菅原四郎，滝川盛量の諸氏に深謝いたします。

なお，この研究の必要性と，この方式による測定につき，かずかずの御助言と御督励を，北海道大学の石田正已教授及び芝浦工業大学の橋本富寿教授より賜わりました。併せてお礼申し上げます。

文　献

1) 藤原潤一 (1971): 水中超音波の水面反射による多重伝搬問題の解析とその応用. 日本音響学会誌, **27**(6), 291-297.

2) 橋本富寿 (1951): 超音波測深並びに魚探の研究. 水産研究会, p. 4.

La mer (Bulletin de la Société franco-japonaise d'océanographie)
Tome 12, N° 1, pp. 26 à 33. Février 1974

Numerical Calculation of Radiative Transfer in the Sea*

Motoaki KISHINO**

Abstract: We suppose that the sea consists of a number of thin horizontal plane parallel layers of equal thickness and in each layer single scattering only occurs. This model was applied to Lake Pend Oreille and Suruga Bay. Using the inherent optical properties of the lake water or seawater, radiance distribution and irradiance were calculated numerically.

After comparing the calculated values with the observed ones, a fairly good agreement was found as expected. Then, we consider that this thin layer method is simple good model of light field in the sea.

1. Introduction

Solar and sky radiant energy falling on the sea surface is partly reflected on the sea surface but, for the most part, refracted and proceeds into the sea. Underwater radiant energy is attenuated as a result of absorption and scattering by seawater itself as well as by suspended particles and dissolved substances. This energy warms seawater and plays an essential role for the primary production. Moreover, the light in the sea presents a large number of problems such as feeding, swimming and orientation of fishes, underwater visibility for divers, underwater photography and television, etc. Then it is certainly one of the most important subjects in optical oceanography to make clear how the light behaves in the sea.

The theoretical study of radiative transfer in the sea was begun by LE GRAND (1939), who considered isotropic scattering of the sunlight only. Subsequently, various experiments have been done by many researchers.

PREISENDORFER (1965) has treated the radiative transfer on the basis of an invariant imbedding concept. He applied a model to Lake Pend Oreille and calculated the radiance in twenty six directions using the observed optical properties of the lake water. After comparing his theoretical result with the Tyler's observed data (TYLER, 1960), he said that this model could be reasonably regarded as a good one of light field. This methods, however, is very complex mathematically, and it is natural that a simple method is desired to solve that problems more esaily with a similar accuracy.

PLASS and KATTAWAR (1969) havs made investigation of radiance in the atmosphere-ocean system based on the Monte Carlo method. This method surely excludes mathematical difficulties contrary to the one mentioned above, but the only shortcoming is to require enormous computation to achieve the result with sufficient accuracy and fine resolution for the angular distribution.

JERLOV and FUKUDA (1960) calculated the radiance distribution in the upper layers of the sea by means of simple integration of scattered light considering only the single scattering of sunlight. The calculated radiance distribution showed a satisfactory agreement with the experimental result. After that, the method was extended to the second-order scattering of the light by KAWANA (1972) and to the third-order by SUGIMORI and HASEMI (1971), but the difference between the observed and calculated values did not vanish increasing with depth on account of neglecting the higher-order scattering. On the other hand, extention of this method up to the higher-order scattering is complicated and requires a long time for computation.

To avoid the difficulty, we consider a set of thin layers in which only the single scattering is taken into account. When the calculation is repeated, it may be expected that the same

* Received January 7, 1974
** The Institute of Physical and Chemical Research, Wakō-shi, Saitama, 351 Japan

effect as in the multiple scattering is produced by the method. Using the optical properties measured in Lake Pend Oreille and Suruga Bay, radiance distribution and irradiance were calculated. From comparison with the observed data, a fairly good agreement was found as expected.

2. Theory

Judging from the results of calculation by JERLOV and FUKUDA (1960), it can be said that the single scattering very conspicuous and the higher-order scattering is negligibly small as far as a thin layer is considered. Here, we suppose that the sea consists of a number of thin horizontal plane parallel layers of equal thickness and in each layer the single scattering only occurs. As shown in Fig. 1, on the top surface of the nth layer we find the downward radiance which has experienced attenuation and single scattering in the $(n-1)$th layer along with the upward radiance which has experienced attenuation and single scattering in the nth layer.

Let Δx be the thickness of thin layer and $(\zeta, \xi=0°)$ be direction of sunlight in the sea. Radiance on the top of surface of the nth layer is given by the following equation:

Irradiance by the direct sunlight, $E_{\text{sun}}(n)$,

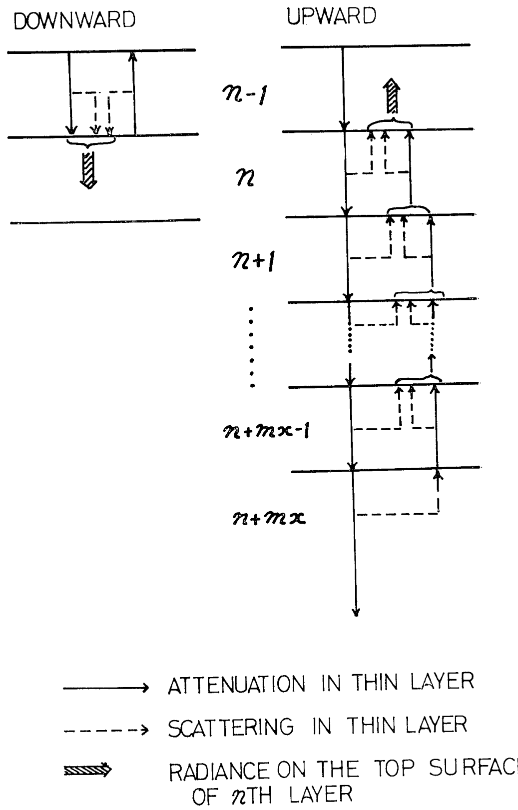

Fig. 1. Flow graph for calculation of radiance.

$$E_{\text{sun}}(n)=E_{\text{sun}}(n-1)e^{-c\Delta x \sec\zeta}.$$

Downward radiance, $L(n, \theta, \phi)$, where θ is $0\leq\theta<\pi/2$

$$L(n, \theta, \phi)=L_{s*}(n, \theta, \phi)+L(n-1, \theta, \phi)e^{-c\Delta x \sec\theta}$$
$$+\int_0^{2\pi}\int_0^{\pi/2} L_{d*}(n, \theta, \phi; \theta', \phi') \sin\theta' d\theta' d\phi' + \int_0^{2\pi}\int_{\pi/2}^{\pi} L_{u*}(n, \theta, \phi; \theta', \phi') \sin\theta' d\theta' d\phi' ,$$

where the first term in the right-hand side is the radiance in the direction (θ, ϕ) produced by the scattering of sunlight in the thin layer, which is given as follows:

$$L_{s*}(n, \theta, \phi)=\begin{cases} E_{\text{sun}}(n-1)\sec\zeta \dfrac{\beta(\Theta)}{c} \dfrac{e^{-c\Delta x\sec\zeta}-e^{-c\Delta x \sec\theta}}{1-\sec\zeta\cos\theta} & (\theta\neq\zeta) \\ E_{\text{sun}}(n-1)\sec^2\zeta\beta(\Theta)\Delta x e^{-c\Delta x\sec\zeta} & (\theta=\zeta) . \end{cases}$$

The second term gives the attenuation of downward radiance in the $(n-1)$th layer. And the third and fourth terms are scattered radiance in the direction (θ, ϕ) produced by the downward radiance in the direction (θ', ϕ') in the $(n-1)$th layer and the upward radiance in the direction (θ', ϕ') in the nth layer, respectively:

$$L_{d*}(n, \theta, \phi; \theta', \phi')=\begin{cases} L(n-1, \theta', \phi')\dfrac{\beta(\Theta')}{c} \dfrac{e^{-c\Delta x\sec\theta'}-e^{-c\Delta x\sec\theta}}{1-\sec\theta'\cos\theta} & (\theta\neq\theta') \\ L(n-1, \theta', \phi')\beta(\Theta')\Delta x \sec\theta' e^{-c\Delta x\sec\theta'} & (\theta=\theta') \end{cases}$$

$$L_{u*}(n,\theta,\phi;\theta',\phi')=L(n,\theta',\phi')\frac{\beta(\Theta')}{c}\frac{1-e^{-c\Delta x(\sec\theta-\sec\theta')}}{1-\sec(\pi-\theta')\cos\theta},$$

and $L(n,\pi/2,\phi)$ is given by

$$L\left(n,\frac{\pi}{2},\phi\right)=E_{\rm sun}(n)\sec\zeta\frac{\beta(\Theta)}{c}e^{-c\Delta x\sec\zeta}+\int_0^{2\pi}\int_0^{\pi}L(n,\theta',\phi')\frac{\beta(\Theta)}{c}e^{-c\Delta x\sec\theta'}\sin\theta' d\theta' d\phi'.$$

Upward radiance, $L(n,\theta,\phi)$, where θ is $\pi/2<\theta\leq\pi$,

$$L(n,\theta,\phi)=L_{s*}(n,\theta,\phi)+L(n+1,\theta,\phi)e^{-c\Delta x\sec(\pi-\theta)}$$
$$+\int_0^{2\pi}\int_0^{\pi/2}L_{d*}(n,\theta,\phi;\theta',\phi')\sin\theta' d\theta' d\phi'+\int_0^{2\pi}\int_{\pi/2}^{\pi}L_{u*}(n,\theta,\phi;\theta',\phi')\sin\theta' d\theta' d\phi',$$

where

$$L_{s*}(n,\theta,\phi)=E_{\rm sun}(n)\sec\zeta\frac{\beta(\Theta)}{c}\frac{1-e^{-c\Delta x(\sec\zeta-\sec\theta)}}{1-\sec\zeta\cos\theta}$$

$$L_{d*}(n,\theta,\phi;\theta',\phi')=L(n,\theta',\phi')\frac{\beta(\Theta')}{c}\frac{1-e^{-c\Delta x(\sec\theta'-\sec\theta)}}{1-\sec\theta'\cos\theta}$$

$$L_{u*}(n,\theta,\phi;\theta',\phi')=\begin{cases}L(n+1,\theta',\phi')\dfrac{\beta(\Theta')}{c}\dfrac{e^{-c\Delta x\sec(\pi-\theta')}-e^{-c\Delta x\sec(\pi-\theta)}}{1-\sec(\pi-\theta')\cos(\pi-\theta)} & (\theta\neq\theta')\\ L(n+1,\theta',\phi')\beta(\Theta')\Delta x\sec(\pi-\theta')e^{-c\Delta x\sec(\pi-\theta')} & (\theta=\theta').\end{cases}$$

In our numerical model, however, the calculation cannot be continued to infinite depth, and we are obliged to find a depth at which the uncertainty of the upward radiance from below does not seriously affect the result of the calculation of light field in the layers above. Let the number of layers at this depth be $(n+mx)$. The upward radiance is given by

$$L(n+mx,\theta,\phi)=E_{\rm sun}(n+mx)\sec\zeta\frac{\beta(\Theta)}{c}\frac{1}{1-\sec\zeta\cos\theta}$$
$$+\int_0^{2\pi}\int_0^{\pi/2}L(n+mx,\theta',\phi')\frac{\beta(\Theta')}{c}\frac{1}{1-\sec\theta'\cos\theta}\sin\theta' d\theta' d\phi',$$

where c is the attenuation coefficient of seawater, $\beta(\Theta)$ is the volume scattering function for scattering angle Θ, which is obtained from the expressions:

$$\cos\Theta=\cos\zeta\cos\theta+\sin\zeta\sin\theta\cos\phi,$$
$$\cos\Theta'=\cos\theta'\cos\theta+\sin\theta'\sin\theta\cos(\phi-\phi').$$

Downward irradiance $E_d(n)$, upward irradiance $E_u(n)$, and scalar irradiance $E_0(n)$ are obtained by integrating over the upper or lower hemisphere, or the sphere, respectively. The results are

$$E_d(n)=\int_0^{2\pi}\int_0^{\pi/2}L(n,\theta,\phi)\cos\theta\sin\theta\, d\theta\, d\phi+E_{\rm sun}(n)$$

$$E_u(n)=\int_0^{2\pi}\int_{\pi/2}^{\pi}L(n,\theta,\phi)|\cos\theta|\sin\theta\, d\theta\, d\phi$$

$$E_0(n)=E_{0d}(n)+E_{0u}(n)$$
$$=\int_0^{2\pi}\int_0^{\pi/2}L(n,\theta,\phi)\sin\theta\, d\theta\, d\phi+E_{\rm sun}(n)\sec\zeta$$
$$+\int_0^{2\pi}\int_{\pi/2}^{\pi}L(n,\theta,\phi)\sin\theta\, d\theta\, d\phi.$$

Depth of nth layer is

$$z=(n-1)\cdot\Delta x.$$

Then, if the inherent optical properties of seawater and the boundary conditions of radiance $L(1,\theta,\phi)$ and irradiance of the direct sunlight $E_{\rm sun}(1)$ are known, the radiance and irradiance at any depth can be obtained.

3. Numerical calculation and discussion

In our calculation, the optical properties observed in Lake Pend Oreille and Suruga Bay are used, which are shown in Table 1. However, since the values of volume scattering function, $\beta(\theta)$, in Lake Pend Oreille were not measured simultaneously with other factors such as radiance distribution and attenuation coefficient in 1957 (TYLER *et al.*, 1959; TYLER, 1960), we had to estimate them from the measured values at the same season in 1960 (TYLER, 1961). The values of $\beta(\theta)$ in parentheses in Table 1 are extrapolated by means of the Spilhaus' method (SPILHAUS, 1965). The extrapolation is made by the equation:

$$\ln \beta(\theta) = A + B\theta + C\theta^2$$

in the range of small angle, and

$$\ln \beta(\theta) = D + E\theta$$

in the range of large angle, where A, B, C, D and E are constants.

Table 1. Optical properties of water in Lake Pend Oreille and Suruga Bay.

Location	Lake Pend Oreille*	Suruga Bay***
Date	1957-3-16～4-28	1969-1-24
Depth	29 m	0～40 m
a	0.117	0.051
b	0.325	0.101
c	0.442	0.152
$\beta(\theta)$	(1960-4-26, 9.2 m)**	(20 m)
0	(2.462)	(1.402)
10	(0.6478)	(0.2315)
20	0.1968	(0.04930)
30	0.06927	0.01356
40	0.02823	0.004806
50	0.01328	0.002002
60	0.006905	0.001115
70	0.004027	0.0007825
80	0.002626	0.0005739
90	0.001919	0.0005126
100	0.001570	0.0005021
110	0.001425	0.0004924
120	0.001386	0.0005895
130	0.001405	0.0007500
140	0.001444	0.001037
150	0.001512	(0.001356)
160	0.001580	(0.001800)
170	0.001628	(0.002361)
180	0.001648	(0.003163)

* After TYLER *et al.* (1959)
** After TYLER (1961)
*** After KISHINO *et al.* (1972)

The layer thickness, Δx, and the number of layers, mx, are important factors in this method. These values were chosen previously after some trials of calculation. Namely, Δx is determined so as to satisfy self-consistency for the absorption coefficient. The absorption coefficient, a, is estimated by the equation:

$$a = \frac{1}{E_0} \frac{d(E_u - E_d)}{dz}$$

based on the calculated irradiance E_d, E_u and E_0, and it was tested whether it accords with the values used originally for the calculation of light field. On the other hand, based on the trial calculations, the reflectance, R, for various values of mx is obtained and the result is shown in Fig. 2. According to the figure, we can recognize that R approaches a constant value gradually as the number of mx increases. Then, mx will be determined when R becomes nearly constant. From these considerations we chose the values of 0.25 m for Δx and 25 for mx in Lake Pend Oreille, while 3.0 m for Δx and 10 for mx in Suruga Bay.

As the boundary condition of $L(1, \theta, \phi)$ in case of Lake Pend Oreille, the values of radiance

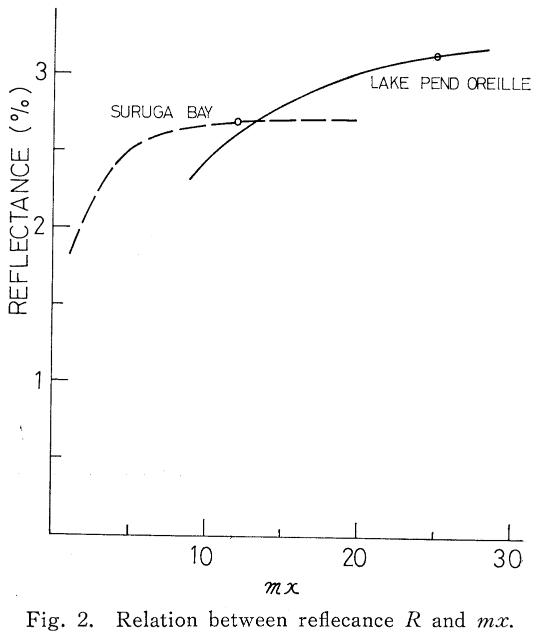

Fig. 2. Relation between reflecance R and mx.

distribution at a depth of 4.24 m observed by TYLER are used (TYLER, 1960). In case of Suruga Bay, we made use of the values of diffused skylight at 40° of the sun altitude, which were measured by RICHARDSON and HULBURT (1949). The ratio of irradiance of the sun to that of skylight on the sea surface was assumed to be 1:0.08181 according to the values observed by KING (1913). Reflection and refraction on the sea surface were also calculated.

In the numerical integration for the solid angle, we used the same method as TYLER *et al.* did (TYLER *et al.*, 1959), and as the increments $\Delta\theta=10°$ and $\Delta\phi=20°$ were adopted.

In Fig. 3 is shown the angular distribution of observed and calculated values of radiance at various depth in the vertical plane including the sun in case of Lake Pend Oreille. The sun altitude is 56.6° and the refraction angle is 24.4°. Although the maximum radiance is smaller and the angular distribution is broader for the calculated values than for the observed ones, both values show a good agreement as a whole.

The vertical distribution of observed and calculated values of radiance in Lake Pend Oreille is shown in Fig. 4 for four directions, the zenith ($\theta=0°$), horizontal ($\theta=90°$, $\phi=0°$),

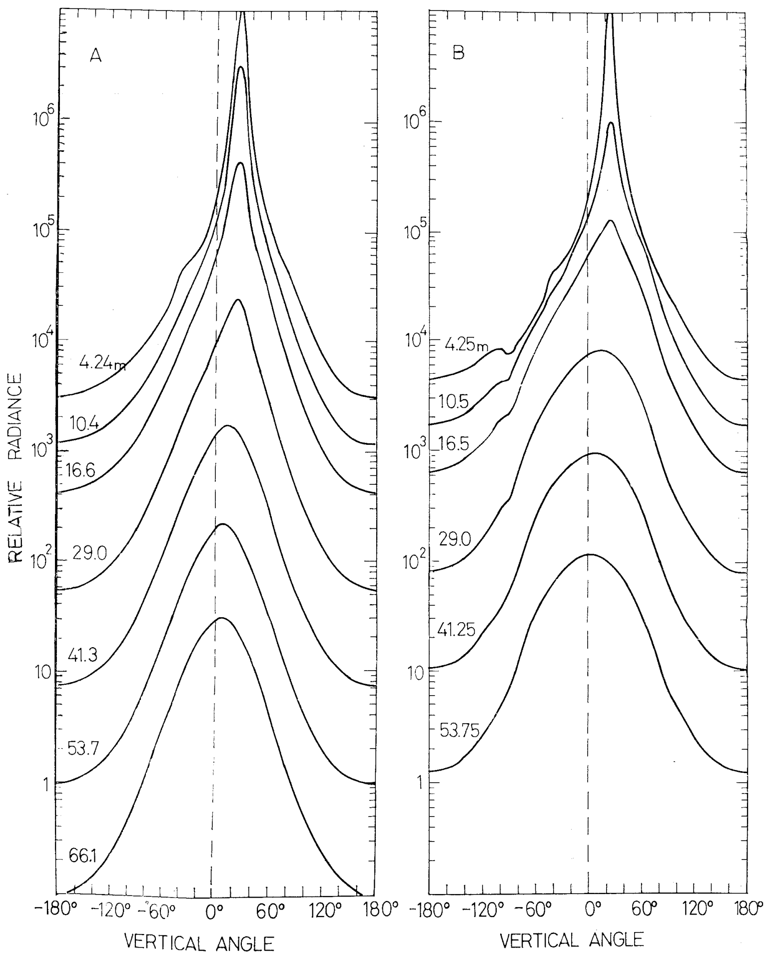

Fig. 3. Radiance distribution in the vertical plane including the sun in case of Lake Pend Oreille.
A: Observed values by TYLER (1960).
B: Calculated values.

nadir ($\theta=180°$) and maximum radiance ($\theta=30°$, $\phi=0°$). The radiance for the zenith direction attains a maximum at a certain depth below the surface, and the existence of such maximum was clearly found in case of the measurements of JERLOV and FUKUDA (1960). If only the single scattering of sunlight is considered, the maximum in radiance appears at the depth z_m:

$$z_m=\frac{1}{c}\,\frac{\ln\sec\theta-\ln\sec\zeta}{\sec\theta-\sec\zeta}$$

The value of z_m is 2.3 m for $\theta=0°$, whereas in our case of thin layer, we have 5.25 m as seen in Fig. 4. Then, it can be said that in the upper layer the downward radiance is also under the influence of higher-order scattering.

Fig. 5 shows the depth profiles of irradiances E_d and E_u and scalar irradiance E_0, which

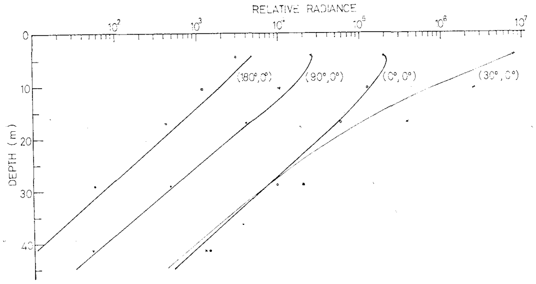

Fig. 4. Vertical profile of radiance in Lake Pend Oreille.
×○△□: Observed values.
———: Calculated values.

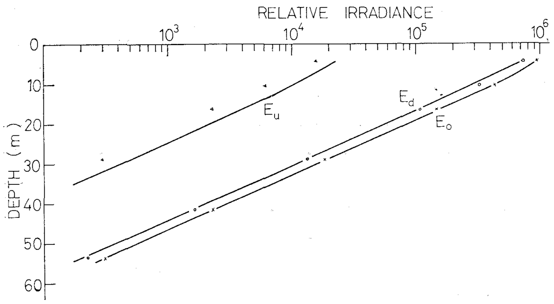

Fig. 5. Depth profile of irradiance and scalar irradiance in Lake Pend Oreille.
×○△: Observed values.
———: Calculated values.

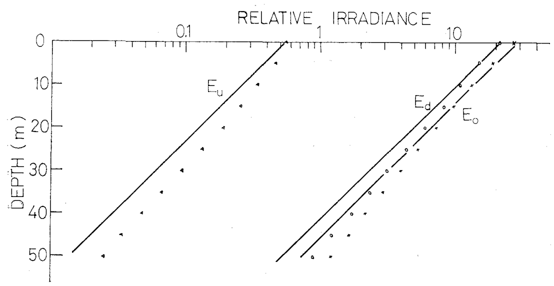

Fig. 6. Depth profiles of irradiance and scalar irradiance in Suruga Bay.
×○△: Observed values.
———: Calculated values.

Table 2. Apparent optical properties in Lake Pend Oreille and Suruga Bay.

Depth (m)	R (%)	D_d	D_u	K_d	a
Lake Pend Oreille					
Measured values					
4.24	2.15	1.247	2.704		
10.4	1.84	1.288	2.727	.153	.115
16.6	2.04	1.291	2.778	.174	.118
29.0	2.27	1.313	2.781	.169	.117
41.3	2.35	1.315	2.757	.165	.117
53.7	2.34	1.307	2.763	.158	.112
Calculated values					
4.25	3.13	1.246	2.501		
10.5	3.58	1.371	2.679	.162	.107
16.5	3.71	1.407	2.729	.167	.107
29.0	3.76	1.423	2.749	.169	.106
41.25	3.77	1.424	2.751	.169	.106
53.75	3.77	1.424	2.751	.169	.106
Suruga Bay					
Measured values					
0	2.38				
10	3.01			.0621	.051
20	3.08			.0637	.053
30	2.91			.0637	.050
40	2.76			.0646	.049
50	2.77			.0662	.048
Calculated values					
0	2.39	1.237	1.945		
9	2.55	1.294	2.038	.0780	.0566
21	2.62	1.325	2.087	.0742	.0524
30	2.63	1.330	2.100	.0742	.0524
39	2.63	1.328	2.101	.0729	.0513
51	2.63	1.320	2.094	.0725	.0513

were obtained from the measurement and calculation of radiance in Lake Pend Oreille. The calculated values of E_d and E_0 present generally a good agreement with the observed values, but the observed upward radiance is smaller than the calculated one. The depth profiles in Suruga Bay is shown in Fig. 6. In this case, the calculated values show somewhat more rapid attenuation than the measured ones.

To understand the difference between the observed and calculated values more clearly, apparent optical properties such as reflectance R, distribution function for downward radiance D_d, for upward radiance D_u, and attenuation coefficient for downward irradiance K_d, and absorption coefficient a, are calculated from the values of E_d, E_u, and E_0, and the result is shown in Table 2.

In case of Lake Pend Oreille, the measured values of D_d are 1.3 on the average, while the calculated values of D_d vary with depth from 1.25 to 1.42. It is found that the angular distribution of calculated radiance becomes broader with depth. The calculated values of reflectance is larger than the measured one. On the other hand, the agreement between the values of D_u and K_d is good, respectively.

In case of Suruga Bay, the calculated values of K_d are larger than the measured ones. Since there is no measurement as to the radiance distribution, comparison cannot be made satisfactorily.

As seen in Figs. 3~6 and Tables 1 and 2, the calculated values show a pretty well agreement with the measured ones. Then, we consider that this method offers a simple model of light field in the sea. But, there exists a small difference between the calculated and observed values, especially, near the maximum of radiance curve and at the upward radiance. These differences are presumably attributed to the uncertainty of the form of volume scattering function, especially, for small angle scattering. In order to check this method well, we need simultaneous measurements of the light field on radiance, irradiance and scalar irradiance, as well as inherent optical properties including c, a, b and $\beta(\theta)$. Of course, the measurement of small angle scattering is essential in all oi them.

Acknowledgments

The author wishes to express his hearty thanks to Principal Scientist S. UNOKI and Scientist N. OKAMI of the Institute of Physical and Chemical Research, for their kind discussion on this work. He is also indebted to his colleagues of this laboratory and to the staff of Computation Center of the Institute.

References

JERLOV, N. G. and M. FUKUDA (1960): Radiance distribution in the upper layers of the sea. Tellus, **12**, 348-355.

KAWANA, K. (1972): Effect of the scattered light on underwater irradiance. Bull. Fac. Fish. Hokkaido Univ., **23**, 82-93.

KING, L. V. (1913): On the scattering and absorption of light in gaseous media, with application to the intensity of sky radiation. Phil. Trans. Roy. Soc. (A), **212**, 375-433.

KISHINO, M., N. OKAMI, G. OSHIBA and T. SASAKI (1972): Optical properties of the water in adjacent regions of the Kuroshio (II). La mer, **10**, 89-94.

LE GRAND, Y. (1939): La pénétration de la lumière dans la mer. Ann. Inst. Océanog., **19**, 393-436.

PLASS, G. N. and G. W. KATTAWAR (1969): Radiative transfer in an atmosphere-ocean system. Appl. Opt., **8**, 455-466.

PREISENDORFER, R. W. (1965): Radiative Transfer on Discrete Spaces. Pergamon, New York, N. Y., 462 pp.

RICHARDSON, R. A. and E. O. HULBURT (1949): Sky-brightness measurements near Bocaiuva, Brazil. J. Geophys. Res., **54**, 215-227.

SPILHAUS, A. F. (1965): Observation of light scattering in the sea water. Ph. D. thesis, Mass. Inst. Technol., Cambridge, 242 pp.

SUGIMORI, Y. and T. HASEMI (1971): Estimation of underwater scattering radiances up to the third order. J. Oceanog. Soc. Japan, **27**, 73-80.

TYLER, J. E., W. H. RICHARDSON and R. W. HOLMES (1959): Method for obtaining the optical properties of large bodies of water. J. Geophys. Res., **64**, 667-673.

TYLER, J. E. (1960): Radiance distribution as a function of depth in an underwater environment. Bull. Scripps Inst. Oceanog., Univ. Calif., **7**, 363-412.

TYLER, J. E. (1961): Scattering properties of distilled and natural waters. Limnol. Oceanog., **6**, 451-456.

海中の放射伝播の数値計算

岸　野　元　彰

要旨：海が等しい厚さの，うすい水平な層によって成り立ち，各層内では一次散乱のみ卓越し，多重散乱は無視出来ると考えた。このモデルをペンドール湖（Lake Pend Oreille）と駿河湾に適用した。両者の固有の光学的性質を用いて，radiance と irradiance が数値的に計算された。

計算値と測定値とを比較した結果，かなり良い一致が見いだされた。従って，この薄層の方法は海中の light field の簡単な良いモデルと考えられる。

La mer (Bulletin de la Société franco-japonaise d'océanographie)
Tome 12, N° 1, pp. 34 à 37. Février 1974

Miscellanées

Analyse préliminaire d'enregistrements de courantomètres à rotor de Savonius*

Kenzo TAKANO** et Mme Hisako KAWAGUCHI***

L'océanographie japonaise s'est peu engagée dans la courantométrie; un effort en ce sens constitue un impératif de plus en plus pressant dans l'étude de la dynamique de l'océan. C'est pourquoi en 1968 nous avons entrepris des mesures de courant par mouillage de courantomètres à rotor de Savonius (Geodyne 102), alors que la technique de mouillage et de récupération dont nous disposions était embryonnaire.

Dans une note précédente, TAKANO et HARA (1970) ont présenté une analyse préliminaire de tous les enregistrements obtenus en 1968 et 1969. L'objet de la présente note est de compléter la précédente par un calcul de corrélations entre les vitesses de courant obtenues à deux niveaux différents.

Le tableau 1 montre les positions et les durées des mesures ainsi que la profondeur.

Comme il a été montré dans la note précitée, d'autres enregistrements sont disponibles mais dans un premier temps nous n'en avons pas tenu compte. En outre, il convient de noter que dans la plupart des mesures, nous avons mis l'accent sur le mouvement de l'eau près du fond; les courantomètres étaient suspendus au sommet d'un tripode posé sur le fond, de façon à se libérer des mouvements perturbateurs dûs à la poussée de l'eau, sauf pour les courantomètres situés à 200 mètres et à 9 mètres au-dessus du fond (cas 4 et 5) qui étaient suspendus à des bouées immergées.

La série des vitesses moyennes sur une minute est analysée de façon suivante: les composantes de période diurne (1500 minutes) et semi-diurne (750 minutes), celle de la période d'inertie ainsi que la composante constante sont déterminées par la méthode des moindres carrés et éliminées de la série. L'analyse spectrale porte alors sur la nouvelle série dépourvue de ces composantes.

Les hodographes de chacune de ces trois composantes périodiques sont des éllipses. Le tableau 2 montre le sens de la rotation des vecteurs vitesses sur ces éllipses: la notation M signifie que les vecteurs vitesses tournent dans le sens des aiguilles d'une montre, la notation I dans le sens inverse. Dans les cas 3 et 4, les sens de la rotation ne s'accordent pas l'un avec l'autre à deux niveaux différents, quelque soit la période. Si deux courantomètres étaient suffisamment rapprochés et que

Tableau 1

N°	latitude	longitude	capteurs au-dessus du fond		durée	profondeur
1	35°11'N,	139°25'E	30 cm,	220 cm	3 jours	750 m
2	35°11'N,	139°25'E	30 cm,	220 cm	22 heures	750 m
3	35°07'N,	139°20'E	40 cm,	330 cm	1,7 jours	700 m
4	39°45'N,	133°52'E	65 cm,	200 m	5 jours	770 m
5	35°12'N,	139°26'E	330 cm,	9 m	25 heures	726 m

* Manuscrit reçu le 1er décembre 1973
** Rikagaku Kenkyusho, Wako-shi, 351 Japon
*** Institut de Recherche Océanique, Université de Tokyo

Tableau 2

N°	hauteur	1500 min.	750 min.	période d'inertie
1	30 cm	I	I	I
	220 cm	I	M	I
2	30 cm	I	I	I
	220 cm	I	I	I
3	40 cm	I	I	I
	330 cm	M	M	M
4	65 cm	I	I	M
	200 m	M	M	I
5	330 cm	I	M	I
	9 m	I	M	M

ces périodes étaient privilégiées, ils devraient tourner dans le même sens. Le désaccord observé dans le cas 3 est dû à l'importance des bruits parasites dans le mouvement de l'eau; dans le cas 4, il peut être plus ou moins attribué à une erreur de mesure qui se manifeste aussi dans le spectre, comme il le sera noté plus loin. A ces exceptions près, l'accord est généralement bon.

Les spectres d'énergie et les cohérences sont présentés sur les figures 1 à 5. Il est à signaler que la durée des mesures n'est pas assez longue pour obtenir un spectre d'énergie pour les basses fréquences. Cela n'empêche tout de même pas de dire que les spectres mettent en évidence une loi en $-5/3$ pour une large bande de fréquence à l'exception du spectre à 200 mètres au-dessus du fond, dans le cas 4. Dans ce dernier cas, les spectres s'écartent considérablement de la courbe en $-5/3$ au delà de 0,5 c/h environ. Cela suggère que la flottabilité de la bouée immergée était trop faible pour maintenir le courantomètre immobile et qu'un bruit de fond a été introduit dans les mesures par les mouvements perturbateurs du courantomètre lui-même.

Les composantes vers l'est de basse fréquence sont cohérentes entre elles mais les composantes vers le nord ne le sont pas. Il est possible que la topographie du fond intervienne dans cette particularité de la cohérence en direction. Bien que la précision de la bathymétrie et du positionnement du site des mesures soit difficile à estimer, les isobathes apparaissent dirigées dans le sens Nord-Sud dans les cas 1 et 2 et dans le sens Est-Ouest dans le cas 3 (voir figure 1 de HARA et TAKANO, 1969 ou figure 2 de TAKANO et HARA, 1970). La direction des isobathes ne s'accorde donc pas toujours avec la direction de la cohérence privilégiée. L'influence de la topographie sur la cohérence donnera sans doute lieu à beaucoup d'études approfondies.

Le manque de cohérence pour toute la gamme des fréquences dans les cas 4 et 5 confirme l'existence d'un bruit de fond important ou la présence des modes baroclíniques supérieurs.

Cette analyse a été faite lorsque l'auteur premier cité était à l'Institut de Recherche Océanique de l'Université de Tokyo.

Bibliographie

HARA, H. et K. TAKANO (1969): Mesure du courant près du fond. La mer, **7**, 27-28. (en japonais)

TAKANO, K. and H. HARA (1970): A preliminary analysis of current meter records. La mer, **8**, 205-228.

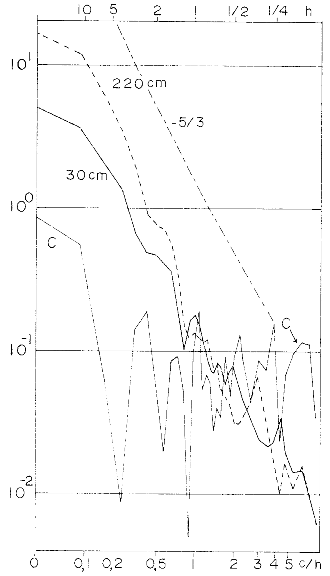

Fig. 1a. Spectres et cohérence des composantes vers l'est dans le cas 1.

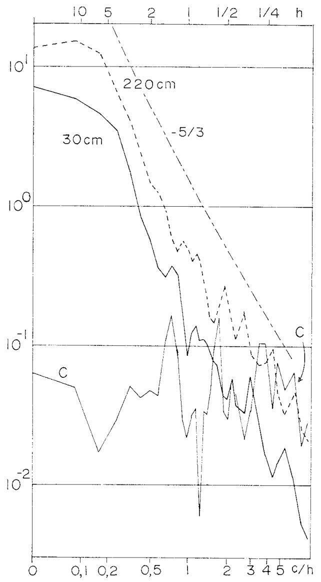

Fig. 1b. Spectres et cohérence des composantes vers le nord dans le cas 1.

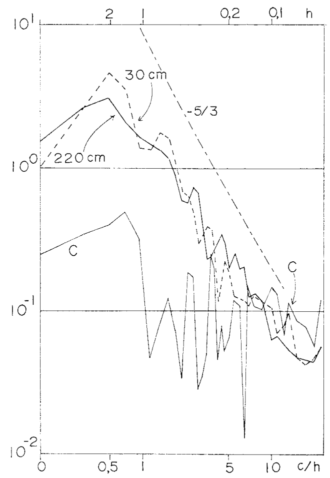

Fig. 2a. Spectres et cohérence des composantes vers l'est dans le cas 2.

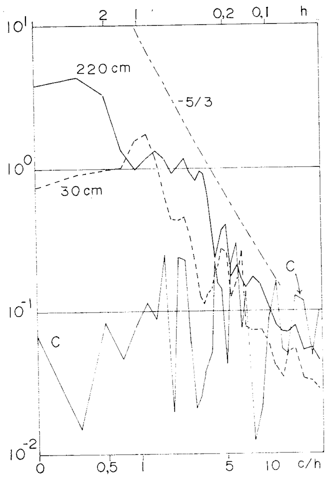

Fig. 2b. Spectres et cohérence des composantes vers le nord dans le cas 2.

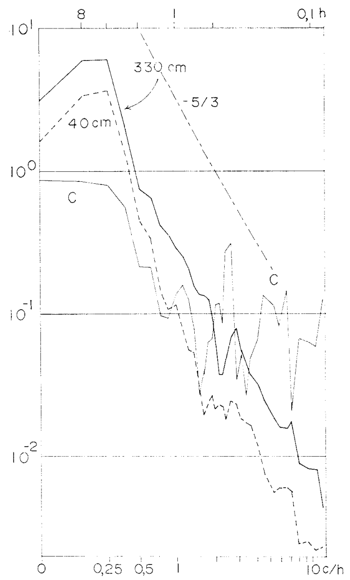

Fig. 3a. Spectres et cohérence des composantes vers l'est dans le cas 3.

Fig. 3b. Spectres et cohérence des composantes vers le nord dans le cas 3.

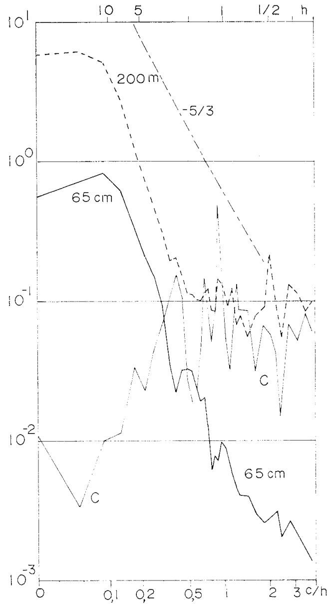

Fig. 4a. Spectres et cohérence des composantes vers l'est dans le cas 4.

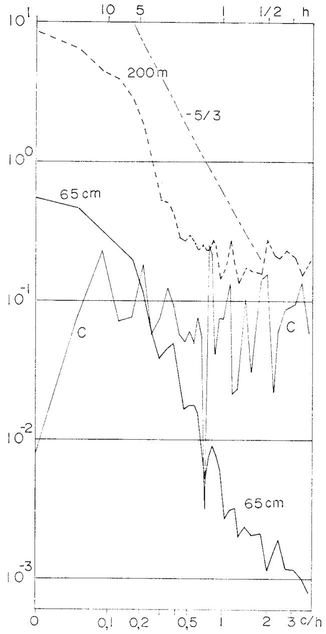

Fig. 4b. Spectres et cohérence des composantes vers le nord dans le cas 4.

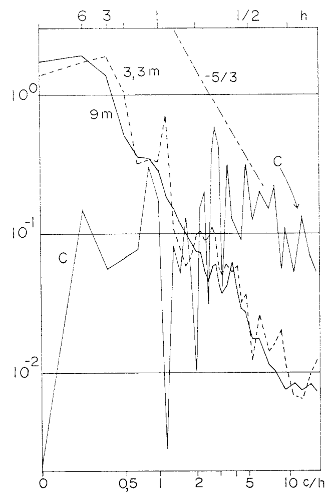

Fig. 5a. Spectres et cohérence des composantes vers l'est dans le cas 5.

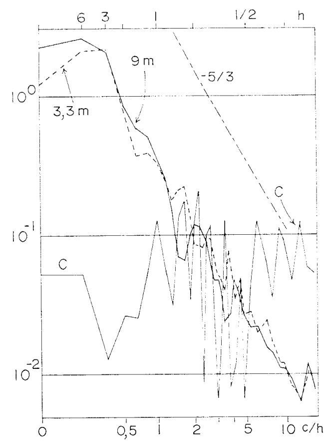

Fig. 5b. Spectres et cohérence des composantes vers le nord dans le cas 5.

La mer (Bulletin de la Société franco-japonaise d'océanographie)
Tome 12, N° 1, pp. 38 à 55 Février 1974

Compte rendu

Recent Aquaculture in Japan*

Yutaka UNO**

1. Preface

The total production by fisheries in Japan was 9,315,000 tons, which was record breaking. Table 1 shows the rough details. The production by shallow sea culture is about 5% of the total in quantity and about 13% in value.

Production by culture in shallow sea mainly consists of yellowtail *Seriola quinqueradiata*, Kuruma prawn *Penaeus japonicus*, oyster *Crassostrea gigas*, pearl oyster *Pinctada martensii*

Table 1. Quantity and value by type of fisheries. Quantity: metric tons, value: million yen (1970).

Type fisheries	Quantity	Value
Distant waters	3, 429, 000	296, 900
Offshore waters	3, 277, 800	236, 500
Coastal waters	1, 890, 900	251, 700
Culture in shallow sea	549, 100	135, 300
Inland waters fisheries and culture	167, 800	48, 700
Total	9, 314, 600	969, 100

Table 3. Annual crop in the shallow waters aquaculture in Japan (1970).

Fish	
Seliola	43, 300 tons
Chrysophrys major	460
Evynnis japonicus	5
Sparus swinbonis	2
Monacanthus (filefish)	63
Trachurus	2
Caranx	36
Other	42
Shrimp (Kuruma shrimp)	301
Octopus	109
Other	94
Bivalves	
Pearl	85
Crassostrea	190, 799
Scallop	5, 675
Other	4
Aquatic plants	
Porphyra	231, 464
Undaria	76, 360
Laminaria	282
Total	549, 083

Table 2. Products of culture in shallow sea. Unit: ton.

Year	Seliola	Kuruma shrimp	Pearl	Oyster	Nori	Other	Total
1960	1, 431	97	48	182, 778	100, 457	1, 017	285, 828
61	2, 036	85	80	172, 895	147, 379		322, 498
62	4, 460	125	69	203, 594	154, 631		362, 897
63	5, 038	179	80	240, 144	144, 531		389, 987
64	10, 321	154	85	240, 564	111, 851		362, 992
65	14, 779	—	99	210, 603	140, 753		379, 797
66	16, 875	—	118	221, 139	128, 440		405, 295
67	21, 169	404	125	232, 200	157, 550		470, 234
68	31, 777	311	112	267, 388	144, 969		521, 941
69	32, 722	290	97	245, 458	134, 320		473, 293
70	43, 354	301	85	190, 799	231, 464		549, 082
71	61, 743	306	49	193, 552	244, 946		608, 390

* Received January 10, 1974
** Tokyo University of Fisheries, Kōnan, Minato-ku, Tokyo, 108 Japan

and Nori *Porphyra*, and their annual production in these years are shown in Table 2, with more detail of the year 1970 in Table 3.

Quite a few species of aquatic animal are commercially cultivated. Among them, the production of oyster and pearl oyster by culture has been stagnant, in spite of the development of its production techniques, because of the narrowing down of the culture ground due to pollution and reclamation of the foreshore. In the cultivation of aquatic plants like Nori, Kuruma prawn, abalone and scallop, production has been increasing and the scale of these species will be larger than before.

Among all the species to which new cultivation techniques are being applied, the author reviews about the empirical techniques of cultivation being applied to Japanese oyster, scallop, Kuruma prawn and abalone.

2. Mass culture of seed for fish farming

In fish farming of specific species, the basic thing is to rear the seed animals of the species and there are two methods for this.

A. Natural seed collecting method
Oyster *Crassostrea gigas*, scallop *Patinopecten yessoensis*, ark-shell *Scapharca broughtonii* and yellowtail *Seliola*, their juveniles are collected in the open sea.

B. Seed culture in tanks
Flatfish *Paraichtys olivaceus*, abalone *Haliotis* and Kuruma prawn *Penaeus japonicus*, the seed cannot be collected in the open sea, therefore, their juveniles are artificially reared in a tank.

In case A, larvae, spawn and grown in the open sea, and collected when they attach themselves to the collecters. In case B, those which cannot be collected in the open sea are reared in tank almost fully artificially and in this case eggs are collected, helped by the use of injection of pituitary hormone, temperature shock or photo-schedule control etc. For the mass rearing of larvae, grown from eggs,

Table 4. The initial food-organisms for larvae in the laboratory. (Added to HIRANO *et al.*, 1963)

Species	Prey	Author
Fugu rubripes	*Mactra* larva, *Artemia* Nauplii	FUJITA, '62, ABE *et al.*, '63
Paralichthys olivaceus	egg and larva of *Echinoidea* and bivales, *Brachionus* sp.	MASUDA, OGASAWARA, '68
Kareius and *Liopsetta*	*Mytilus* larva, *Brachionus*.	MITO, '69, KURATA, '56
Seliora	*Echinoidea* and Bivalves' egg and larva	HARADA *et al.*, '69
Mylio macrocephalus	oyster larva	HIRANO, '69
Chrysophris major	*Echinoidea* egg and oyster larva. Copepod nauplii	HIRANO, '69, YAMASHITA, '60
Stichopus japonicus	*Monas* sp.	IMAI, '50
Echinoidea	*Skeletonema costatum*, *Chaetoceros calcitrans*	YAMABE, '62, UNO *et al.*, '63
Crassostrea gigas	*Monas* sp.	IMAI, '48
C. virginica	*Isochrysis*, *Monochrysis*	DAVIS *et al.*, '58
Ostrea edulis	*Platymonas* sp.	COLE, '37
Scapharca broughtonii	*Monas* sp., *C. calcitrans*,	KANNO, '63
	Phaeodactylum tricornutum	Aomori Pre., '58
Meretrix lusoria	*C. calcitrans*, *Syclotellla nana*	SAGARA, '62
Patinopecten yessoensis	*C. calcitrans*	YAMAMOTO *et al.*, '50
Haliotis	*Navicula* sp., *Ectocarpus* sp, *Coconeis* sp, *Melosira* sp, *Amphora* sp, *Platymonas*, *C. calcitrans*, Gametophyte and Sporophyte of *Eisenia*	SAGARA, INO, KIKUCHI, UNO
Sepia esculenta	*Neomysis japonica*	OSHIMA *et al.*, '61
Octopus vulgaris	Zoea of *Crangon* and *Palaemo*	Hyogo Pre. St., '62
Penaeus japonicus	*Skeletonema costatum*	HUDINAGA, '42
Portunus trituberculatus	*Artemia* Nauplii	MAEKAWA, '61

knowledge of feeding ecology for the purpose of nutrition and environmental conditions are very useful.

Larvae which are hatched out from eggs, grow on the nutrition provided by their own yolk for 3 to 10 days but they will die with the exhaustion of yolk if they fail to obtain food from outside. In other words, they can-

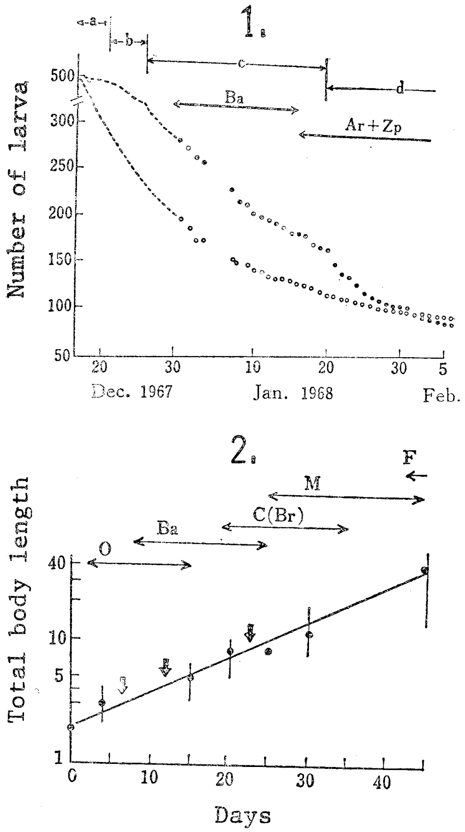

Fig. 1. Variation of survival rate of the larva, Japanese sole, *Kareius bicoloratus* in relation to trophic levels. a: egg, b: prelarva, c: postlarva, d: metamorphosis stage. Ba: rotifer, Ar: *Artemia* nauplii, Zp: zooplankton collected in the sea. Black circle: egg spawned in the pond, white: spawned artificially. (MITO *et al.*, 1969)

2. Relationship between the foods and growth of larva, black sea bream *Mylio macrocephalus*. O: larva of oyster, Ba: Barnacle nauplii, Br: *Artemia* nauplii, M: *Neomysis*, F: raw fish meal. Arrows show the critical point of larva. (Modified from FUSHIMI *et al.*, 1968)

not survive through this stage without feeding. Foods are, at this stage, called the initial foods and they are very important, particularly for aquatic animals. Table 4 is a list of the initial foods. Essential characteristics for the initial foods differ from species to species but generally they are:

A. Taking into consideration size, motion and floating ability, it should be easy to be caught by larvae.
B. Easily digested and rich in nutrition.
C. Non-toxicating.
D. Can be produced in large quantities.

As larvae grow larger they require food of higher trophic level and this in other words, means they show size preference with their

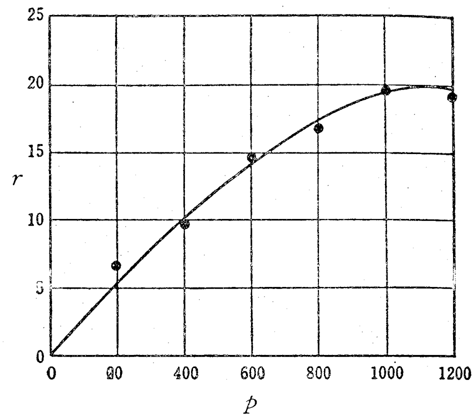

Fig. 2. Relation between the ration, r and concentration of food, p of the larva, *Macrobrachium nipponense* in the laboratory. (UNO, 1971)

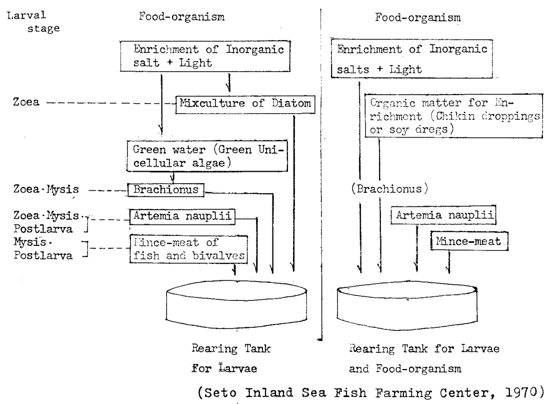

Fig. 3. The scheme of the culture food-organism.

growth and, therefore, when rearing larvae, it is necessary to change foods to match their growth. An example is shown in Fig. 1.

There have been many studies on initial foods but the one known as the most effective with widest application is brackish rotifer *Brachionus plicatilis*, for fish larvae and diatom *Chaetoceros calcitrans* for bivalve larvae. In recent years, in addition to these, active sludge (bacteria flock), has also been used as an initial food. When using this active sludge, seawater in the rearing tank is agitated continuously by agitating apparatus.

When rearing larvae, density of food is important. Even if there is a good food is used meeting all the above conditions, it its density is low, ration of larvae will be small and a good result cannot be expected. This theory is formulated by IVLEV (1961).

$$r = R(1 - e^{-kp})$$

r: ration, R: maximum ration, p: density of food organisms, k: constant.

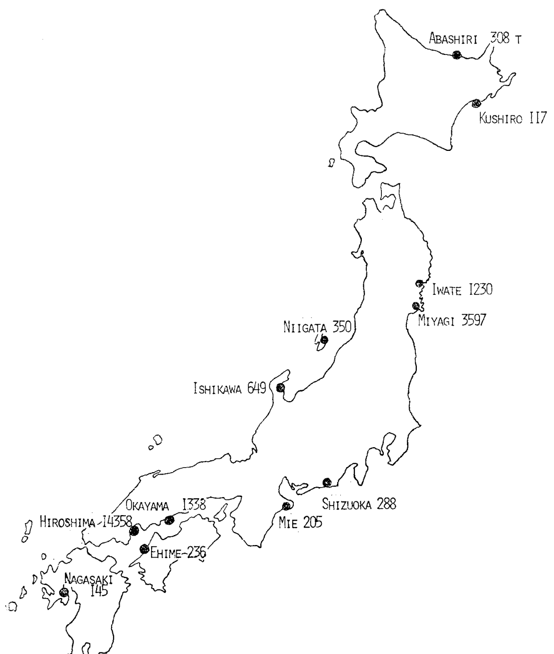

Fig. 4. Main productions of Japanese oyster, *Crassostrea gigas*. Numerals show the annual catch, 1970.

If we take as an example the freshwater prawn *Macrobrachium nipponense*, it is like Fig. 2, $r = 22.63\ (1 - e^{-0.344p})$ (UNO, 1971). In addition, it goes without saying that environmental conditions such as temperature and salinity of seawater should be well suited to the growth of the rearing animal.

In Japan, mass production of seed is being carried out in tanks conferming to all the conditions mentioned above, as a result of many studies concerning these conditions. Among other aspects in developing rearing techniques special attention is being paid to establishing a system for dealing with food organisms in the rearing tank. One of the example is the rearing of Kuruma prawn, which is shown in Fig. 3.

3. Oyster culture

In Japan, oyster culture is being done mainly with *Crassostrea gigas*. There are 17 species of oysters but commercial culture has been made only with *C. gigas* and *C. rivulgris* of which the latter is, however, in very small quantities. Main culture grounds of *C. gigas* are shown in Fig. 4, and the annual harvest is shown in Table 5. Of many places, Hiroshima and Miyagi areas are the biggest producing areas with a production of 23,149 tons (without shell) in 1970. Production in recent years has been very stagnant, as mentioned before, because of the narrowing down of the culture area, due to industrial pollution and

Table 5. Annual catch of oyster culture, tons, excluded shell.

Year	Total	Main products	
		Hiroshima	Miyagi
1960	25,977	16,753	3,717
61	23,352	16,444	4,248
62	30,075	17,370	4,778
63	35,990	22,217	4,792
64	33,506	22,429	5,109
65	34,463	23,295	3,457
66	35,361	25,417	3,993
67	38,037	28,438	3,727
68	40,928	31,188	3,814
70	23,149	14,358	3,597
71	27,836	16,362	3,605

reclamation of the foreshores. Areas now being used for oyster farming total 3,253.3 ha, which consist of:

Sowing culture	209.6 ha
Bamboo culture	181.6
Hanging culture	
Raft method	2,013.1
Long-line method	576.7
Rack method	272.4
Total	3,253.4

The majority of production is by raft method. The sequence culture is:

Seed oyster culture, growing culture, and harvesting.

1. Seed oyster culture (Fig. 5)

Japanese oyster spawns in the months between June and October. After the swimming larval stage that continues from 10–14 days after being spawned, they settle to rock substratum and start sessile life. During the transition period from pelagic from to sessile from collectors made from a number of empty oyster or scallop shells strung together on a wire passing through a hole made in each shell

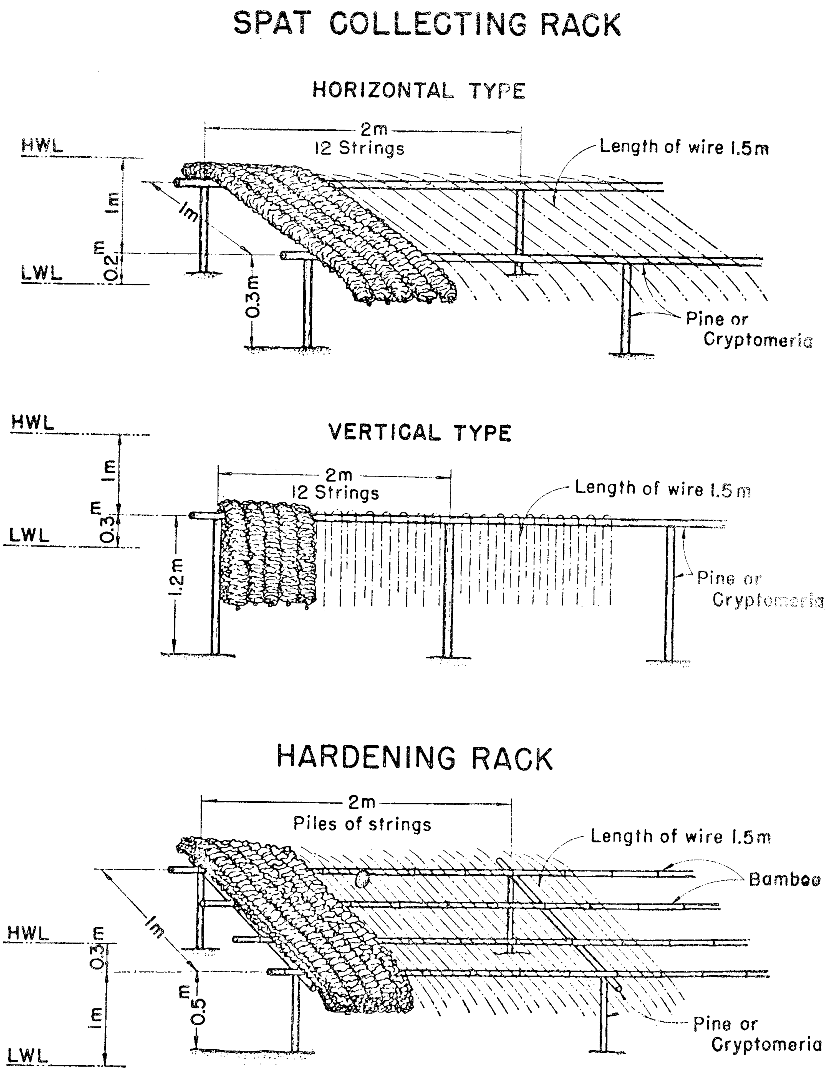

Fig. 5. Seed oyster culture Miyagi Prefecture. (CAHN, 1950)

are hung on a rack suspended in midwater. The correct timing for putting the collectors into the sea is important as it decides the success or failure of spat collection. To decide the correct timing, when the main spawning run of the year is observed, start regular counting of the larvae in the sea and when full grown larvae are observed check the settling condition of spats by using a test piece of collector. The collectors on which spats have settled are stacked on hardening racks and the spats are hardened in order to make them strong enough to undergo long transportation and high temperatures during export shipments. As a result of this process the spats become the hardened seeds which are also widely recommended for domestic culture as they are very resistant to the pollution of the environment and therefore guarantee stable production.

2. Growing culture (Figs. 6, 7 and 8)

Oysters can be cultivated by the sowing method, bamboo method and hanging method of which the hanging method is predominant. The hanging method is applied to sea-farming of all the bivalves and its advantages are:

1) Surface space in the sea can be used more efficiently. At the same time culture grounds are not dependent on bottom conditions.

2) Animals can take in more food constantly.

Oyster culture has a long history and in

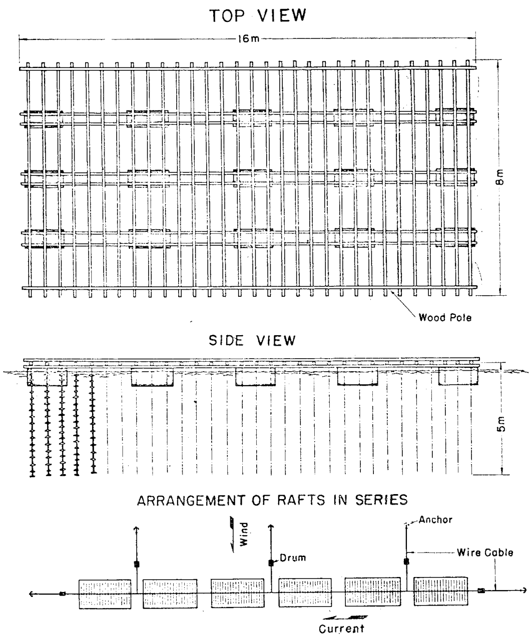

Fig. 6. Raft method of oyster culture Kanawa-jima, Hiroshima Prefecture. (CAHN, 1950)

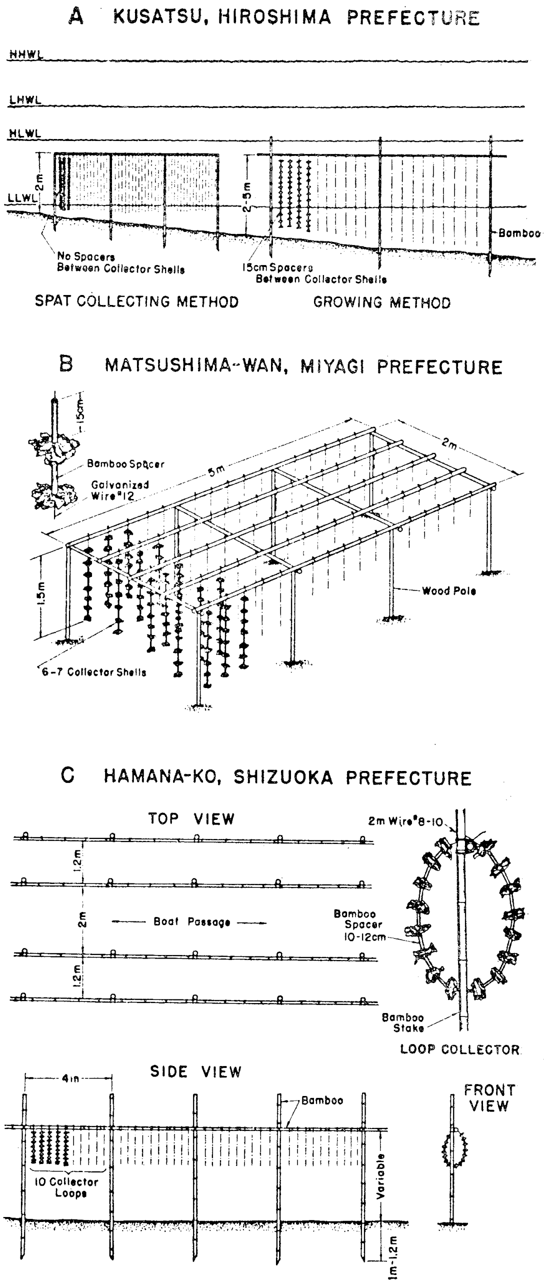

Fig. 7. Rack method of oyster culture. (CAHN, 1950)

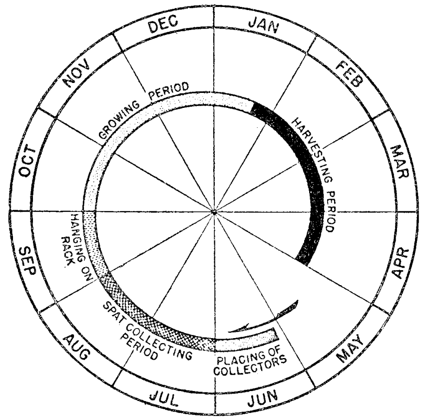

Fig. 8. Seasonal activities of rack culture method, one-year crop at Hiroshima Pre. (left figure) and seed oyster culture method at Miyagi Pre. (right figure). (CAHN, 1950)

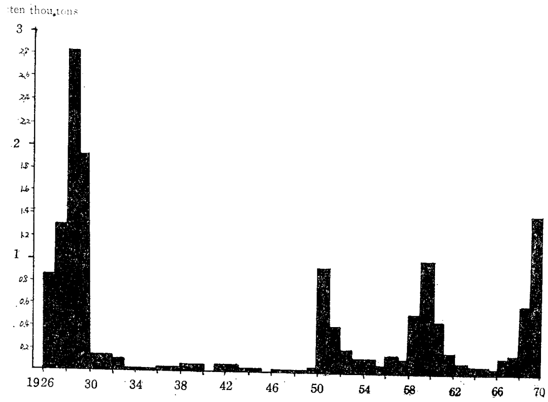

Fig. 9. Total catch of scallop between 1926~70 in Mutsu Bay.

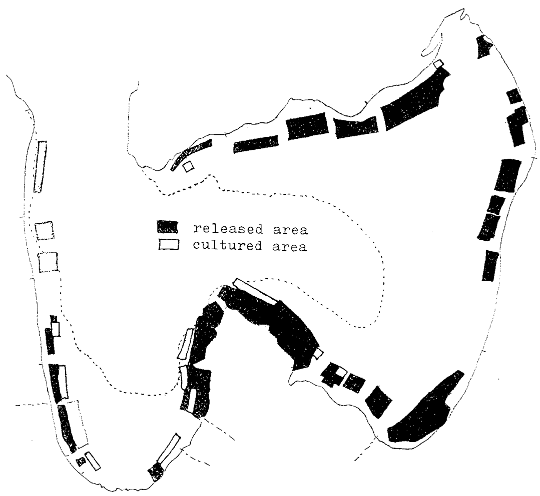

Fig. 10. The released area and cultured area of scallop in Mutsu Bay.

Table 6. Annual yields of spats in Mutsu Bay.

Item \ Year	1966	1967	1968	1969	1970	1971
Total no. of equipments	101	228	683	1,000	2,049	2,467
Total no. of collector ($\times 10^3$)	32	98	305	582	1,513	2,486
Mean no. of attached spats per collector	201	1,012	2,089	405	10,124	10,734
Total no. attached spats ($\times 10^6$)	3	176	893	229	15,725	38,283
Total no. of spats used for intermediate culture ($\times 10^6$)	1	75	325	85	1,594	2,087
Rate of use for intermediate culture in %	33.3	42.6	29.4	37.1	10.1	5.5
Total no. of spats for bottom culture ($\times 10^6$)	—	52	324	37	1,215	1,447
Total no. of seed for hanging culture ($\times 10^6$)	—	2	23	27	79	126
Total no. of seed soled to other localities ($\times 10^6$)	—	2	14	10	95	140

Japan it can be said to be the origin of all sea farming type fisheries. As the oyster culture grounds are bays and esturies, they are now flooded by industrial effluents and sewage which give rise to red waters and explosive propagation of fouling animals. Because of these phenomena and the biodeposition which lowers the productivity of the culture grounds, production of oyster in Japan has been badly affected, giving rise to a serious problem for the oyster producers.

Table 7. The possibility of scallop production in Mutsu Bay. (HIRASAWA, 1972)

	Total	Stocking	Culture
	ton	ton	ton
Total	189,000	148,000	41,000
The area of fishing right	117,000	106,000	11,000
stocking area	73,000	72,000	1,000
mixing area	21,000	20,000	1,000
cultivated area	23,000	14,000	9,000
The open sea in the bay	72,000	42,000	30,000

4. Scallop culture

In Japan, Scallops *Patinopecten yessoensis*, are mainly produced in Hokkaido and Aomori

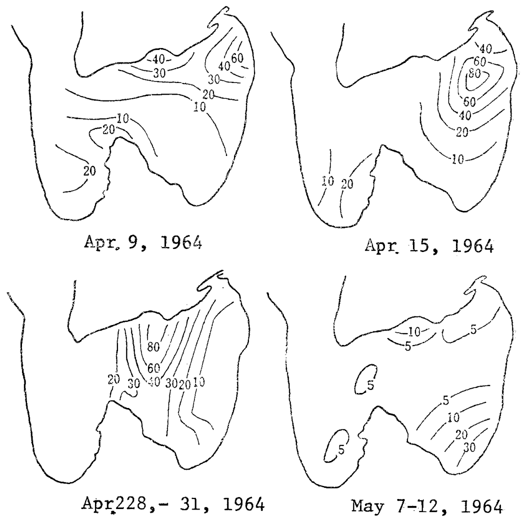

Fig. 11. Distribution of larvae, *Patinopecten yessoensis* in Mutsu Bay. (ITO *et al.*, 1967) Numerals show the density of larva (Ind./m^3).

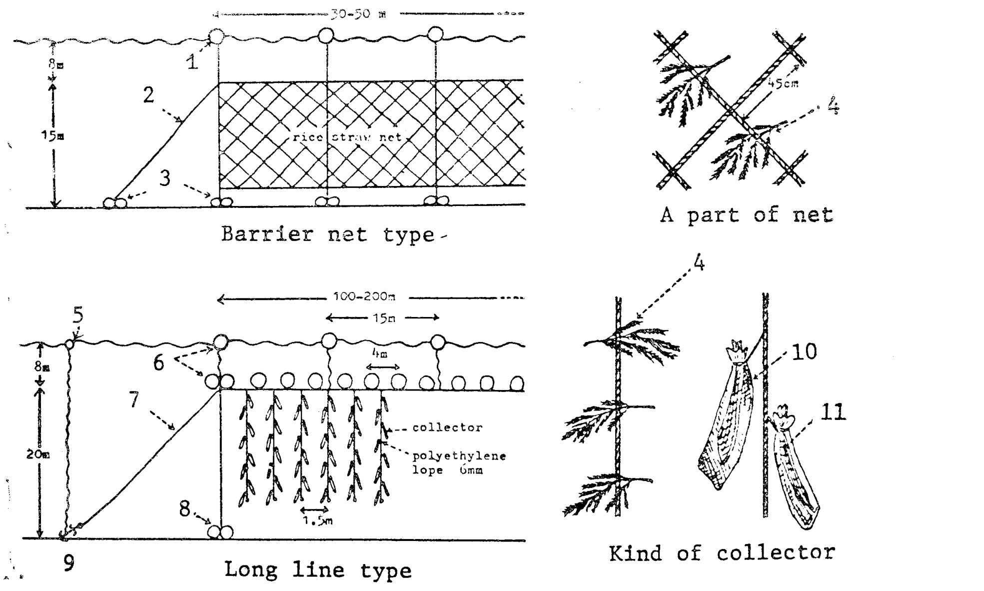

Fig. 12. Equipments for natural spats collection. (ITO *et al.*, 1972)
1: float, 2: rice straw rope, 3: sand bag, 4: Japanese cedar leaves, 5: float, 24 cm, 6: float, 36 cm, 7: polyethylene rope, 16-18 mm, 8: sand bag, 9: anchor, 40-50 kg, 10: polyethylene net for covering, 11: polyethylene or nylon.

Prefecture by fishing, but of late there has been remarkable progress in culture techniques and its culture grounds are fast expanding. In 1970 production by fishing was 16,639 tons while that by culture reached 5,675 tons. The annual landings in Mutsu Bay in 1926-70 are shown in Fig. 9. Up to 1966, production was mostly by fishing annual production varied widely from year to year. Since 1966, with the commercial introduction of scallop culture, fishing grounds have also been expanding and in 1970 production there reached 15,000 tons. The situation in 1970 is explained in Fig. 10. There are still many unexploited fishing grounds and production is expected to reach 30,000 tons in the near future.

The tend in the development of seed scallop culture is shown in Table 6. In 1970, the total number of collected spats was 28,283 million out of which 2,087 million spats were culture to be seed scallop, about 5.5 % of the collected spats. Therefore, it is possible to increase the production further, by expanding the culture grounds. Table 7 gives an estimate of possible production which is 189,000 tons, consisting of 73,000 tons by sowing culture, 21,000 tons by combination of sowing and hanging culture, 23,000 tons by hanging culture and 72,000 tons by offshore fisheries. This corresponds to 6.7 times of the largest annual production in the past (HIRASAWA, 1972).

Japanese scallop start to spawn the water temperature reaches ca. 9°C and this is from the end of May through to the end of June in Lagoon Saroma, Hokkaido and from March through to April in Mutsu Bay, Aomori Prefecture. One adult scallop discharge more than 100 million eggs. To collect spats it is necessary to make tests to determine the spawning season each year and the occurrence and distribution of swimming larvae in the sea. One such example is shown in Fig. 11, where will find big fluctuation in larval distribution over a short period, which may be attributable to wind direction, wind force and tidal currents. The detailed mechanism of these fluctuations will be known before long. When full grown veligers appear, collectors, as illustrated in Fig. 12, put into the sea. The spats that are attached to the Japanese ceder leaves grow to 6-10 mm in shell length in July and Augus and they stay on the ceder leaves, attached by their bysuss untill the end of September when they reach about 15 mm in shell length and

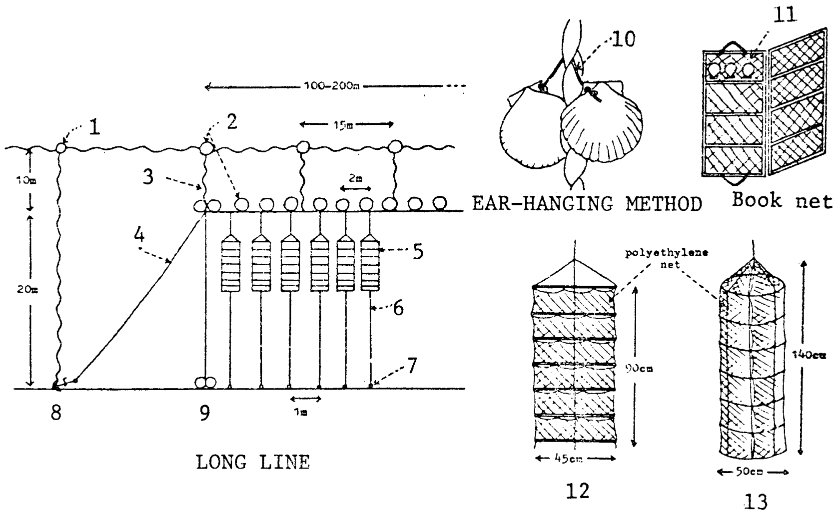

Fig. 13. Various equipments for hanging culture.
1: float, 24 cm, 2: float, 36 cm, 3: polyethylene rope, 16-18 mm, 5: lantern net, 6: polyethylene rope, 6 mm, 7: weight, 500 g, 8: anchor, 40-60 kg, 9: sand bag, 40 kg, 10: nylon string, 1.8-2.0 mm, 11: polyethylene net, 12: pocket net, 13: lantern net with seven compartments. (ITO *et al.*, 1972)

then release themselves naturally from the collectors and begin their benthos life.

Collected spats are reared to be seed scallops. They are put in a net of 1-5 mm mesh and cultivated by the hanging method, and as they grow larger they are selected according to size from time to time and transferred to pearl-nets of bigger mesh where they are cultivated to about 3 cm shell-length. All this process is by the hanging method, of which an example is shown in Fig. 13. Various nets are employed such as book nets, lantern nets and pocket nets and for cultivation, netted spats are hung in water with a depth of 10-30 m. Growth of the spats depends on the conditions of the culture grounds such as water temperature, availability of food plankton, tidal current and others but among them the water temperature seems to be the most important factor, as shown in Figs. 14 and 15, and spats grow faster in the southern waters. Scallops are known to die if the water temperature exceeds 23°C.

In hanging culture, scallops grow very slowly in waters less than 5 m deep while with oysters, quite the opposite. Therefore, it is worth trying to examine the possibility of combined culture of oysters and scallops (Fig. 16).

The sowing method, which requires no materials is the simplest culture method but this is very much influenced by the bottom conditions of the culture grounds. In Mutsu Bay, sites with a depth of 5 to 30 m having fine sand, coarse sand or pebbles on their bottom and exposed to the tidal current are thought to be suited to the sowing method. Optimum density of population is said to be 5

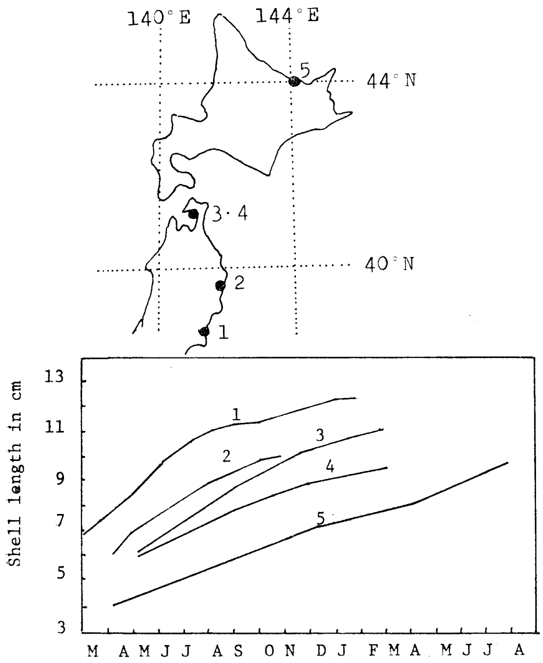

Fig. 14. Growth of the scallop cultured with hanging method in various localities, Tohoku region and Hokkaido, Japan.

1: Kesennuma Bay, Miyagi Pre., Ear-hanging method, 2: Ofunato Bay, Miyagi Pre., Ear-hanging method, 3: Mutsu Bay, Aomori Pre., Lantern net, 4: Mutsu Bay, Pocket net, 5: Lagoon Saroma, Hokkaido, Pocket net. (ITO *et al.*, 1971)

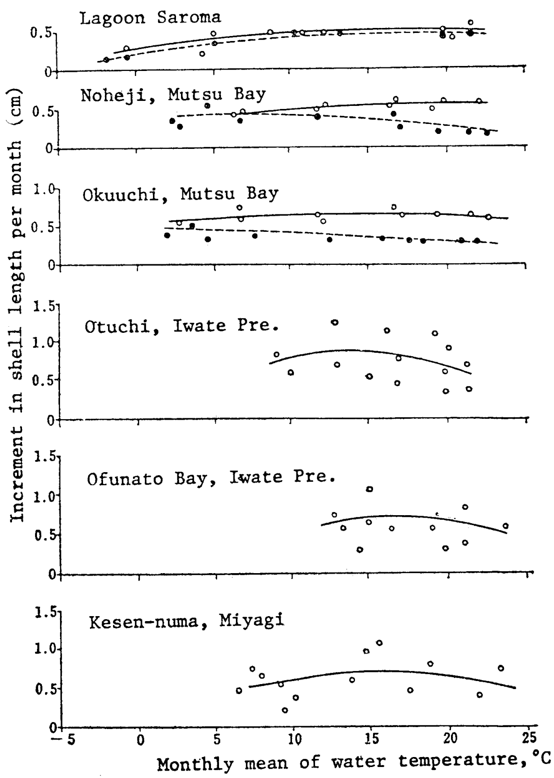

Fig. 15. Monthly growth rate of *Patinopecten yessoensis* in relation to water temperature. Black circle: one year old after culture, white circle: two years old. (ITO *et al.*, 1971)

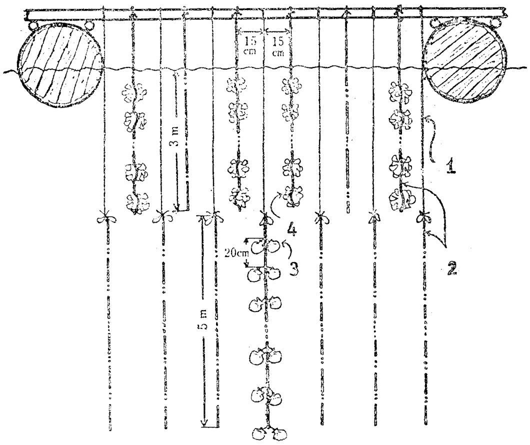

Fig. 16. The hanging culture of scallop in combination with oyster (*Ostrea edulis*).
1. Manila rope, 6 mm, 2. Straw rope coated with coal tar, 2 cm, 3. Scallop spat, 4. Oyster spat. (ITO *et al.*, 1971)

Table 8. The economic efficiency per ha of culture and stocking. (HIRASAWA, 1972)

Item \ Method	culture	stocking
Catch (piece)	36,000	31,300
Landing value (thou. yen)	1,080	751
Cost (thou. yen)	405	247
Income (thou. yen)	675	504

or 6 scallops per square meter. Grown scallops are harvested by dredging 2 to 3 years after sowing.

Economic comparison of hanging culture and sowing culture is show in Table 8 where the former shows higher productivity. Table 9 shows the outline of scallop culture business according to the scale of the business. Class A, using 5 sets of hanging racks each with long-line 100 m in length shows high productivity of labor is lower. Class C is just the opposite of class A. From Table 9 the productivity of scallop culture can be calculated and this is shown in Table 10. From this, the optimum size of scallop culture business in Mutsu Bay is said to be class B (HIRASAWA, 1972).

Table 9. Cost and income of scallop culture by farm scale. (HIRASAWA, 1972)

Item \ Scale		A (5 set)	B (10 set)	C (20 set)
Landing value (yen)		1,900	3,110	5,758
Cost		544	1,088	2,902
equipment		62	121	253
cage		163	272	504
seed		79	132	250
wage		90	400	1,600
dep. etc		150	163	295
Income		1,356	2,022	2,856
Catch	(piece)	66,000	108,000	199,000
	(tons)	11.9	19.4	35.9
Family labor	(man)	2	2	2
	(woman)	1	1	1
Worker woman-days		90	400	1,600

Table 10. Productivity of scallop culture. (HIRASAWA, 1972)

Item \ Scale	A	B	C
Cost per shell (yen)	5.2	9.9	14.5
Income per family labor (thou. yen)	502	756	1,056
Value added per laborer (yen)	172	210	189
Income per long line (yen)	271	211	190
Income per 1 ha (yen)	753	631	396

5. Kuruma prawn culture

Following Fudinaga's study (FUDINAGA, 1942), great progress has been made during the past 20 years in the study of the pond-culture of Kuruma prawn but the studies were mainly focussed on the production of seed prawns with little attention paid to the problem of rearing prawning juveniles to adults. In recent years there has been remarkable progress in the studies of intensive pondculture and it has become possible to produce 2 kg per square meter.

The Japanese government established the Seto Inland Sea Fish Farming Center to restore and increase the marine resources in the area. After many feasibility studies on the rearing of prawns from their seeds they now produce 173 million larvae per year including both fish and shellfish to stock the open sea with them.

As Kuruma prawn, they developed a technique to produce 24 million postlarvae by using a 1,200-ton tank and studies are now being made from standpoint of ecology and other aspects about stocking the sea with the seeds.

Notwithstanding the increase in production of Kuruma prawn seeds, production of this prawn by pound culture was only 301 tons in 1970 and the main reasons for this stangation in pond culture are firstly, a good portion of the seeds thus produced are liberated in the open sea, secondly many of the sites suitable for pond culture have already been exploited and not much room is left for new exploitation and thirdly the technique for intensive pond culture has not yet been fully developed, in particular, not much is known about feeding.

The spawning season for Kuruma prawn in Japan is from May through to October, and the season comes earlier in southern waters. During the spawning season, parent prawns with matured roe are caught and placed in a spawning tank (10×10×2.5 m) in batches of 50 to 100 prawns to a tank. If the temperature of the water is kept at 28°C, they spawn on the day they are caught or the following day. If the spent prawns are removed, the spawning tanks become larvae rearing tanks. The

Table 11. Life history phase of *P. japonicus*. (KURATA, 1972)

Phase	From begins	Duration[a] in days	Approx. body length (mm)		Life form	Habitats
			Male	Female		
Embryo	Fertilization	0.6	0.24[b]		Planktonic	Offshore
Larva	Hatching	14—15	0.3—5.0		do	do
Juvenile	Metamorphosis	30	5—25		Planktonic-Benthic	Offshore-Esttary
Adolescent	Development of secondary sex characters	60	25—90[c]	25—110[d]	Benthic	Estuary-Sound
Subadult	Onset of gonad maturation	?	90—100[e]	110—125[e]	do	Sound-Offsho re
Adult	Completion of gonad maturation	?	100—220[f]	125—262[f]	do	Offshore

a) Approximate number of days in summer.
b) Diameter of egg. (mm)
c) Minimum size with jointed petasma.
d) Minimum size with stopper.
e) Minimum size with ripe gonads.
f) Maximum size ever found.

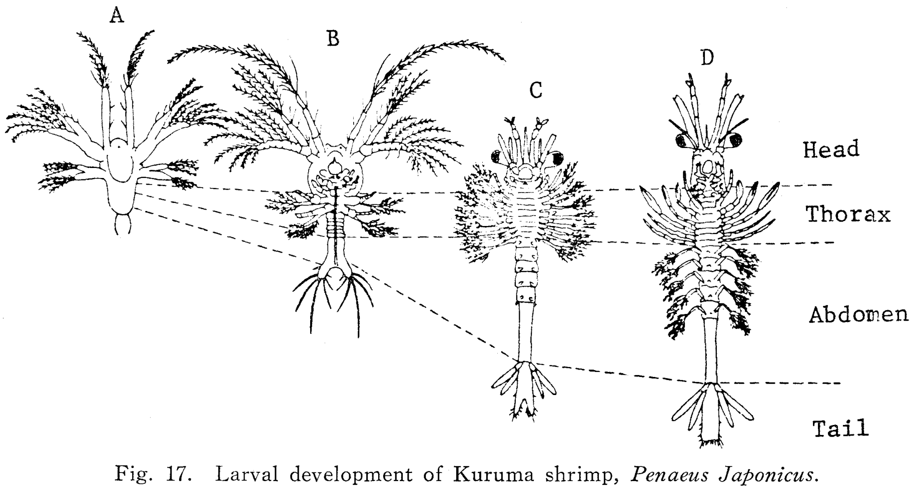

Fig. 17. Larval development of Kuruma shrimp, *Penaeus Japonicus*. A. Nauplius, B. Protozoea, C. Zoea, D. Megalopa (Postlarva). (KURATA, 1972)

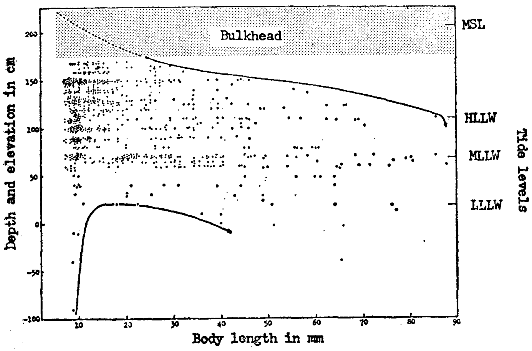

Fig. 18. Vertical distribution of *P. japonicus* juveniles and adolescents in the intertidal zone exposed at low tide, Saijo, Aug.-Sep., 1971. Each dot represents one individual. (KURATA, 1972)

larvae emerge from the eggs as nauplius in about 28°C. Nauplius moult six times and pass into the zoea. Zoea pass into mysis after 3 moultings and mysis pass into postlarvae after 3 moultings. During this larval period, feeding is controlled as shown in Fig. 3 using diatom, *Brachionus*, *Artemia* and minced meat of bivalves and fish, depending on the stage of development. Postlarvae, after about 30 days rearing in tanks, grow to 9 to 12 mm size and becomes seeds for stocking and pond culture. The seed thus produced are mostly used to stock the sea and partly for pond culture.

The life history of Kuruma prawn is shown in Table 11 and Fig. 17. In view of their life cycle, the best time to liberate the stocking seeds in the sea is when the prawns, becoming adolescents 70-90 mm in size, start benthos life. In this period, their habitat is mainly in an intertidal zone and when they grow to a size of 40-90 mm they gradually extended their

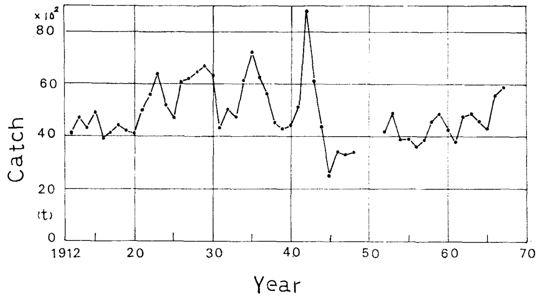

Fig. 20. Fluctuations in the landings of Japanese abalones, *Haliotis*.

living spheres into deeper water (Fig. 18). Prawns are preyed on the fish and other predators when they are liberated in the sea and, therefore, the intertidal zones with many tidal pools provide havens for the young prawns. Optimum stocking rate is considered to be 10 to 20 pieces per square meter.

Problems connected with pond culture are the difficulty in preparing good quality formulated diets and the deterioration of the quality of the water in the rearing tanks due to feeding. As prawns stay in the bottom sand during the day time they are also affected by the decomposition on the bottom due to their own biodeposits and food remnants. Many studies have been made to solve these problems and the most advanced methods of pond culture have by SHIGENO (1972) the following characteristics.

1. Tank water is kept clean, (free from deterioration), by supplying large quantities of seawater.
2. In order to maintain a good environment for the prawns which stay in the sand-beds during the day, the tank is made with a double bottom with sand of 10-15 cm thick and the water is discharge through this

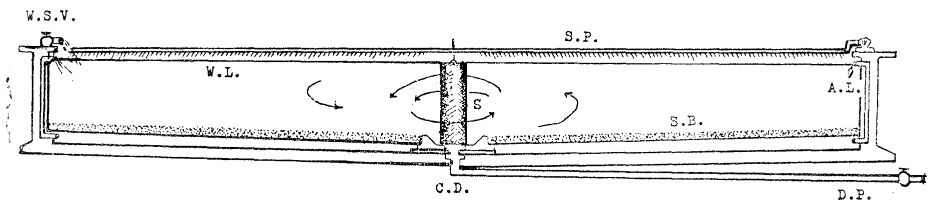

Fig. 19. Side view of round tank used for experiment.
WSV: water supply valve, WL: water level, CD: central drain, S: screen, SP: shower pipe, SB: sand bed, AL: air lift, DP: drain pipe. (SHIGENO, 1972)

sand bed during the day time, (by overflowing at night).

3. A round tank is used and with a shower pipe, a strong circular movement is given to the water in the pond and this automatically collects food remnants and moulted skeletons in the center of the pond for discharge.
4. In the hope of achieving quicker growth, a formulated diet having a protein content similar to the prawn itself is being developed.

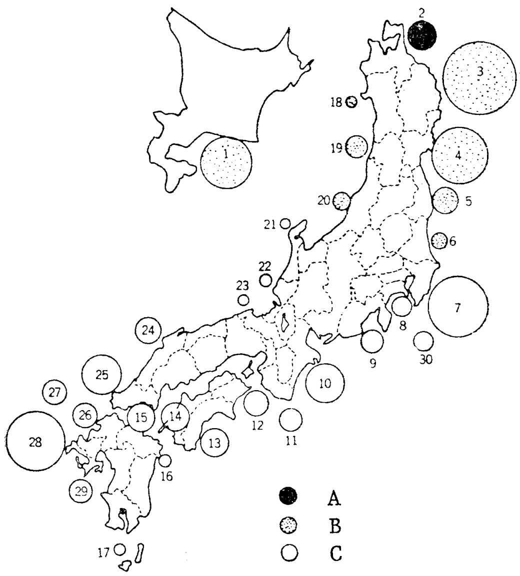

Fig. 21. Showing the distribution of *Haliotis* in Japan, basing on the commercial catch. A: *Haliotis discus hannai, H. discus, H. sieboldi,* and *H. gigantea,* B: *H. discus hannai,* C: *H. discus, H. sieboldii* and *H. gigantea.*
1: Hokkaido, 574 tons, 2: Aomori, 280, 3: Iwate, 1283, 4: Miyagi, 693, 5: Fukushima, 83, 6: Ibaragi, 39, 7: Chiba, 750, 8: Kanagawa, 65, 9: Shizuoka, 91, 10: Mie, 384, 11: Wakayama, 116, 12: Tokushima, 106, 13: Kochi, 33, 14: Ehime, 109, 15: Oita, 103, 16: Miyazaki, 7, 17: Kagoshima, 9, 18: Akita, 14, 19: Yamagata, 45, 20: Niigata, 37, 21: Ishikawa, 26, 22: Fukui, 29, 23: Kyoto, 22, 24: Shimane, 102, 25: Yamaguchi, 315, 26: Fukuoka, 105, 27: Saga, 83, 28: Nagasaki, 710, 29: Kumamoto, 67, 30: Tokyo, 79.

Fig. 19 is an example of a representative round pond. The tank has a 1,000 m^3 capacity with a 23 m diameter, 2.5 m deep, double bottom with 15 cm thick sand, average water supply of 1,620 tons per day and the pond is used for rearing during six months between September and February with postlarvae P44 population of 80,000 pieces (mean body weight 0.068 g) fed with formulated diet; survival rate is 93.0 %; production efficiency 2.65 kg per square meter (186 pieces per square meter); and about 1 ton of prawns is produced. The basic ingredients of the formulated diet are squid meal, mysid shrimp meal, brine shrimp meal, petroleum yeast, marine yeast, fish meal active sludge, gluten, soya bean protein, whale meal and casein. These twelve kinds of protein containing materials are mixed and formed into a thread like shape and dried to a moisture content of 10 %. Crude protein content of this formulated diet is more than 60 %.

6. Haliotis culture

Annual landing of abalone in Japan in the past 60 years has fluctuated between 4,000 and 8,000 tons as shown in Fig. 20. Fig. 21 shows the industrial distribution of abalone, of which the commercial species are *H. discus hannai, H. discus, H. sieboldii, H. gigantea* and *H. diversicolar spertexta.* In the last several years it has become possible to produce seeds of these varieties. As it takes at least 4 to 5 years for abalone to grow to adult size it is advisable to increase production by the stocking method rather than by the culture method.

In order to increase the production of abalone through stocking in fenceless natural environment, much ecological knowledge is needed about their distribution, migration and habitat.

As shown in Fig. 22, abalone spawns when the water temperature comes down to 20°C. Regarding spawning, a water temperature of 20°C can be taken as a physiological constant. Utilizing this natural factor, a temperature shock given to mature parent abalone, induces spawning and fertilized eggs can be obtained. The eggs thus obtained are hatched out in approximately 18 hours at a water temperature of 20°C, and after 3 or 10 days of pelagic stage, the larvae settle down to benthos life. As initial foods, they eat primarily small size unicellular algae such as *Platymonas* sp., *Navicular* sp., *Cocconeis* sp., gametophyte and sporophyte of *Eisenia*. As they grow to a shell-length of about 3 mm they feed on small common algae and with their further growth they like to eat large algae, particularly brown algae such as *Eisenia*, *Undaria* and *Laminaria*. For seed production, water temperature and salinity are important factors. Fig. 23 shows the outcome of the experiments on temperature-salinity combinations which influence the process of swimming larvae metamorphosing into benthos. Optimum range is with water temperature of 16-24°C, and salinity of more than 30 ‰. Fig. 23.A illustrates a seed collection system worked out on the basis of the above conditions. The collector used is made of transparent corrugated polyethylene sheets the surfaces of which are covered with diatom which have attached themselves beforehand. This type collector spats can be collector spats can be collected in a density of 40,000-50,000 per 3.3 m².

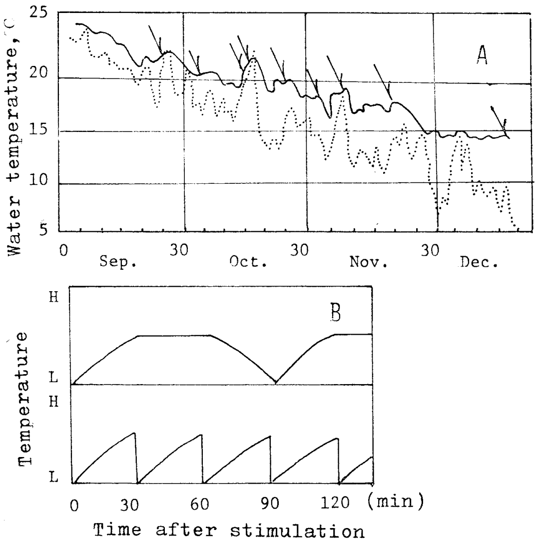

Fig. 22. Relationship between temperature and spawning of *Haliotis*. (From Data of Chiba Pre. Fish. Res. Stn., 1962)

A. Showing the spawn of *H. discus* (arrow) under laboratory condition.

B. Two methods for promoting spawn by temperature control.

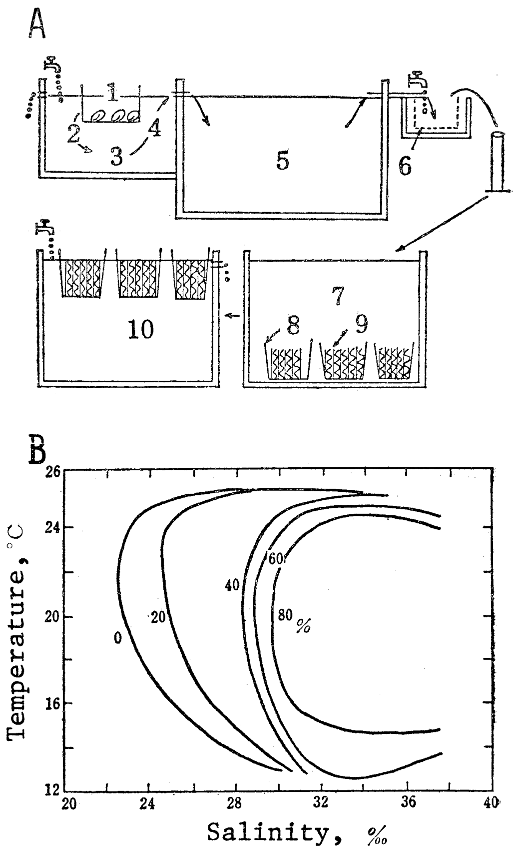

Fig. 23. A. The Scheme showing the rearing method.

1: adult shell, 2: fertilization, 3: hatch out, 4: floating of larva, 5: rearing tank for larvae, 6: filer, 7: collecting tank for spat, 8: basket, 9: corrugated polyethylene sheets, 10: nursery tank for spat. (KIKUCHI, 1964)

B. The effect of the combinations of temperature and salinity on the metamorphosis rate of larva, *H. discus*.

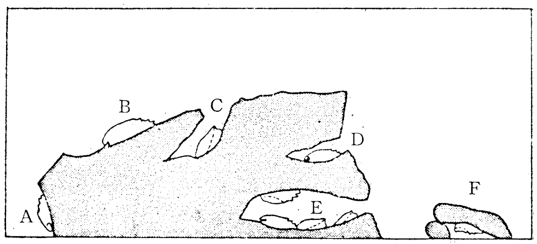

Fig. 24. Typical rocky habitat of Japanese abalone.

A. rock wall, B. exposed surface, C. crevice, D. ledge, E. cave, F. place beneath stone.

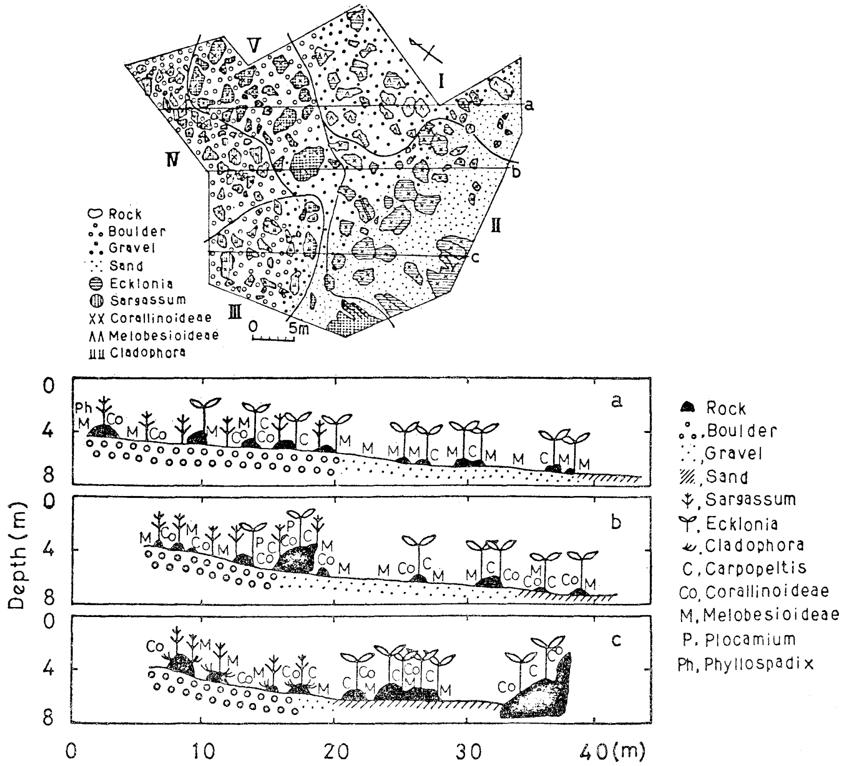

Fig. 25. Physical bottom conditions and vegetation (upper), and bottom profiles of the transections at a, b and c lines in upper figure, (UNO *et al.*, 1972)

Collected spats are reared until they reach a shell length of 3 cm and are then released in the open sea for stocking. Abalones prefer to live in particular areas of a rocky shore as illustrated in Fig. 24. As to their ecology in a natural environment, much information has been obtained through observations which the author has made by diving. Abalone are found distributed in a concentrated fashion in a particular microhabitat, and the individuals that make a home of such a microhabitat tend to occupy that partucular place and, therefore, stocking abalones cannot settle in those places which have former occupants. Abalones migrate vertically and those placese which have former occupants. Abalones migrate vertically and they move to shallower water when the water temperature drops in winter. Smaller abalones migrate gradually to deeper water as they grow larger. In releasing for stocking, therefore, it is necessary to select suitable sites with due regard to such ecological characteris-

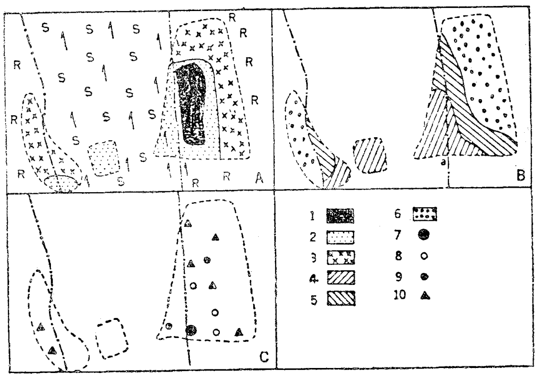

Fig. 26. Showing the distribution of abalone, *Haliotis discus hannai* in relation to structure man-made reef and food algae and water current in the field.
A. Distribution of N-type concrete block (1: piled up area, 2: 1 block/1-4 m^2, 3: 1 block/10-20 m^2).
B. Density of food algae (4: 1-3 kg/block, 5: less than 1 kg/block, 6: rare).
C. Density of abalone (7: more than 15/block, 8: 15-9/block, 9: 4-8/block, 10: 1-3/block).
Dotted lines area, S and R show the area of block distributed, sand and rock bottoms, respectively. (After Ibaragi Pre. Rep., 1965)

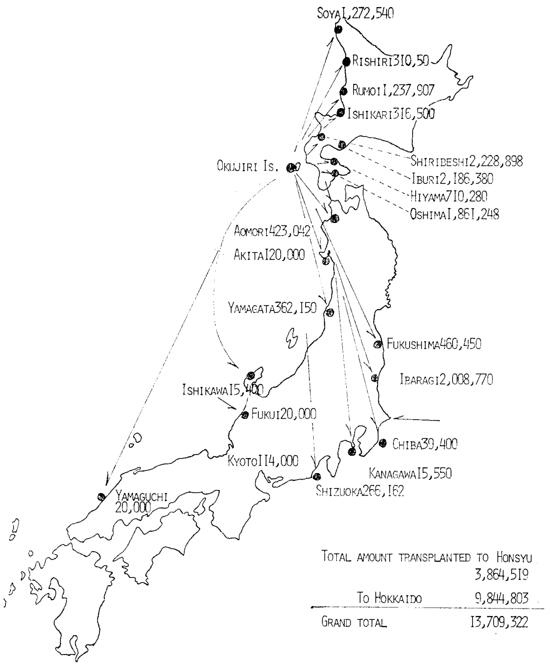

Fig. 27. Transplantation of abalone spat, *Haliotis discus hannai* occurred in Okujiri Is., Hokkaido through 1965–1968.

tics of abalone. Fig. 25 shows the result of researches concerning bottom profiles and it is known that the larger indviduals prefer to live in kelp zones in Zone II.

From many studies, it has been established that the habitat for abalone should meet with the following minimal conditions:

1. A shore reef of a type that shelters the place from sunshine.
2. Food algae is abundantly available.
3. Accessible to a tidal current that helps the concentrated distribution of abalone.

When the bottom conditions are not suitable for abalone, N-type concrete blocks are laid to provide man-made reefs for abalone. It can be seen from Fig. 26, that the distribution of abalone is concentrated in those areas where the above-mentioned three conditions are well fulfilled.

An example of seed abalone stocking in Japan is shown in Fig. 27. Though of a northern species, 14 million individuals of *H. discus hannai* were transplanted to southern waters in the 1965–68 period. The outcome, shown in Fig.

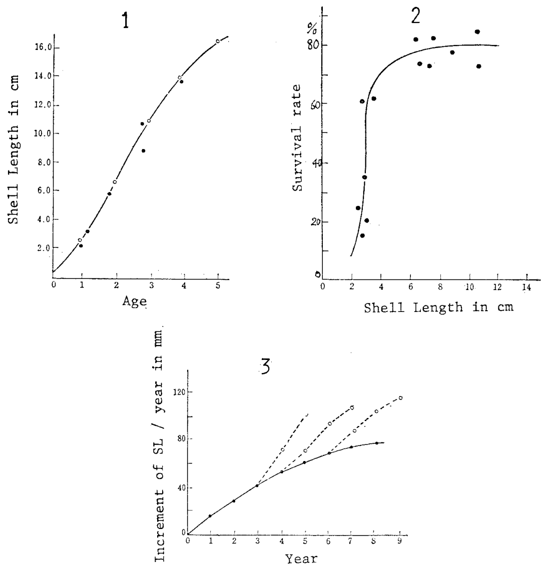

Fig. 28. Showing the growth of the abalone spats stocked sea.

1. Growth of the spats artificially collected. Black circle, *H. discus*. White circle, *H. gigantea*.

2. Survival rate of the stocked spats after one year in relation to the size (shell length), *H. gigantea* (Kanagawa Fish. Res. Stn., 1969)

3. Growth of stocked abalone, *H. discus hannai* introduced to Ibaragi Pre. Solid line, growth of the native ground, Okujiri Is., Hokkaido (1970).

28–3, revealed that their growth was much faster there than in their place of origin. The survival rate of stocking abalone depends on the bottom conditions in the stocking area, but generally speaking, the rate is higher with indivials of larger size. Artificically collected spats grows to a shell length of 2.3 cm in the first year, 6.7 cm in the second year, 10.7 cm in the third year, 13.9 cm in the fourth year and 17.6 cm in the fifth year.

References

CAHN, A. R. (1950): Oyster culture in Japan. General Headquarters, Natural Resources Section, Rep., **134**, 1–80.

FUSHIMI, T., K. KITAJIMA and M. OUCHI (1968): Study on the mass-rearing of larvae of *Chrysophrys major*. Bull. Hiroshima Pre. Fish. Res. Stn., No. 1, 37–48.

HIRASAWA, Y. (1972): A study on the use of fishing ground, management and distribution of Japanese scallop culture in the Bay of Mutsu. Preprints of International Ocean Development Conference Tokyo, 1972, 1702-1714.

HIRANO, R. and Y. OSHIMA (1963): On the rearing larvae of marine animals and their foods. Bull. Jap. Soc. Sci. Fish., **29**(3), 282-297. (in Japanese)

HUDINAGA, M. (1942): Reproduction, development and rearing of *Penaeus japonicus* Bate. Jap. J. Zool., **10**, 305-393.

ITO, S., F. TSUBATA, K. TAKEDA, M. CHIBA and Y. NAGATANI (1967): Studies on the aquaculture of the Japanese scallop. (1) Seed scallop collecting experiment. Rep. Aquaculture Center of Aomori Pre., No. 9, 1-22. (in Japanese)

ITO, S. *et al.* (1971): Techniques on the scallop culture. Through culture at shallow waters, Chap. III, Development of scallop culture. Kosei-sha-Koseikaku, pp. 187-263.

IVLEV, V. S. (1961): Experimental ecology of the feeding of fishes (translated from the Russian by D. SCOTT). Yale Univ. Press., p. 22.

KANNO, H. (1970): On the relationship between the occurrence of pelagic larvae and attached spats in Okunai. The Aquiculture, **17**(3), 121-134. (in Japanese)

KIKUCHI, S. (1964): Study on the culture of abalone, *Haliotis discus hannai* Ino. Contribution at the 1964 Peking Sym. GEN 041, 185-202.

KURATA, H. (1972): Certain principles pertaining to the penaeid shrimp seedling and seeding for the farming in the sea. Bull. Nansei Reg. Fish. Res. Lab., **5**, 33-75.

SHIGENO, K. (1972): New technical aspect on the cultivation of prawn *Penaeus japonicus*. Preprint of the second International Ocean Development Conference, Tokyo 1972, **2**, 1726-1738.

UNO, Y. (1971): Studies on the aquaculture of *Macrobrachium nipponense* (De Haan) with special reference to breeding cycle, larval development and feeding ecology. La mer, **9**(2), 123-128.

UNO, Y., Y. KOIKE and H. MONMA (1972): Ecological studies on the propagation of the Japanese abalone (Genus *Haliotis*)—I. Distribution and movement of *Haliotis sieboldii* in the natural environment. La mer, **10**(2), 43-49. (in Japanese)

ERRATA

Volume 11, No. 4 (1973), p. 219, column 1, line 31: Change "80-130 mg" to "80-130 μg".

p. 220. Replace Fig. 1 with the following:

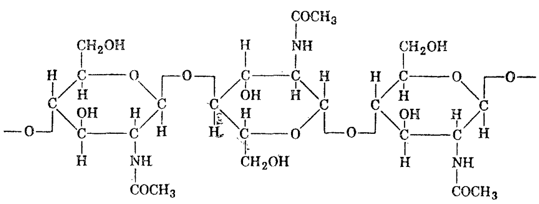

学　会　記　事

1. 昭和48年12月20日と12月28日に，東京水産大学において第2回及び第3回日仏海洋学会賞受賞候補者推薦委員会が開かれ，審議の結果，昭和49年度受賞候補者として松生洽氏を推薦することとし，この旨森田委員長から会長に報告した。

2. 昭和49年2月25日，東京水産大学において編集委員会が開かれ，第12巻第1号の編集が行われた。

3. 会員の住所，所属の変更。

氏　名	新住所又は新所属
関川　正	福島県いわき市泉町下川字八合 79-1 いわき製作所
楠　宏	東京都板橋区加賀 1-9-10 国立極地研究所
冨永　政英	鹿児島市鴨池町 52 鹿児島大学工学部海洋土木開発工学科
長谷川　隆	豊田市竜神町飛越 37　松風荘3号
日本海洋産業K.K.	東京都新宿区西新宿 2-6-1 新宿住友ビル内私書箱47号
日本アクアラングK.K.	東京都品川区東品川4-9-26 南産業ビル内

4. 交換及び寄贈図書。

1) 海洋機器開発，**5**(11, 12)，**6**(12).
2) 研究実用化報告，**22**(10, 11).（電通研）
3) 国立科学博物館専報，No. 6, 1973.
4) 海洋産業研究資料，**5**(1).
5) 日本航海学会論文集，50 号.
6) 鯨研通信，268, 269 号.
7) 日本プランクトン学会報，**20**(1).
8) なつしま，No. 5.
9) 広島大学水畜産学部紀要，**12**(2).
10) 国立科学博物館研究報告，**16**(4).
11) Ocean Age, **6**(1～3).
12) Boletin Informativo, N° 1～6.
13) Science et Pèche, N° 227, 228.
14) Bulletin de l'Association de Géographes Françis, N° 410, 1973.
15) Bulletin de l'Institut de Géologie de Bassin d'Aquitaine, N° 13, 1973.
16) Revue des Travaux de l'Institut des Pèches Maritimes, Tome XXXVII.

賛助会員

旭化成工業株式会社	東京都千代田区有楽町 1-12-1
井出利明	釧路市白金町 11
株式会社内田老鶴圃新社　内田悟	東京都千代田区九段北 1-4
梅林弘直	東京都千代田区大手町 2-2-1　新大手町ビル7階　極東貿易株式会社
株式会社大林組	東京都千代田区神田司町 2-3
小樽舶用電機株式会社	小樽市色内町 1-20
株式会社オルガノ	東京都文京区本郷 5-5-16
株式会社　オーシャン・エージ社	東京都千代田区神田美士代町 11-2　第1東英ビル
海上電機株式会社	東京都千代田区神田錦町 1-19
社団法人　海洋開発産業技術協会	東京都港区六本木 4-1-13
株式会社　海洋開発センター	東京都港区赤坂 1-9-1
協同低温工業株式会社	東京都千代田区神田佐久間町 1-21　山伝ビル
協和商工株式会社	東京都新宿区下落合 1-513 第二正明ビル
栗山ゴム株式会社	大阪市東淀川区西中島町 1-195
小松川化工機株式会社	東京都江戸川区小松川 1-2645
小山康三	東京都文京区本駒込 6-15-10　英和印刷社
三信船舶電具株式会社	東京都千代田区内神田 1-15
三洋水路測量株式会社	東京都港区新橋 5-23-7　三栄ビル
シュナイダー財団極東駐在事務所	東京都港区芝琴平町 38　日本ガス協会ビル
昭和電装株式会社	高松市福岡町 467
大洋電機株式会社	東京都千代田区神田錦町 3-16
株式会社高瀬鉄工所	東京都江戸川区松江 1-11-15
株式会社鶴見精機工作所	横浜市鶴見区鶴見町 1506
帝国酸素株式会社	神戸市兵庫区高松町 22-1
東亜港湾株式会社	東京都千代田区四番町 5
東京工材株式会社	東京都中央区築地 4-2　築三ビル
株式会社東京久栄	東京都中央区八重洲 3-3　八重洲口会館
東京製綱繊維ロープ株式会社	東京都中央区日本橋室町 2-8　古河ビル
東京レプ株式会社	東京都豊島区池袋 2-1120　ローズマンション 302 号
株式会社東邦電探	東京都杉並区上高井戸 5-327
東洋海洋開発株式会社	東京都中央区宝町 3-4
東レ株式会社	大津市苑山 3-2-1
中川防蝕工業株式会社	東京都千代田区神田鍛冶町 2-1　東京建物ビル
株式会社ナック	東京都中央区銀座 1-5-6
日本アクアラング株式会社	東京都品川区東品川 4-9-26　南産業ビル
日本海事広報協会海の世界編集部	東京都港区琴平町 35　船舶振興ビル
日本海洋産業株式会社	東京都新宿区西新宿 2-6-1　新宿住友ビル
日本テトラポッド株式会社	東京都港区新橋 2-1-13 新橋富士ビル9階
日本テレスコム株式会社	東京都港区六本木 4-11-10　六本木富士ビル
社団法人　日本能率協会	東京都港区芝公園25号地
日本無線株式会社	東京都港区芝桜川町 25　第五森ビル
有限会社ハラダ電機製作所	東京都豊島区池袋 8-3292
ヒエン電工株式会社	堺市松屋町 1-3
深田多満男	東京都港区芝虎ノ門8　虎ノ門実業会館　深田サルベージ株式会社
藤田潔	東京都中央区銀座西 7-6　株式会社ビデオプロモーション
藤田峯雄	東京都江東区南砂 1-3-25　株式会社　中村鉄工所
芙蓉海洋開発株式会社	東京都千代田区大手町 2-3-6 タイムライフビル
フランス物産株式会社	東京都千代田区神田小川町 3-20-2 増淵ビル
古野電気株式会社	東京都中央区八重洲 4-5　藤和ビル
丸文株式会社	東京都中央区日本橋大伝馬町 2-1-1
三井海洋開発株式会社	東京都千代田区霞ケ関 3-2-5　霞ケ関ビル3002号室
三菱重工業株式会社	東京都千代田区丸の内 2-5-1
株式会社吉田製作所	東京都台東区上野 3-13-9
吉野計器製作所	東京都北区西ケ原 1-14
株式会社離合社	東京都千代田区神田鍛冶町 1-2　丸石ビル
株式会社渡部計器製作所	東京都文京区向丘 1-7-17

Exploiting the Ocean by...

T.S.K. OCEANOGRAPHIC INSTRUMENTS

REPRESENTATIVE GROUPS OF INSTRUMENTS AND SYSTEMS

T.S－デジタル塩分計

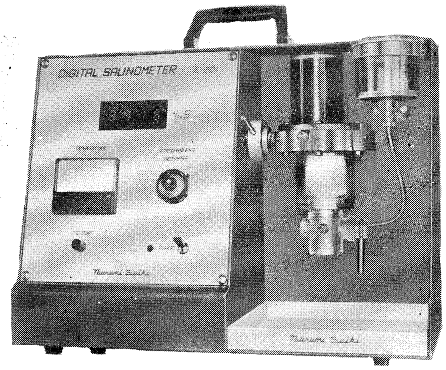

本卓上塩分計は，電磁誘導方式による卓上塩分計T.S－Eシリーズのデジタル表示型として開発されたものであります。

迅速な卓上塩分計を！のご要望に応えわずか数十秒で測定し結果が得られますので測定の迅速性と相まって取扱操作の効果的な省力化および測定者による測定誤差をなくする卓上塩分計の決定版であります。

特　長

- デジタル表示(直読)
- 高精度
- 使用法簡単
- 迅速測定

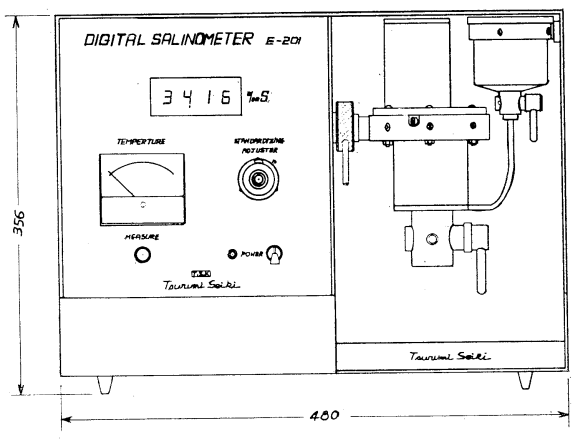

仕　様

測定範囲	0～36‰S
精　　度	±0.01‰S
自動温度補償範囲	5～30℃
所要水量	80c.c.
電　　源	A.C 100V
重　　量	約20kg

THE TSURUMI SEIKI CO., LTD.

1506 Tsurumi-cho Tsurumi-ku, Yokohama, 〒230 Japan

CABLE ADDRESS	TELEPHONE	TSK. USA.
TSURUMISEIKI Yokohama	045-521-5252～5	3510 Kurtz St.,
	TLX; 3823750 TSK JPN J	San Diego, Calif, 92110, U.S.A

IWAMIYA INSTRUMENTATION LABORATORY

長期捲自記流速計

(NC-Ⅱ)

本流速計は海中に設置し、内蔵した記録器に流速流向を同時に記録するプロペラ型の流速計で約20日間の記録を取る事が出来ます。但し流速は20分毎に3分間の平均流速を又流向は20分毎に一回、共に棒グラフ状に記録しますから読取が非常に簡単なのが特徴となって居ります。

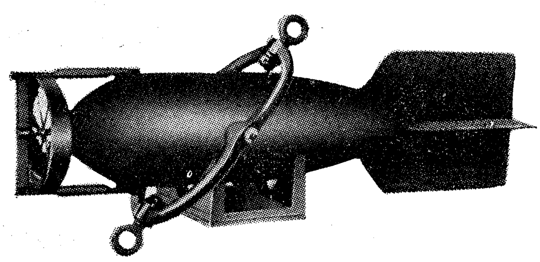

(外器)

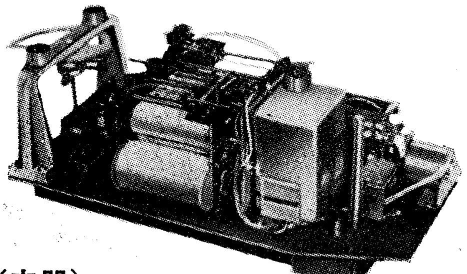

(内器)

プロペラはA，B，C三枚一組になって居り

A(弱流用)………1 m/sec
B(中流用)………2 m/sec
C(強流用)………3 m/sec

迄で一枚毎に検定してあります。

弱流ペラーに依る最低速度は約4cm/secです。

フース型長期捲自記検潮器

(LFT-Ⅲ)

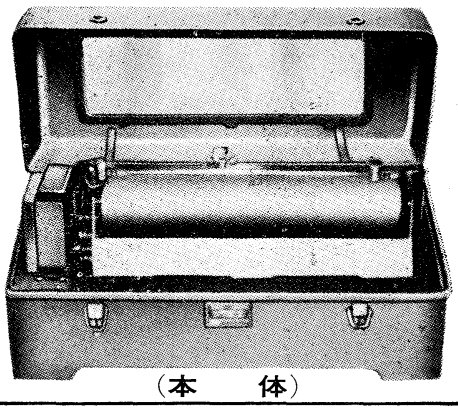

(本　体)

営業品目

階段抵抗式波高計
ケーブル式波高計
フース型検潮器
小野式自記流速計
自記水位計
港施型土圧計
理研式水中カメラ
その他海洋観測諸計器

協和商工株式会社

東京都豊島区目白4丁目24番地1号
TEL (952) 1376代表 〒171

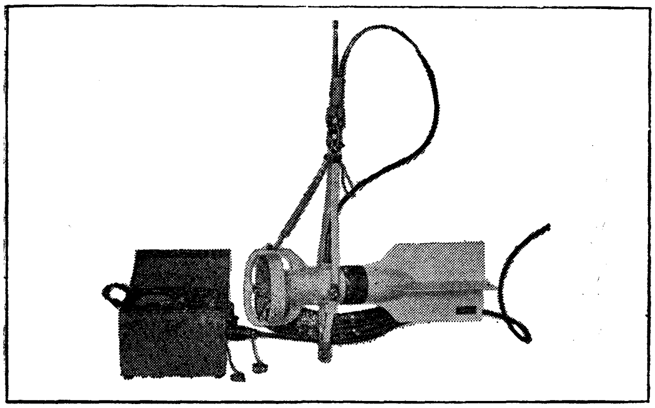

Direct-Reading Current &
Direction Meter

Model

CM-2

Catalogues are to be sent immediately upon receipt of your order products

Products

KM-2 : Direct Reading Knot-Meter for Trawl-Boats to Control Adequate Speed

ET-5 : Electric Meter of Water Temperature

ECT-5: Electric Conduction and Temperature Meter for Chlorine

TOHO DENTAN CO.,LTD.

Office: 1-8-9, Miyamae, Suginami-Ku, Tokyo. Tel. Tokyo (03) 334—3451～3

AUTO-LAB PORTABLE S-T BRIDGE

Model 602

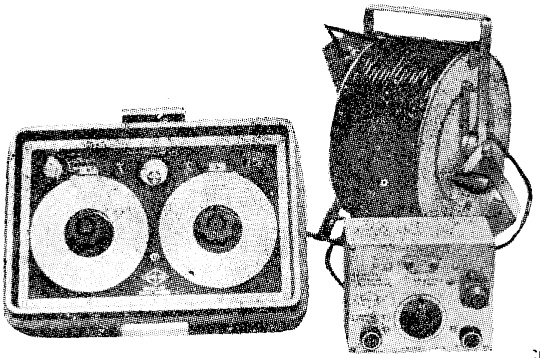

オート・ラブ誘導起電式精密塩分計に引続いて，開発された温度と塩分の現場測定用の可搬型海洋測器です。温度，塩分ともダイアルで直読出来，簡便で堅牢しかも高精度なソリッドステートのユニット結合構造の最新鋭計器です。

温　度 ： 0～35°C 1/2 確度 ±0.1°C

塩　分 ： Scale 1. 0～32 ‰S 確度 ±0.1 ‰S

Scale 2. 32～42 ‰S 確度 ±0.03 ‰S

電　源 ： 電池 9 V，200 時間使用可能

追加附属品

ステンレス製ケーブルリール

半自動式電極プラチナイザー

製 造 品 目

転倒温度計各種

電気式水温計各種

採水器・海洋観測機器

気象用・理化学用温度計

サーモレンジャー・ミグスター　温度調節器

日本およびアジア総代理店

株式会社 渡部計器製作所

東京都文京区向丘 1の7の17

TEL (811) 0044 (代表) 〒 113

(カタログ御希望の方は誌名御記入の上御請求下さい)

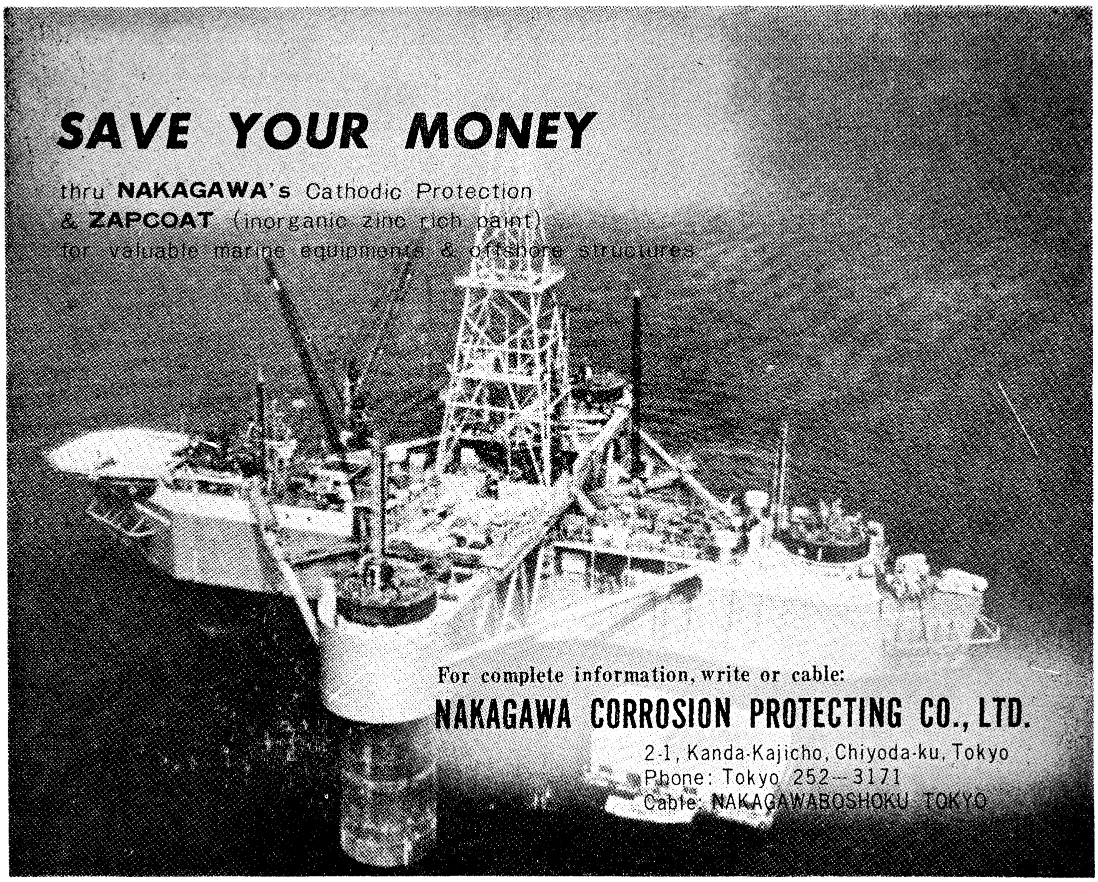
SAVE YOUR MONEY
thru NAKAGAWA's Cathodic Protection
& ZAPCOAT (inorganic zinc rich paint)
for valuable marine equipments & offshore structures
For complete information, write or cable:
NAKAGAWA CORROSION PROTECTING CO., LTD.
2-1, Kanda-Kajicho, Chiyoda-ku, Tokyo
Phone: Tokyo 252－3171
Cable: NAKAGAWABOSHOKU TOKYO

昭和49年2月25日 印刷
昭和49年2月28日 発行

うみ 第12巻 第1号

定価 ¥400

編集者 今村豊
発行者 佐々木忠義
発行所 日仏海洋学会
財団法人 日仏会館内
東京都千代田区神田駿河台2-3
郵便番号:101
電話 (291) 1141
振替番号:東京96503

印刷者 小山康三
印刷所 英和印刷社
東京都文京区本駒込6-15-10
郵便番号:113
電話 (941) 6500

第 12 巻　第 1 号

目　　次

Tome 12　　N°1

SOMMAIRE